Virginia Commonwealth University
VCU Scholars Compass

Theses and Dissertations | Graduate School

2012

PREPARATION AND EVALUATION OF DECONSTRUCTION ANALOGS OF 7-DEOXYKALAFUNGIN AS AKT INHIBITORS

Sudha Korwar
Virginia Commonwealth University

Follow this and additional works at: https://scholarscompass.vcu.edu/etd

 Part of the Pharmacy and Pharmaceutical Sciences Commons

© The Author

Downloaded from
https://scholarscompass.vcu.edu/etd/387

This Thesis is brought to you for free and open access by the Graduate School at VCU Scholars Compass. It has been accepted for inclusion in Theses and Dissertations by an authorized administrator of VCU Scholars Compass. For more information, please contact libcompass@vcu.edu.

PREPARATION AND EVALUATION OF DECONSTRUCTION ANALOGS OF 7-DEOXYKALAFUNGIN AS AKT INHIBITORS

A thesis submitted in partial fulfillment of the requirements for the degree of Master of Science at Virginia Commonwealth University.

by

SUDHA KORWAR
Bachelor of Pharmacy, Manipal University, India, May 2010

Director: Dr. KEITH C. ELLIS
Assistant Professor, Department of Medicinal Chemistry

Virginia Commonwealth University
Richmond, Virginia
July, 2012

Acknowledgement

First and foremost, I would like to thank my advisor Dr. Keith C. Ellis for his guidance and support over the last two years. His patience, knowledge, optimism and encouragement have helped me overcome the obstacles encountered during my research. One could not wish for better advisor.

I would like to thank Dr. Montserrat Samso, my committee member and mentor over the past two years. Her encouragement and support cannot be expressed in words.

I would like to thank Dr. John C. Hackett, my committee member, for reading my thesis.

I would like to thank my lab mates, Jenson Verghese and Lauren Gaskell, for helping me get started with the synthesis. They have immensely helped me throughout my research by giving me valuable advice, being very patient and encouraging at all times. I would like to thank the Ellis Group post-doctoral fellow Dr. Thuy Nguyen for performing the assays and for giving me invaluable advice. It has been a wonderful experience working in the Ellis Group.

I would like to thank the Samso Group members Drs. Demetrio Santiago, Vanessa Cabra, Pablo Castro Hartmann; and Tyler Steele for their support.

I would like to thank my parents and my sister for giving me support and encouragement at all times, as always.

Table of Contents

List of Tables

List of Figures

List of Figures

List of Figures

List of Figures

List of Figures

Abstract

PREPARATION AND EVALUATION OF DECONSTRUCTION ANALOGS OF 7-DEOXYKALAFUNGIN AS AKT INHIBITORS

SUDHA KORWAR, M. S.

A thesis submitted in partial fulfillment of the requirements for the degree of Master of Science at Virginia Commonwealth University.

Virginia Commonwealth University, 2012

Director: Dr. KEITH C. ELLIS
Assistant Professor, Department of Medicinal Chemistry

Pyranonaphthoquinone lactones have been recently found to be selective inhibitors of the serine-threonine kinase AKT/PKB. AKT/PKB plays a major role in tumorigenesis, hence these compounds have a great potential to act as anti-cancer agents. They act by a novel bioreductive alkylation mechanism of inhibition of AKT/PKB.

In this work, 7-deoxykalafungin, a pyranonaphthoquinone lactone and its deconstruction analogs were synthesized. The structural features of the compounds necessary to inhibit AKT1 potently and selectively were determined. It was observed that compounds with a pyran ring were more

potent in inhibiting AKT1. Conversely, flexible compounds were found to be weak inhibitors of AKT1. Also, presence of a lactone ring was found to be favorable in inhibiting AKT1. Of the compounds tested, 7-deoxykalafungin was the most potent inhibitor of AKT1 (IC_{50} = 0.28 µM against AKT1) and compound **4-61** was the most potent inhibitor of PKA (IC_{50} = 0.43 µM against PKA).

CHAPTER 1

INTRODUCTION

1.1 Protein phosphorylation

Proteins can be regulated by reversible covalent modifications such as phosphorylation, acetylation, hydroxylation, methylation, etc. The most commonly encountered modification is phosphorylation (**Figure 1**) which is carried out by protein kinases.[1]

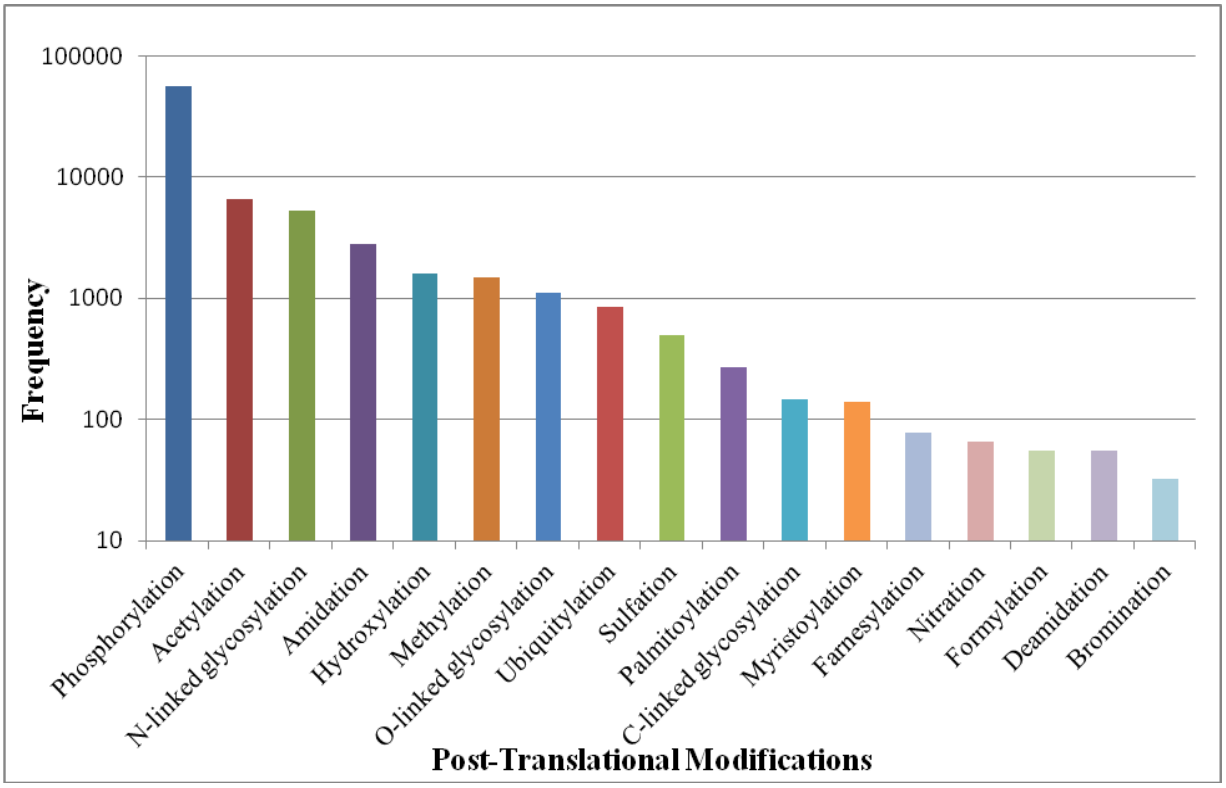

Figure 1. Frequency of post-translational modifications[1]

Protein kinases are regulatory enzymes that transfer a phosphate group from ATP to the substrates resulting in activation or inactivation of the substrates. They require a divalent metal ion such as Mg^{2+} for their activity. A total of 518 protein kinases have been found in humans to

date. The residues that are most commonly phosphorylated are serine (~76-90%), threonine (~10-20%) and tyrosine (~0.05-4%). The less commonly phosphorylated residues are histidine, aspartic acid and glutamic acid. There are 8 major groups of protein kinases AGC (PK**A**, PK**G**, PK**C**); CAMK (**Ca**-Cal**m**odulin dependent protein **k**inases); CMGC (**C**DK, **M**APK, **G**SK3, **C**LK); TK (**T**yrosine **K**inases); TKL (**T**yrosine **K**inase **L**ike kinases); STE (homologs of yeast kinases); RGC (**R**eceptor **G**uanylate **C**yclases) and CK1 (**C**asein **K**inase **1**).[2]

1.2 AGC kinases

AGC kinases are a subfamily of protein kinases that have a similar catalytic kinase domain as that of cAMP-dependent protein kinase (PK**A**), cGMP-dependent protein kinase (PK**G**) and protein kinase C (PK**C**).[3] To date, 60 human AGC kinases have been found. A general structure of an AGC kinase is shown below. (**Figure 2**) It consists of a large carboxy terminal lobe (C-lobe) in the activation segment, a small amino terminal lobe (N-lobe), αC helix connecting both the lobes, a turn motif and a hydrophobic motif. In order for an AGC kinase to be activated, it has to be phosphorylated in two highly conserved motifs – the 'activation segment' or 'T-loop' present in the catalytic domain and 'hydrophobic motif' present in the non-catalytic domain. Some AGC family members contain a Pleckstrin Homology (PH) domain. In many AGC kinases phosphorylation of the 'turn motif' helps in maintaining the integrity of the kinase.[4] The 'bilobal kinase fold' affords one molecule of ATP between the N-lobe and the C-lobe which acts as the phosphate donor during the phosphorylation reactions. [5] The AGC kinases phosphorylate a variety of proteins, most of which contain basic residues at the N-terminal position of the phosphorylated serine or threonine residues. They play a very important role in various cellular functions and are found to be implicated in many diseases such as cancer and diabetes.

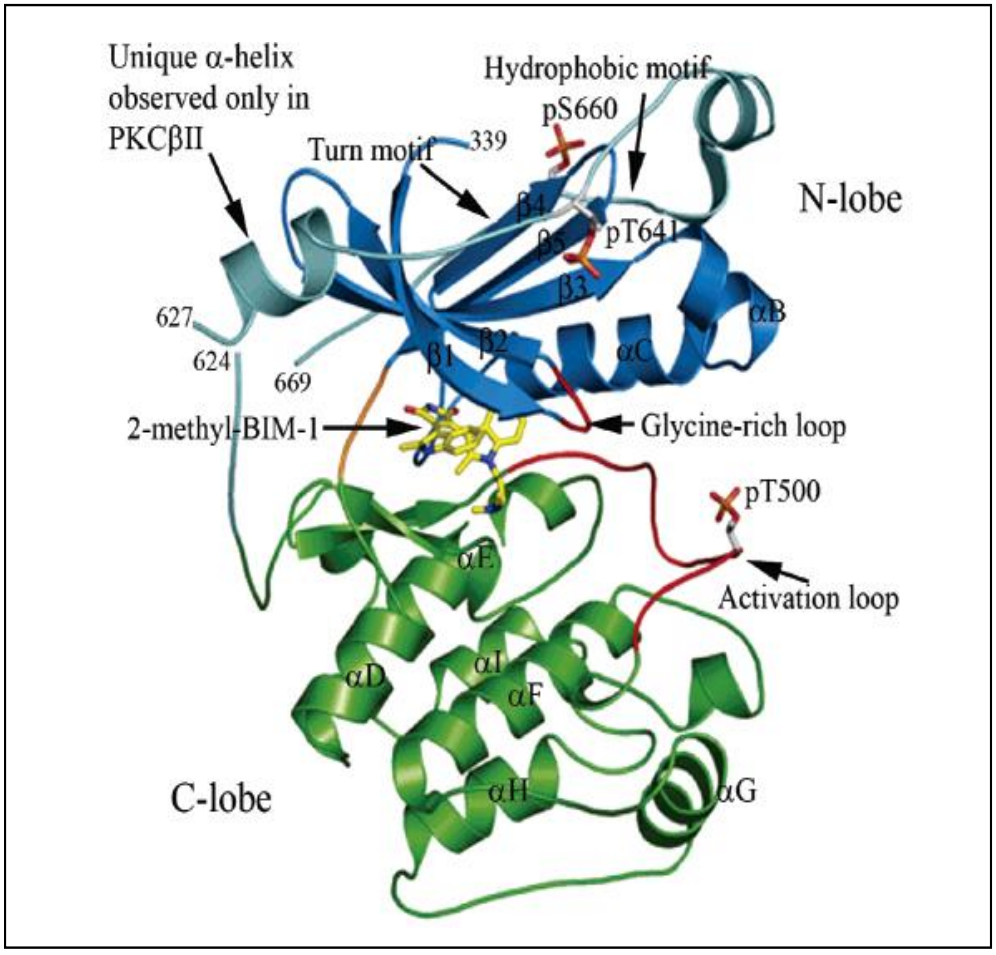

Figure 2. Structure of catalytic domain of human PKC II in complex with an inhibitor

"Reprinted with permission from Grodsky, N.; Li, Y.; Bouzida, D.; Love, R.; Jensen, J.; Nodes, B.; Nonomiya, J.; Grant, S. Structure of the catalytic domain of human protein kinase C β II complexed with a bisindolylmaleimide inhibitor. *Biochemistry*. **2006**, *45*, 13970-13981. Copyright 2006, American Chemical Society.

1.3 AKT Introduction

Akt was first identified in 1987 by Stephen Staal in a mouse strain that spontaneously developed lymphoma in the thymus caused by a transforming retrovirus.[6] The viral oncogene was termed *v*-Akt. The cellular homolog of this viral oncogene found in humans was termed Akt1 (the first identified isoform in humans). AKT exists as three isoforms AKT1 (PKBα), AKT2 (PKBβ) and AKT3 (PKBγ) encoded by three separate genes. Akt1 is ubiquitously distributed in many tissues and is responsible for growth and survival of cells.[7] Akt2 is found mainly in adipocytes and muscle cells; it is responsible for glucose homeostasis.[8] Akt3 expression is restricted to brain and testes. AKT has an N-terminal PH domain, a kinase (catalytic) domain and a C-terminal regulatory region containing a hydrophobic motif. The catalytic domain of AKT is very similar to that of other PKA and PKC family members.

The three isoforms of AKT share different levels of homology in different domains. (**Table 1**)

Table 1. Percent sequence similarity between AKT isoforms[9]

PAIR	PH domain	LINK region	Catalytic domain	C-terminal extension
AKT1/AKT2	80 %	46 %	90 %	66 %
AKT1/AKT3	84 %	40 %	88 %	76 %
AKT2/AKT3	76 %	17 %	87 %	70 %

1.3.1 Phosphorylation sites

The isoforms of Akt have different phosphorylation sites. (**Figure 3**) The serine and threonine residues (shown in red) are necessary for the activation of Akt, whereas the other sites are found to be constitutively phosphorylated.[10]

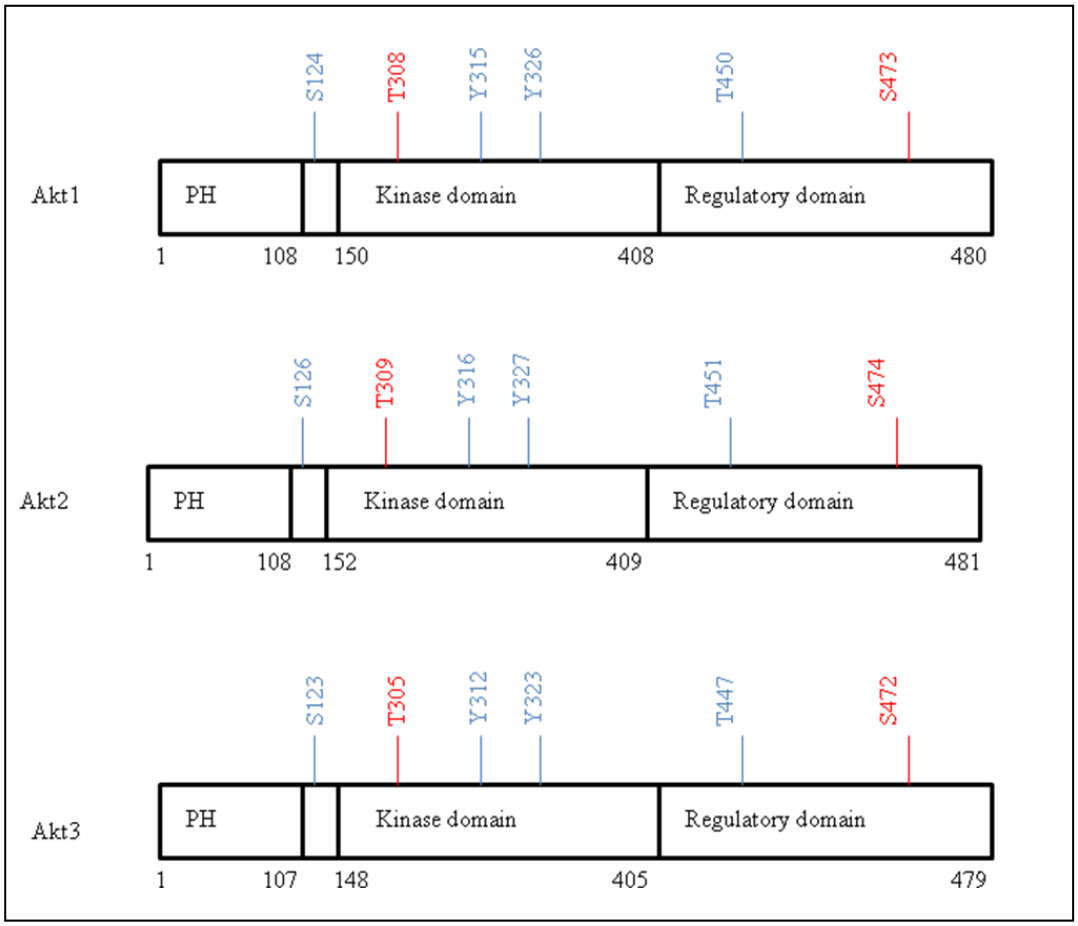

Figure 3. Phosphorylation sites on the isoforms of Akt

1.3.2 Crystal structure of AKT1

A crystal structure of full-length AKT has not been reported to date. The PH domain and the catalytic domains have been crystallized separately. The first crystal structure of AKT1 (1-123 amino acids bound to phosphoinositol-3,4,5-triphosphate) was reported by Thomas *et al.* [11]

The crystal structure of AKT2 (146-481 amino acids bound to GSK3-peptide and AMP-PNP) was reported by Yang *et al* in 2002.[12] In this structure, S474 phosphorylation on the hydrophobic motif helps in the ordering of αC helix by promoting the interaction between the hydrophobic motif and the N-lobe of kinase domain. This αC helix then interacts with the phosphorylated

T309 in the activation segment. This results in conformational change and activation of the enzyme.

1.4 Regulation of AKT by upstream processes

AKT is regulated by and regulates a wide range of factors - a few of which are discussed below.

1.4.1 Positive regulation of Akt

AKT is positively regulated by a number of factors that result in its phosphorylation.

1.4.1.1 Phosphatidylinositol 3-Kinase (PI 3-Kinase) mediated activation of AKT/PKB

It has been found that Akt is activated by PDGFR β (Platelet-Derived Growth Factor Receptor β) through PI 3-Kinase.[13] PDGFR is a tyrosine kinase receptor. Upon stimulation, it undergoes dimerization.[14] This activates its intrinsic kinase activity leading to the autophosphorylation of its tyrosine residues Y740 and Y751 which in turn leads to the binding of PI 3-Kinase to its phosphorylated tyrosine residues. PI 3-Kinase has a regulatory subunit (p85) and a catalytic subunit (p110). When stimulated by the growth factor, PI 3-Kinase binds to the phosphorylated tyrosine residues Y740 and Y751 of the growth factor receptor through its regulatory subunit and gets activated. Once activated, it phosphorylates inositol residues to form PIP2 and PIP3 through its catalytic domain. PIP3 then binds to Akt at its PH domain which results in the translocation of Akt to the plasma membrane and its subsequent activation **(Figure 4).**

1.4.1.2 Role of Phosphoinositide Dependent Kinases (PDKs) in the activation of AKT/PKB

It is found that Akt1 is phosphorylated on its serine and threonine residues even before it undergoes activation by the growth factors. For instance, S124 and T450 in mouse Akt1 undergo phosphorylation constitutively.[15] This phosphorylation makes Akt more prone to subsequent phosphorylations. T308 and S473 residues that lie in the activation loop of the kinase domain

and in the carboxy terminal of the kinase, respectively, are found to be very crucial in the activation of Akt by growth factors. 3-Phosphoinositide Dependent Kinase 1 (PDK1) has been found to phosphorylate Akt at its T308 residue. This kinase was cloned and purified

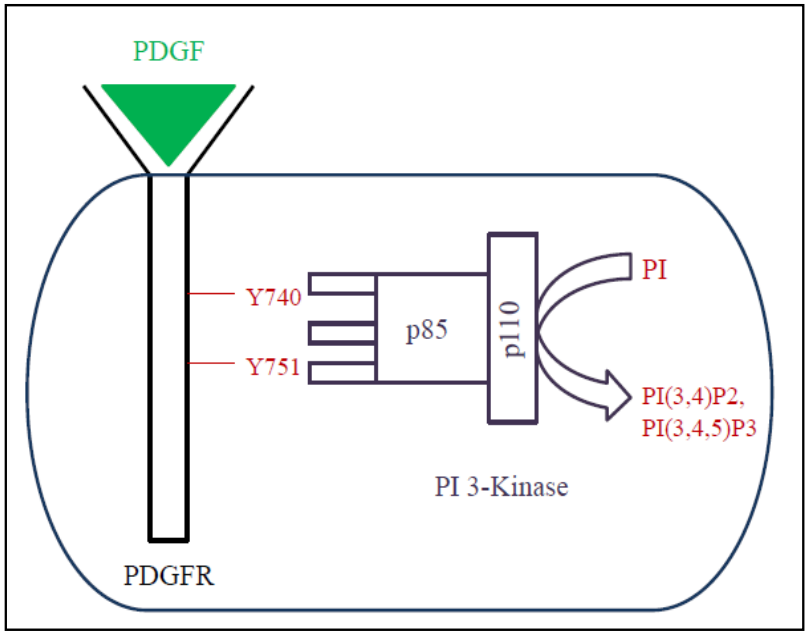

Figure 4. Activation of PI 3-Kinase by PDGF

in 1997.[16] PDK1 binds with a high affinity to PIP3 through its PH domain's C-terminus. Some studies show that upon stimulation by growth factors, PDK1 is translocated to the plasma membrane[17]and phosphorylates Akt. Whereas other studies suggest that PDK1 does not translocate upon stimulation by growth factors.[18] However, very little PDK1 remains bound to the plasma membrane in non-stimulated cells. The PDK1 in the plasma membrane might be responsible solely for the phosphorylation of Akt and other substrates present in the membrane and the one in the cytoplasm might be responsible for the phosphorylation of other cytosolic proteins. PDK1 does not phosphorylate S473 by itself.[19] The kinase that phosphorylates S473 has been in debate for a very long time. Several kinases have been proposed. Delcommenne *et al*

have found that a serine-threonine kinase named Integrin-Linked Kinase 1 (ILK-1) phosphorylates S473 *in* vitro.[20] Whereas, Balendran *et al.* suggest that both PDK1 and PDK2 might be the same enzyme and the ability to phosphorylate S473 and/or T308 specifically depends on the interaction of PDK1 with other components within the cell.[21] They have found that the kinase domain of PDK1 interacts with the carboxy terminal region of Protein Kinase C-Related Kinase (PKN2 or PRK2). This region has been named PDK1-Interacting Fragment (PIF). PIF has the same consensus sequence as that of PDK2 with just one difference – the serine 473 is replaced by an aspartic acid residue. Once PDK1 interacts with PIF, it is converted to an enzyme form that phosphorylates both T308 and S473 in Akt/PKB. They have also ruled out the possibility of autophosphorylation at S473 residue by Akt itself once T308 is phosphorylated by PDK1. **(Figure 5)**

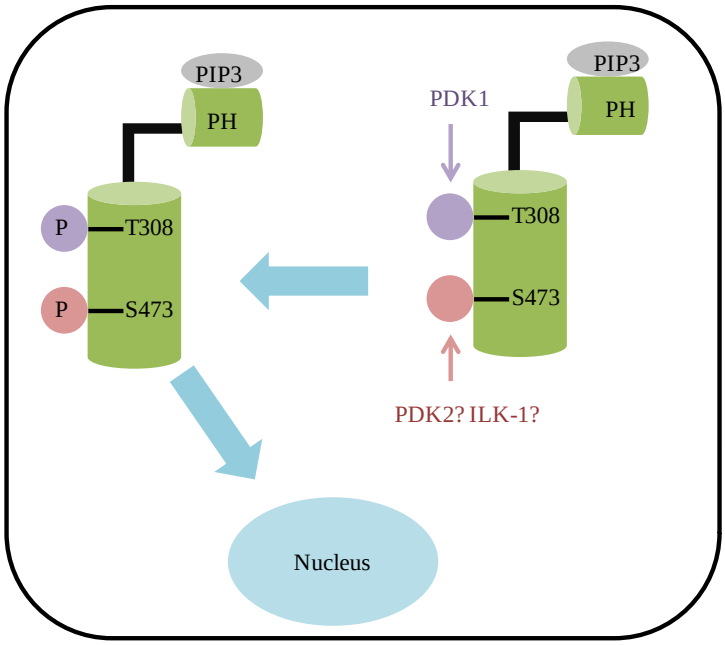

Figure 5. Phosphorylation of AKT1

But recently, it has been found that S473 is phosphorylated by PI3-Kinase-related Kinase (PIKK) super family members - mammalian Target Of Rapamycin Complex 2 (mTORC2)[22] under normal growth conditions and DNA dependent Protein Kinase (DNA-PK) under conditions of stress.[23] AKT1 is phosphorylated constitutively at Thr450 in its turn motif. This is essential for the stabilization and the prevention of dephosphorylation of the hydrophobic motif.[4]

1.4.1.3 Integrin-mediated stimulation of AKT[24]

Integrins are heterodimeric receptors on the cell surface that are involved in the adhesion, differentiation, migration, growth and survival of cells. When a cell gets attached to the fibronectin receptors in the extracellular matrix by the action of integrins, the Focal Adhesion Kinase (FAK), a tyrosine kinase in the cytoplasm, gets activated by the phosphorylation of its tyrosine residue by integrins. This in turn stimulates the interaction of FAK with p85 subunit of PI 3-Kinase[25] resulting in the phosphorylation of PI 3-Kinase and hence its activation. As a result, PI 3-Kinase phosphorylates the D3 position of inositol ring to form PI(3,4)P2 and PI(3,4,5)P3. This activates the Akt signaling pathway by the binding of phosphoinositides to the PH domain of AKT.

1.4.1.4 B cell Antigen Receptor (BCR) mediated activation of PI 3-Kinase:

It has been found that the B Cell antigen Receptors (BCR) activate Akt signaling pathway by activating PI 3-Kinase.[26] The role of Akt in the survival of B cells is not exactly known. It might play a role in enhancing the protein synthesis in B cells.

1.4.1.5 Miscellaneous

Angiotensin II,[27] hydrogen peroxide,[28] CD28, CD5, GPCRs, μ receptors have been found to activate Akt signaling through PI 3-Kinase.

1.4.2 Negative regulation of Akt

Dephosphorylation is the major means by which Akt is negatively regulated. This is achieved by the action of various phosphatases aided by the short half-lives of phosphorylated T308 and S473 residues.

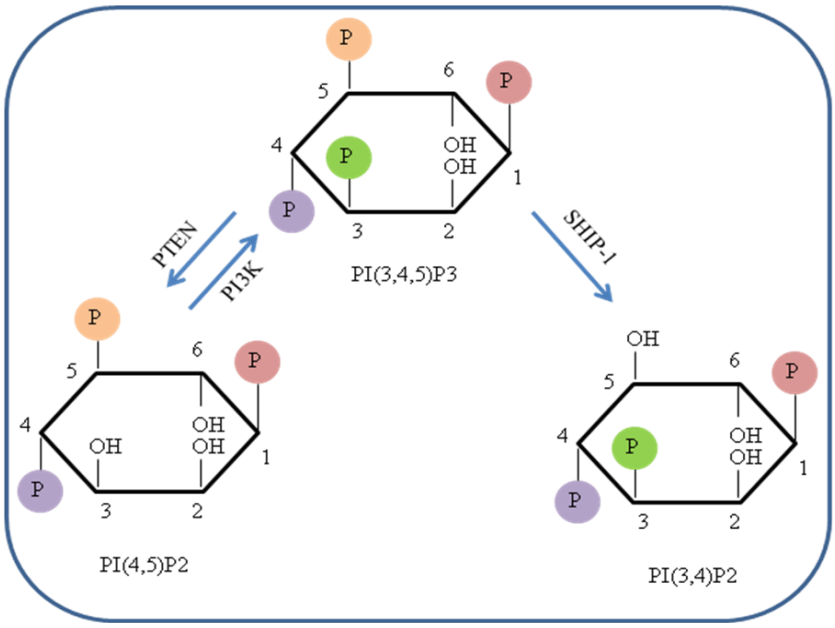

Figure 6. Dephosphorylation of phosphoinositides

1.4.2.1 Dephosphorylation by PTEN (Phosphatase and Tensin Homologue deleted on chromosome 10)

PTEN is a tumor suppressor gene present on the human chromosome 10 in the 10q23 region.[29] It is also referred to as MMAC1 (Mutated in Multiple Advanced Cancer 1). PTEN has been found to be implicated in many types of human cancers such as glioblastomas, melanomas, etc. It contains a catalytic motif homologous to that present in protein tyrosine phosphatases. PTEN has been found to be a lipid phosphatase with 3-phosphoinositide specific phosphatase activity.[30] It dephosphorylates PI(3,4,5)P3 to form PI(4,5)P2 (**Figure 6**). Thus it inhibits PI 3-Kinase activity,

thereby inhibiting the Akt/PKB pathway.[31] This inhibition by PTEN is found to affect only the basal PKB activity, it does not affect the pathway when Akt is stimulated by growth factors.[30] Some other studies have shown that PTEN inhibits the cell migration and focal adhesion by causing tyrosine dephosphorylation of FAK, thereby inhibiting FAK.[32]

1.4.2.2 Dephosphorylation by SHIP (SH (Src Homology)-2 containing Inositol 5′ Phosphatase)

SHIP is a **5′** specific lipid phosphatase that breaks down PI(3,4,5)P3 to PI(3,4)P2. SHIP1 is present in hematopoietic cells and SHIP2 is found in non-hematopoietic cells. It has been found that in myeloid cells, SHIP inhibits Akt pathway which is stimulated by the growth factors.[33] This is in contrast to PTEN which only inhibits the basal activity of Akt/PKB. In myeloid cells, when cytokine receptors are stimulated by the cytokines, they get activated and in turn activate PI 3-Kinase and induce tyrosine phosphorylation of SHIP. Activation of PI 3-Kinase results in the formation of PI(3,4,5)P3. The phosphorylated SHIP is then translocated to the plasma membrane by interaction with Shc (Src homology and collagen). In the membrane, SHIP dephosphorylates PI(3,4,5)P3 to PI(3,4)P2 (**Figure 6**). This results in the inactivation of Akt/PKB pathway. Aman *et al*. have reported that SHIP inhibits the activation of Akt/PKB pathway in B cells.[34]

1.4.2.3 PH domain

PH domain acts as both positive and negative regulator of Akt. In a cell, Akt is present in a constitutively inactive state in the cytoplasm due to the interaction between its PH domain and the kinase domain.[35] This intramolecular interaction does not allow the threonine residue to be exposed to PDK1, hence it remains unphosphorylated. When 3-phosphoinositides bind to the PH

domain, the conformation of Akt changes, its activation/catalytic loop is exposed, resulting in the phosphorylation of T308 by PDK1.

1.5 Downstream processes of Akt - Cellular functions

Akt is known to phosphorylate several proteins. In order for a protein to be phosphorylated by Akt, it must have the consensus sequence of Arg-X-Arg-Y-Z-Ser/Thr-Hydrophobic and bulky residue (where X - any amino acid, Y and Z – small amino acids other than Gly).[36] Around a thousand proteins in the cell contain this consensus sequence, of which 50 have been characterized as AKT substrates till date. These substrates can be classified as:

1.5.1 Cell cycle progression regulators

These include Glycogen Synthase Kinase 3β, p21, p27, cyclin D1, etc.

1.5.1.1 Glycogen Synthase Kinase (GSK) 3α and 3β

Glycogen synthase is a constitutively active enzyme that is involved in the rate-determining step of glycogen synthesis. It exists as two isoenzymes in mammals – α (51 kDa) and β (47 kDa). The phosphorylated form of this enzyme is inactive and the non-phosphorylated form is active. GSK3 is known to phosphorylate four clustered serine residues named 3a – 3d in Glycogen Synthase enzyme. This inhibits the GS enzyme. In order for GS to be phosphorylated by GSK3, the priming site (the serine residue at +4 position with respect to the target serine residue) on GS has to be phosphorylated. This is done by Casein Kinase 2.

It is found that, in response to insulin[37] and other growth factors such as Epidermal Growth Factor (EGF),[38] GSK3α is phosphorylated at serine 21 residue and GSK3β is phosphorylated at serine 9 residue by Akt/PKB. This inhibits GSK, as a result, glycogen synthase remains in a dephosphorylated/active state resulting in the synthesis of glycogen.

GSK3 phosphorylates and inhibits many proto-oncogenes such as c-Jun, c-Myc, β-catenin, etc.

- β-catenin - once phosphorylated by GSK3β, it gets degraded due to the action of the proteosome, hence the cell dies. Thus Akt promotes cell survival by inhibiting GSK3β due to phosphorylation.
- c-Jun - it is a part of the transcription factor complex called AP1 (Activator Protein 1). Once phosphorylated by GSK3 at 3 residues, it loses its DNA-binding affinity. Hence, the trans-activation of its effector genes does not occur.[39] Akt protects the activity of c-Jun by inhibiting GSK3.
- eIF-2B - GSK3 phosphorylates the eukaryotic Initiation Factor-2B *in vitro*. eIF-2B regulates the levels of eIF-2 which plays an important role in translation

1.5.2 Cell survival/death regulators

These include Forkhead transcription factors, BAD, caspase-9, p53, etc.

1.5.2.1 Forkhead transcription factors

Forkhead transcription factors[40] such as DAF-16 (in *Caenorhabditis elegans*); FKHR, FKHR1 and AFX (in humans) cause apoptosis in cells. They contain a Nuclear Localization Sequence or Signal (NLS) consisting of ForkHead DNA-binding domain and a domain made up of basic amino acids. This NLS is responsible for importing these factors into the nucleus of a cell. Inside the nucleus, they bind to certain elements on the DNA and bring about apoptosis of the cells. For example, FKHR1 is found to bind to the DNA Response Element known as ForkHead Response Element (FHRE) resulting in the activation of Fas ligand gene (a death gene). Akt has been found to inhibit these transcription factors.[41] When survival factors are present, Akt phosphorylates 3 sites in FKHR1 – T32, S253 and S315. The phosphorylation of T32, S253 (to a major extent) and S315 (to a minor extent) causes FKHR1 to bind to a scaffolding protein 14-3-3

in the cytoplasm. The S253 phosphorylation site overlaps with the domain made up of basic amino acids. This gives a negative charge to the otherwise positively charged domain. Thus, the NLS gets disrupted and no longer transports FKHR1 into the nucleus and gets sequestered in the cytoplasm to the scaffolding protein. Hence, the apoptotic genes are not activated. As a result, the cell survives (**Figure 7**).

1.5.2.2 BH3-only protein BAD (B-cell lymphoma-2 Associated Death promoter)

BAD is a Bcl-2 Homology domain 3 (BH3)-only protein. In its dephosphorylated state, it binds to prosurvival Bcl-2 family members (such as BCL-X_L) and inactivates them, leading to apoptosis. In the presence of survival factors, AKT phosphorylates S136 on BAD; causing binding of 14-3-3 proteins to the complex of BAD and BCL-X_L. This helps in the phosphorylation of S155 of BAD by kinases. This phosphorylation leads to the dissociation of BAD from BCL-X_L, thereby preventing apoptosis. [42,43]

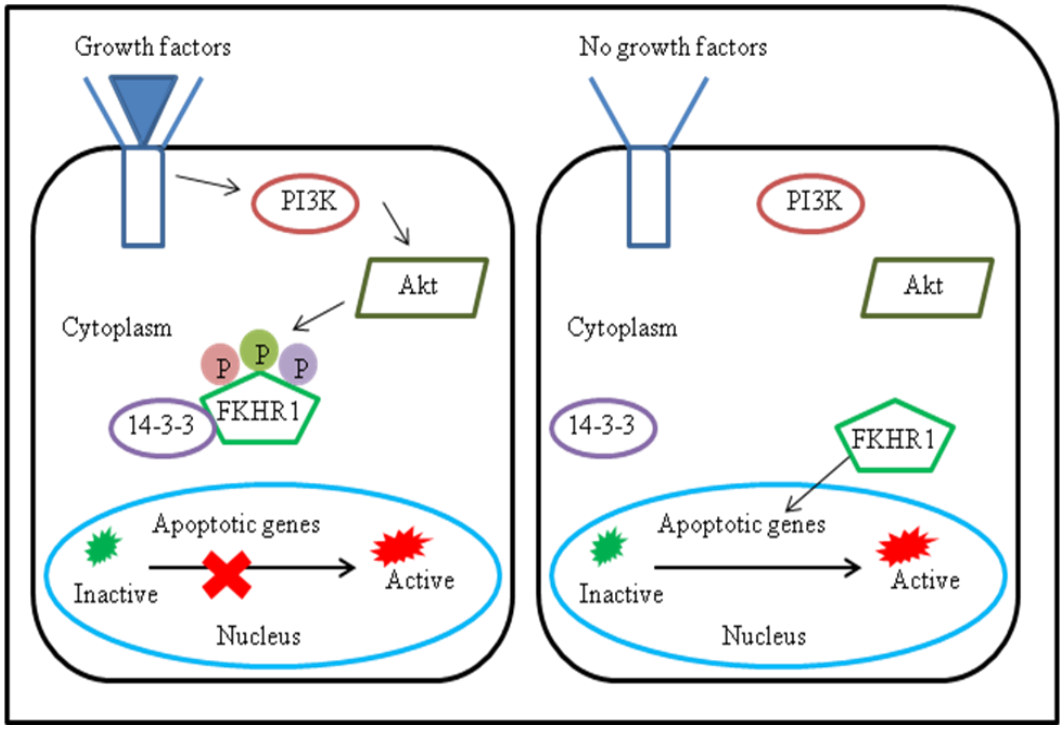

Figure 7. Regulation of FKHR1 by AKT

1.5.3 Protein synthesis or cell growth regulators

These include Tuberous Sclerosis Complexes 1/2 (TSC1/2), mTORC1 (mammalian Target Of Rapamycin Complex 1), 4E-binding protein-1 (4E-BP1), etc.

1.5.3.1 mTORC1 and Tuberous Sclerosis Complexes 1/2 (TSC1/2)

AKT indirectly activates mTORC1 (**Figure 8**). AKT phosphorylates TSC2 at multiple sites (in the TSC1-TSC2 complex).[44] This prevents TSC1-TSC2 complex from hydrolyzing GTP on Rheb to GDP. Thus, Rheb-GTP accumulates in the cell, which activates mTORC1.[45] mTORC1 then phosphorylates downstream targets such as 4E-BP1 (4E-Binding Protein 1), resulting in translation of mRNA leading to cell survival. mTORC1 also phosphorylates IRS-1 (Insulin Receptor Substrate-1) resulting in its degradation. This acts as a negative feedback mechanism of AKT signaling pathway. [46]

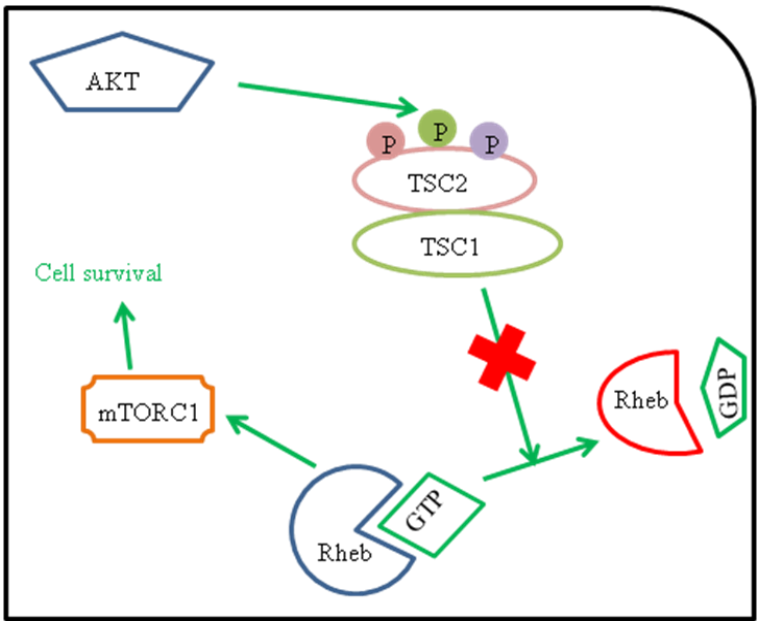

Figure 8. Regulation of mTORC1 by AKT

1.6 AKT signaling pathway and cancer

Alterations of AKT have been implicated in many types of cancers.

1.6.1 AKT gene over expression and amplification

Alteration of AKT gene expression was first identified in 1992 in human cancer.[47] Akt2 was found to be amplified and over expressed in ovarian carcinoma cell lines, 12% of primary ovarian carcinomas and 3% of breast carcinomas.[48] When Akt2 is over expressed, it could make the cells excessively responsive to normal levels of growth factors, leading to cell proliferation.[49] Akt2 has also been found to be over expressed and/or amplified in pancreatic cancer cell lines and 10-20% of primary pancreatic carcinomas.[50] The expression of AKT2 protein has been reported to be elevated in 40% of hepatocellular carcinomas.[51] It has been found to increase invasiveness and metastasis in human ovarian and breast cancer cells by up regulating integrins.[52] The amplification of Akt1 and Akt3 are not common in cancers.

1.6.2 AKT hyper activation

Activation of AKT has been reported in many types of human cancers (**Table 2**).[53,54] Correlation between AKT activation and disease advancement/poor prognosis has been reported. AKT1 kinase activity was found to be increased in 40% of breast and ovarian cancers, >50% of prostrate carcinomas.[55] AKT2 kinase activation was found in 30-40% of pancreatic cancers.[56]

1.6.3 AKT signaling pathway alterations

The activation of AKT signaling pathway can occur by a variety of mechanisms. Over expression of growth factor receptors (wild-type) hyper-sensitize the cells to normal levels of growth factors leading to AKT activation.[57] Constitutive activation of AKT could be caused by mutant receptors.[58] Mutations in PIK3R1 gene (which encodes PI3-kinase) have been detected in

a few colorectal and ovarian tumors.[59] Mutations and inactivation of PTEN (a negative regulator of AKT) have been reported in endometrial and prostrate cancers.[60]

Thus, AKT is an appealing target for cancer therapy.

Table 2. Activation of AKT in human cancers

Tumor type	% Tumors with active AKT
Glioma	~ 55
Thyroid carcinoma	80 - 100
Breast carcinoma	20 - 55
Small-lung cell carcinoma	~ 60
Non-small-cell lung carcinoma	30 - 75
Gastric carcinoma	~ 80
Gastrointestinal stromal tumors	~ 30
Pancreatic carcinoma	30 - 70
Bile duct carcinoma	~ 85
Ovarian carcinoma	40 - 70
Endometrial carcinoma	> 35
Prostrate carcinoma	45 - 55
Renal cell carcinoma	~ 40
Anaplastic large-cell lymphoma	~ 100
Acute myeloid leukemia	~ 70
Multiple myeloma	~ 90

CHAPTER 2

INHIBITORS OF AKT

Because of the sequence similarity among the isoforms of AKT, it has been a challenge to develop isoform-specific inhibitors. The sites on AKT enzyme against which inhibitors can be developed are: ATP binding site, phosphoinositide binding site on the PH domain, substrate binding site and allosteric site. Different types of inhibitors developed to date are discussed below.

2.1 ATP-Competitive inhibitors

ATP is essential for kinase activity. Preventing binding of ATP to AKT is one of the approaches to inhibit the enzyme. The ATP binding site is conserved among AKT, PKA and PKC. Many inhibitors of PKA, PKC and kinases in other families have been found to inhibit AKT and their structures have been optimized to improve selectivity towards AKT. For example, analogs of balanol (a non-selective kinase inhibitor) have been developed. (**Figure 9**) Compound **2-1** has an IC_{50} of 2 nM against PKA and 4 nM against AKT1 *in vitro*.[61] The potent PKA inhibitor **2-2** (**H-89**) (IC_{50} 0.035 µM against PKA, 2.5 µM against AKT1) has been optimized to give compound **2-3** (**NL-71-101**) which has an IC_{50} 9 µM against PKA and 3.7 µM against AKT1 *in vitro*.[62] During a high-throughput screening, Abbott researchers found the bispyridine compound **2-4** to be an AKT1 inhibitor (IC_{50} 5 µM).[63] Based on this scaffold, several 3,5-disubstituted pyridine analogs were developed (**Figure 10**). They were found to be ATP-competitive inhibitors both *in vitro* and *in vivo*. The most potent inhibitor in this series was compound **2-5** (K_i = 0.16 nM against AKT1).[64]

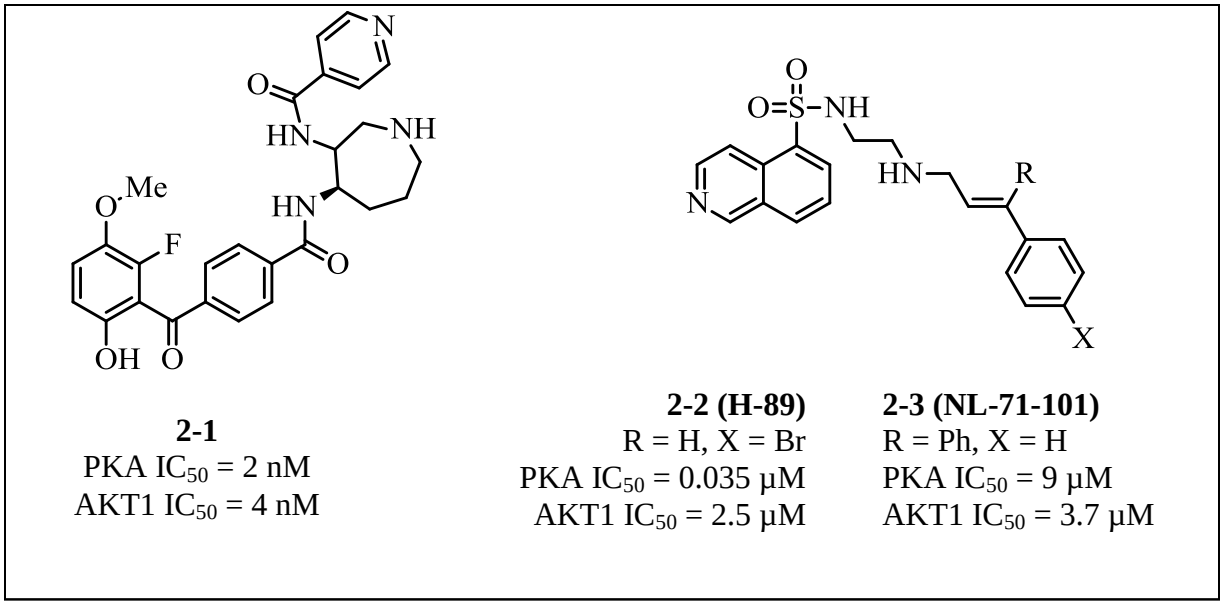

2-1
PKA IC_{50} = 2 nM
AKT1 IC_{50} = 4 nM

2-2 (H-89)
R = H, X = Br
PKA IC_{50} = 0.035 µM
AKT1 IC_{50} = 2.5 µM

2-3 (NL-71-101)
R = Ph, X = H
PKA IC_{50} = 9 µM
AKT1 IC_{50} = 3.7 µM

Figure 9. Early ATP-competitive inhibitors

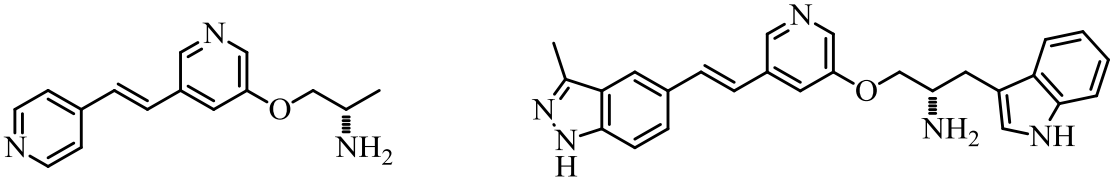

2-4
AKT1 IC_{50} = 5 µM

2-5
AKT1 K_i = 0.16 nM

Figure 10. 3,5-disubstituted pyridine analogs as ATP-competitive AKT inhibitors

In 2008, Glaxo Smith Kline reported lead optimization studies on two compounds (**2-6** and **2-7**) that were identified in a high-throughput screen as AKT inhibitors.[65] These studies resulted in the development of the compound **2-8** (**GSK690693**) which is an ATP-competitive, AKT kinase inhibitor (IC_{50} 2, 13 and 9 nM against AKT1, AKT2 and AKT3 respectively) (**Figure 11**). It was

co-crystallized with the kinase domain of AKT2 (148-481) and the X-ray co-crystal structure was reported. (**Figure 12**) Accordingly, this compound occupies the ATP-binding pocket. The interactions observed are the hydrogen bonds between N5 of oxadiazole ring and NH of Ala232 in the hinge region; NH of piperidine ring and Glu236 carboxylic acid group in the substrate binding region. A hydrogen bond network between hydroxyl group of the alkyne, Glu200 carboxylic acid group and NH of Phe294. This OH group might have displaced the water molecule in the enzyme. The intramolecular hydrogen bond between exocyclic NH of the oxadiazole ring and N3 of the imidazopyridine ring appears to keep both the rings coplanar.

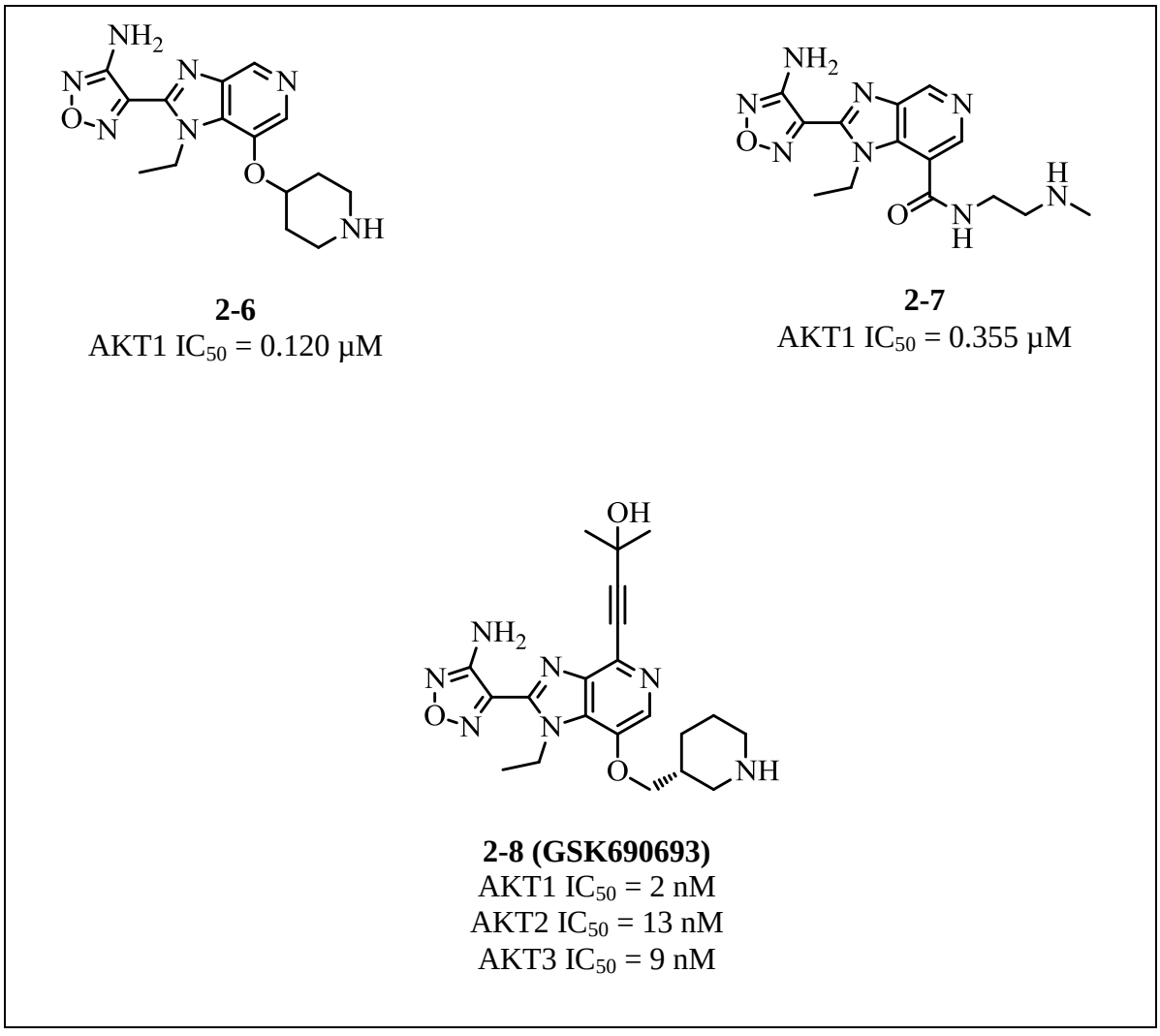

Figure 11. Oxadiazole containing AKT inhibitors

GSK690693 has been found to inhibit GSK3β phosphorylation *in vivo* and cause inhibition of the tumor xenograft (BT474 - breast carcinoma) growth in mice. It is currently in clinical trials to treat solid tumors and hematological malignancies in patients.

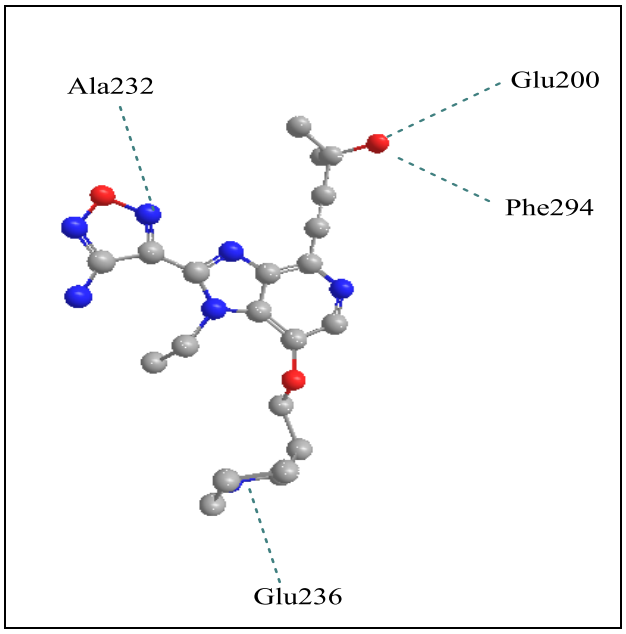

Figure 12. Model of GSK690693 showing interactions with AKT2 (148-481 residues)[65]

During a high-throughput screen, Pfizer identified a pyrrolopyrimidine compound **2-9** as an AKT1 inhibitor (IC_{50} 210 nM).[66] Analogs of this compound were synthesized (**Figure 13**) and the best analog **2-10** (IC_{50} 151 nM) was co-crystallized with the kinase domain of AKT1. In this structure, two nitrogens of the pyrrolopyrimidine ring are involved in hydrogen bonding interactions at the hinge region; two nitrogens of the triazole ring are involved in hydrogen bonding with two water molecules and π-stack with Phe161; and there is one intramolecular hydrogen bond between the NH of aniline and one nitrogen of the triazole (**Figure 14).** Thus, rigidity can be tolerated here. Based on this, imidazopiperidine analogs were synthesized. The compound **2-11** was the most potent one (IC_{50} 42 nM). **2-11** was co-crystallized with the kinase domain of AKT1 (**Figure 14).** The interactions in **2-11** are – two hydrogen bonds between the

nitrogens on the imidazole ring and glutamate 234 and aspartate 292 (in contrast to water molecules as in compound **2-10**) in the region where ribose of ATP binds. There is no π-stacking as the Phe 161 is pushed away. The pyrrolopyrimide ring shows similar interactions as that in **2-10**. Further analogs were prepared and the spiro compound **2-12** was found to be a very potent AKT1 inhibitor (IC_{50} 2.4 nM) and to inhibit tumors *in vivo*.

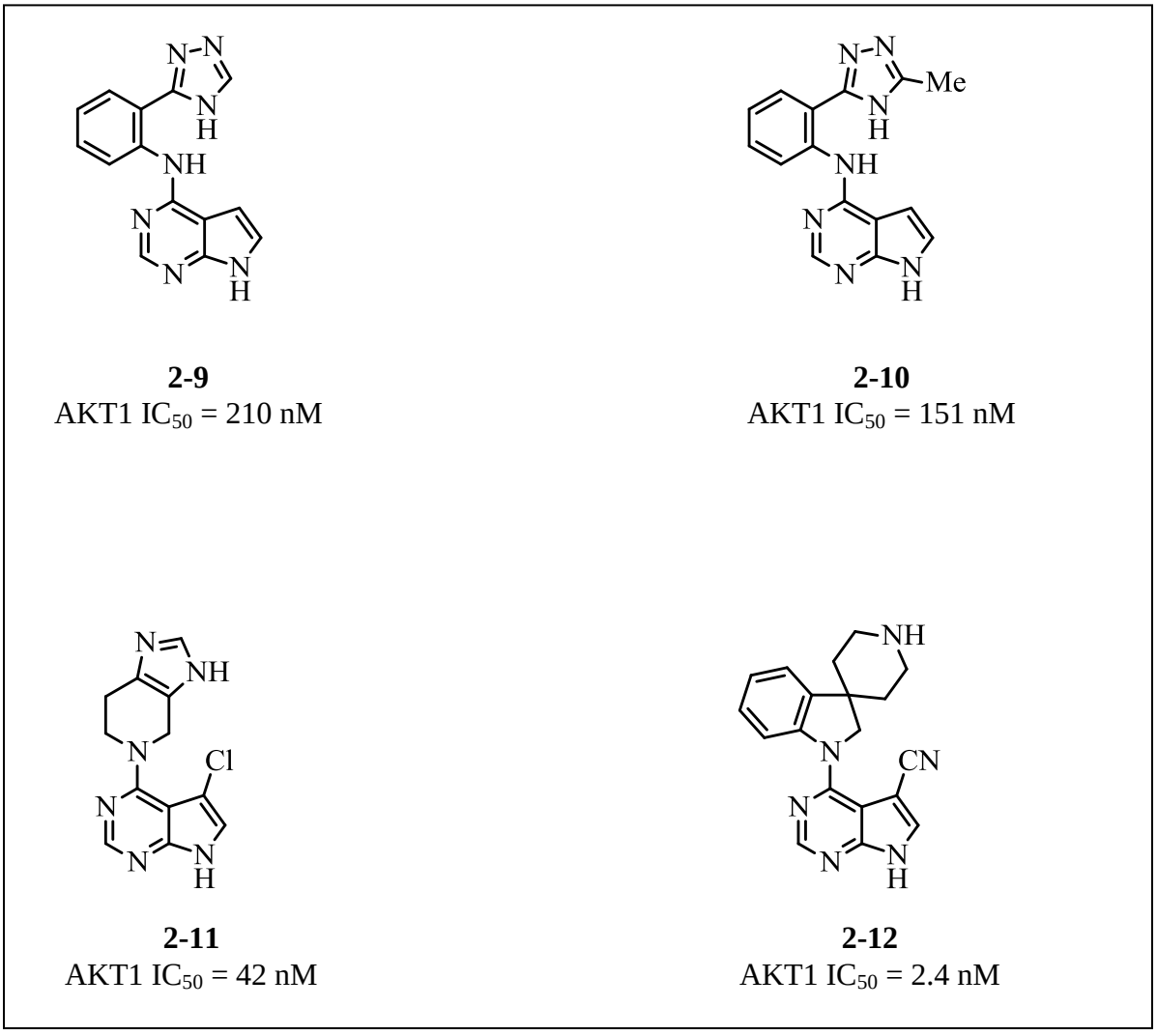

Figure 13. Pyrrolopyrimidine analogs as ATP-competitive AKT inhibitors

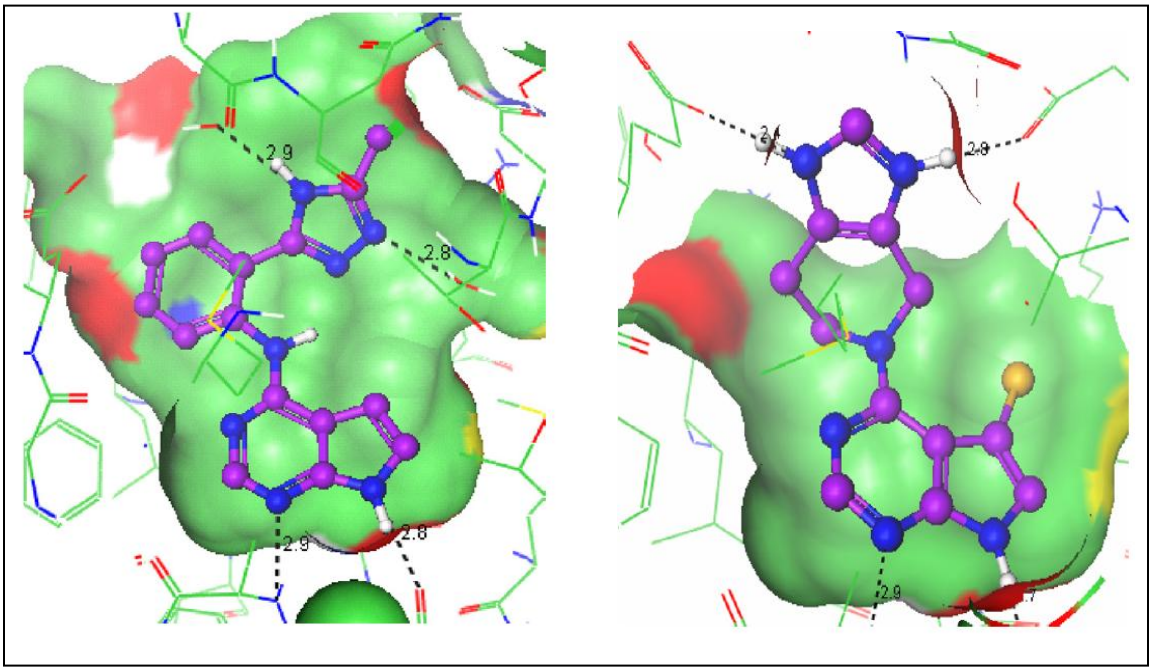

Figure 14. AKT1 kinase domain co-crystals with pyrrolopyrimidine inhibitors

"Reprinted from Lippa, B.; Pan, G.; Corbett, M.; Li, C.; Kauffmam, G. S.; Pandit, J.; Robinson, S.; Wei, L.; Kozina, E.; Marr, E. S.; Borzillo, G.; Knauth, E.; Barbacci-Tobin, E. G.; Vincent, P.; Troutman, M.; Baker, D.; Rajamohan, F.; Kakar, S.; Clark, T.; Morris, J. Synthesis and structure based optimization of novel Akt inhibitors. *Bioorg. Med. Chem. Lett.* **2008**, 18, 3359-3363, Copyright 2008, with permission from Elsevier."

2.2 Drugs that target PH domain

PI(3,4,5)P3 binds to AKT and subsequently facilitates translocation to the plasma membrane resulting in activation of AKT. Blockade of PIP3 binding would thus prevent the translocation and activation of AKT. A crystal structure of the PH domain of AKT bound to PI(3,4,5)P3 has been reported.[11]

It is found that D3 and D4 phosphate groups of the inositol interact with basic residues (lysine, arginine) in the phosphoinositide binding site on the PH domain. These ionic interactions are very essential for phosphoinositide binding to AKT (mutations of the basic residues to non-basic residues resulted in the decrease/abolition of phosphoinositide binding). The D5 phosphate is not much involved in binding to the PH domain as it faces the solvent and interacts with some water molecules.

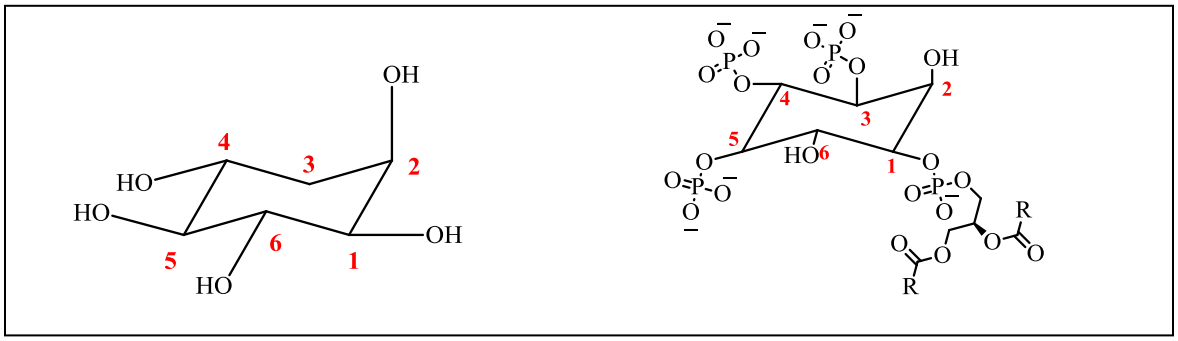

Figure 15. D-3-deoxy-myo-inositol and PI(3,4,5)P3

Several phosphoinositide analog inhibitors have been developed. This approach was based on the observation that D-3-deoxy-myo-inositols (**Figure 15**) inhibit the growth of transformed cells.[67] These inositols lack the hydroxyl group at the 3⁻position, so they cannot be phosphorylated by PI3K. Analogs of phosphatidyl-myo-inositol were made, such as compounds **2-13** (**DPI**) which has IC_{50} 35 µM in HT-29 cells[68] and **2-14** (**DPIEL**) that has IC_{50} 2.1 µM in HT-29 cells, which is more stable than **2-13** (**DPI**) inside cells as it is resistant to phospholipases.[69]

The crystal structure of IP(1,3,4,5)4 with the PH domain of AKT showed that the equatorial phosphates at 1,3,4 and the axial OH group at 2 position (oriented inside the binding pocket) of inositol ring are involved in hydrogen bonding at the phosphoinositide binding site. By the use of molecular modeling of PH domain of AKT, phosphatidylinositol ether lipid analog inhibitors have been developed.[70] Compound **2-15** (**PIA5**) was found to be very potent (IC_{50} 4.13 µM in

H1703 cells) (**Figure 16**). Based on docking studies, it has been hypothesized that the substituted hydroxyl group at position 2 is oriented outside the binding pocket. Hence, in order to maximize hydrogen bonding interactions at the other positions, the ring has to be rotated; this results in the reorientation of the lipophilic side chains. This could change the conformation of the PH domain subsequently leading to the inactivation of AKT. These analogs were found to inhibit the phosphorylation of only the targets downstream of AKT. Their ability to cause apoptosis was higher in cells that had a higher AKT activity compared to cells with low AKT activity. The major problem with these compounds is their poor pharmacokinetics because of their low solubility and a tendency to form aggregates. Replacement of the phosphate group by a carbonate group diminished their AKT inhibition activity. Dimers of the compounds were also found to be inactive. Nevertheless, this binding pocket is not a suitable target for drug development as it is shallow.[9]

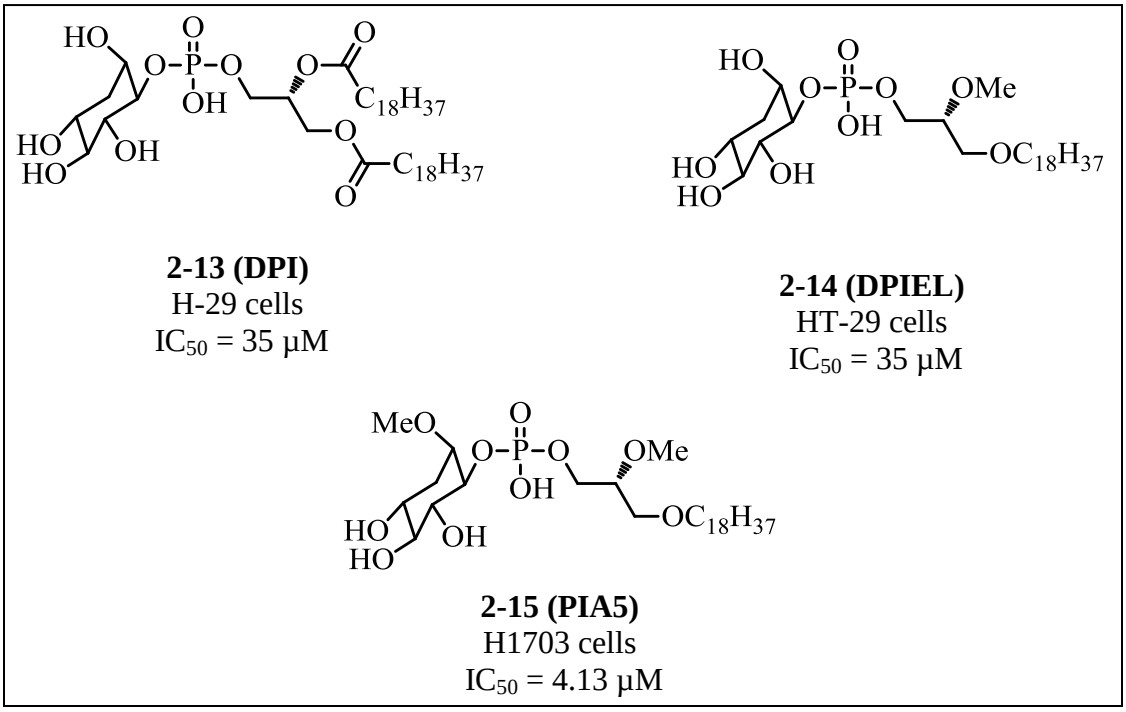

Figure 16. Phosphatidylinositol analog inhibitors of AKT

2.3 Inhibitors that bind at the substrate binding site

These inhibitors have a greater selectivity compared to the first two classes. They can be further classified as -

2.3.1 Pseudosubstrate peptidic inhibitors

A 14-mer peptide called AKTide-2T (**2-16**) which has the sequence ARKRERTYSFGHHA had been identified as an inhibitor of AKT (K_i 12 μM against mouse AKT1) which binds to the substrate-binding site by Obata et al in 2000.[71] Later, in 2004, Luo et al constructed a 20-mer peptide (**2-17**) which was a hybrid between **AKTide-2T** and 16-24 amino acids of FOXO3 (VELDPEFEP). Peptide **2-17** is more potent than **2-16** probably due to higher number of interactions with AKT. Several analogs were made (**Table 3**). When the serine at position 17 was changed to alanine (**2-18**), the inhibition increased most likely because this peptide binds to the substrate-binding site, but can neither be phosphorylated nor can detach from the site. The inhibition decreased when Ser17 was changed to Aspartate (**2-19**; most likely because the carboxy group of Asp occupies the site of phosphate of ATP). Peptides **2-20** and **2-21** had Alanine and Aspartate at position 15 respectively. Except peptide **2-17** (which inhibited SGK also), all other compounds were found to selectively inhibit AKT. It was found that a peptide must have at least 17 amino acids in order to inhibit AKT effectively (**Table 4**). These compounds inhibited GSK3 phosphorylation but not growth (the peptides might be not be stable over time) in HeLa cells. The peptides were found to be highly selective towards AKT (over other kinases).[72]

Table 3. Pseudosubstrate peptidic inhibitors of AKT1

Number	Peptide sequence	AKT1 K_i (μM)
2-16 (AKTide-2T)	ARKRERTYSFGHHA	12
2-17	VELDPEFEPRARERTYSFGH	1.11
2-18	VELDPEFEPRARERTYAFGH	0.11
2-19	VELDPEFEPRARERTYDFGH	10.6
2-20	VELDPEFEPRARERAYAFGH	0.095
2-21	VELDPEFEPRARERDYAFGH	>16

Table 4. Minimum number of amino acids required for peptide inhibitors

Number of amino acids	Peptide sequence	AKT1 K_i (μM)
8	Ac-ERTYAFGH	>100
11	Ac-RARERTYAFGH	15.86
14	FEPRARERTYAFGH	1.97
14	Ac-FEPRARERTYAFGH	1.44
17	Ac-DPEFEPRARERTYAFGH	0.26
20	VELDPEFEPRARERTYAFGH	0.18
20	Ac-VELDPEFEPRARERTYAFGH	0.098

2.3.2 Peptidic substrate-mimetic inhibitors

In 1996, Alessi et al had identified the minimum consensus sequence of a substrate to be phosphorylated by AKT as RXRYYS/TZ (X-any amino acid, Y-small residues except glycine, Z-bulky hydrophobic residue). While testing the phosphorylation of various peptide sequences by AKT1, they found two peptide sequences that had very low K_m values and high specificity for AKT1 compared to MAPKAP kinase-1 and p70 S6 kinase : RPRTSSF (K_m 5 μM) and GRPRTSSF (K_m 8 μM).

In 2002, the X-ray crystal structure of activated AKT in complex with GSK3β (10 residue sequence) and an ATP analog was published.[12] This showed that the sequence GRPRTTSFAE is bound to the substrate binding site via many interactions (**Figure 17**). This sequence is similar to the one reported by Alessi et al in 1996 (GRPRTSSF). In 2007, Hamilton & coworkers utilized the sequence GRPRTTSF (8 residues) to make about 35 analogs. It was found that the three residues (GRP) at N-terminal hydrophilic region were not necessary. They could be replaced by an acetyl group. The arginine at the 4th position was very essential. The Threonine residues at positions 5 and 6 were not necessary; they could be replaced by *p*-amino benzoic acid. The Serine at position 7 could be changed to a Valine. Phenylalanine at position 8 was necessary to make hydrophobic interactions. A hydrophobic ring could be added to the C-terminal phenylalanine in order to increase the binding interactions at the C-terminal region. Another hydrophobic group could be added to the N-terminus. These modifications led to the development of a potent AKT1 inhibitor **2-22** (IC_{50} 14 μM) (**Figure 17**). This shows that only 3 amino acid residues out of 8 are necessary to inhibit AKT and they can be linked by non-peptidic groups to improve the hydrophobicity of these compounds which is essential for cell permeability.[73]

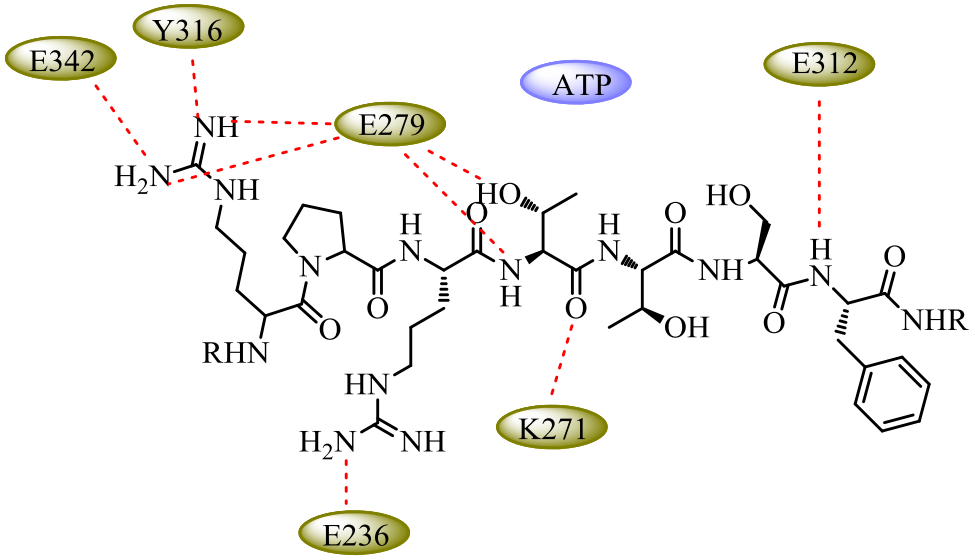

GSK3β (10 residue sequence) interacting with AKT1 residues

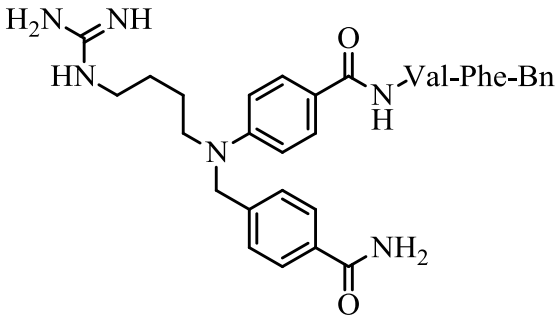

2-22

AKT1 IC_{50} = 14 μM

Figure 17. Peptide substrate-mimetic inhibitors

Non-peptide substrate-mimetic inhibitors: By using docking studies, improvements were made on the peptidic substrate-mimetics to give the first non-peptide substrate-mimetic inhibitors **2-23, 2-24** of AKT (**Figure 18**). These compounds are more hydrophobic and rigid compared to the peptidic compounds.[74]

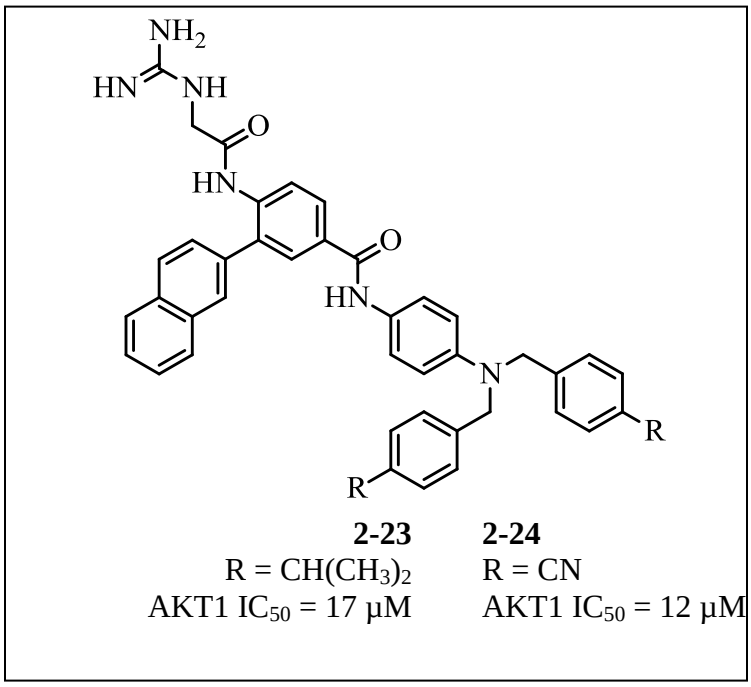

2-23 R = $CH(CH_3)_2$, AKT1 IC_{50} = 17 µM

2-24 R = CN, AKT1 IC_{50} = 12 µM

Figure 18. Non-peptide substrate-mimetic inhibitors

2.4 Allosteric inhibitors

These inhibitors not only specific for AKT over other kinases, but are also AKT isoenzyme specific. Barnett et al had identified compound **2-25** (IC_{50} 4.6 µM against AKT1 and >250 µM against AKT2, AKT3, SGK) as a selective AKT1 inhibitor (**Figure 19**). Based on the observation that **2-25** was active only against AKT1 containing a PH domain and showed non-competitive inhibition of AKT1 with respect to ATP and peptide substrate; a model for the allosteric inhibition of AKT was proposed.[75] According to this model (**Figure 20**), these types of inhibitors bind to a site which is formed only when PH domain is present. This site could be formed due to the conformational changes resulting from interaction of PH domain and kinase domain or it could be present at the interface of both the domains. When bound to this site, the

inhibitor locks up AKT in a "closed" conformation and does not allow it to interact with PDK1, thereby preventing its phosphorylation and subsequent activation.

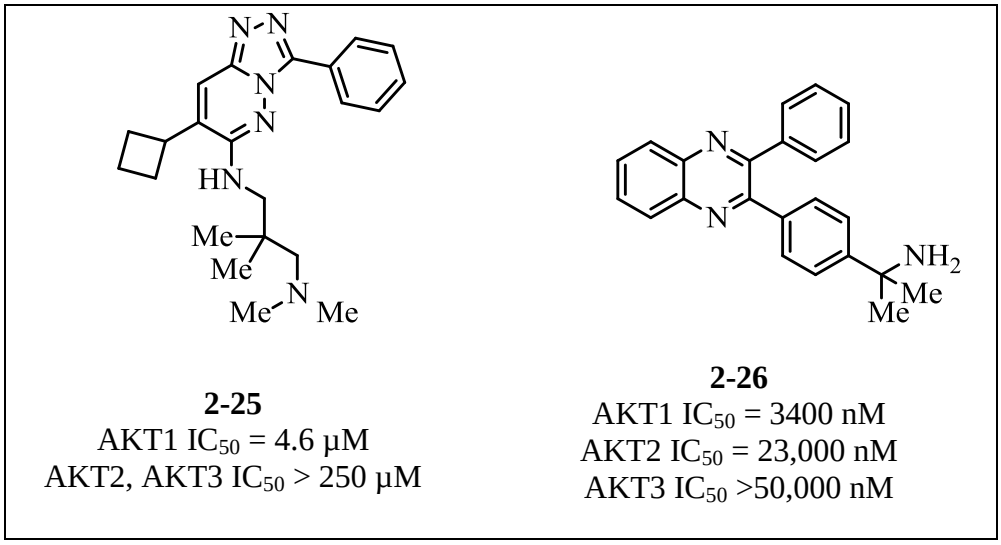

2-25
AKT1 IC_{50} = 4.6 µM
AKT2, AKT3 IC_{50} > 250 µM

2-26
AKT1 IC_{50} = 3400 nM
AKT2 IC_{50} = 23,000 nM
AKT3 IC_{50} >50,000 nM

Figure 19. Early isoform-specific allosteric AKT inhibitors

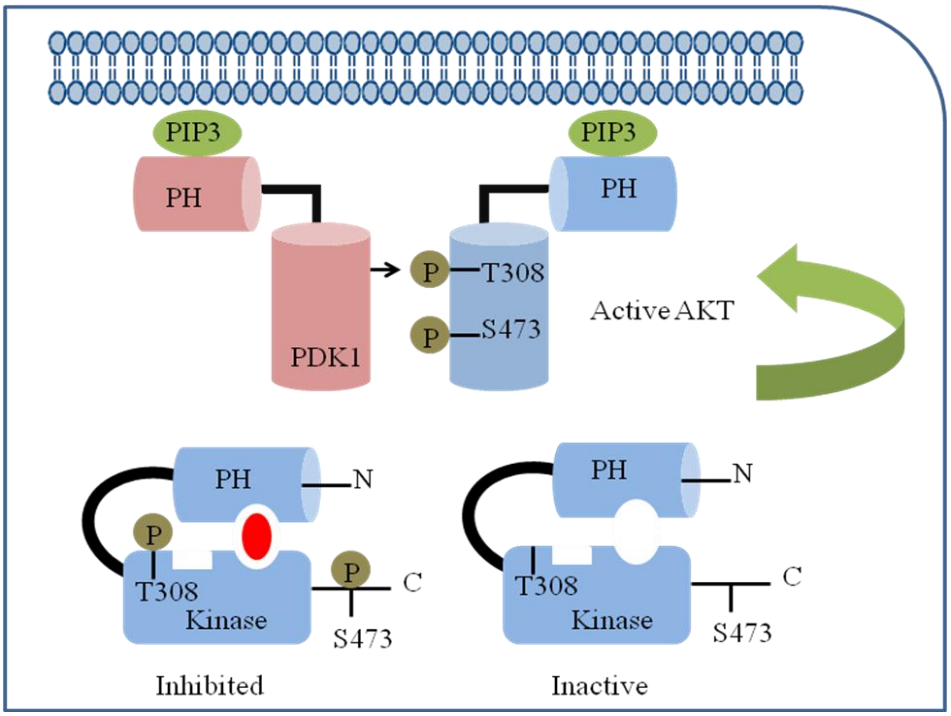

Figure 20.[76] Model for the allosteric inhibition of AKT

In 2005, Merck reported a series of isoenzyme-specific allosteric AKT inhibitors which were PH domain dependent.[77] During a high-throughput screen targeted at identifying AKT inhibitors, they identified the compound **2-26** (**Figure 19**) to be specific to AKT over other kinases and also specific to AKT1 (IC_{50} s 3400 nM; 23,000 nM and >50,000 nM against AKT1; AKT2 and AKT3 respectively). This compound was inactive in Akt mutants lacking the PH domain. Several analogs of **2-26** were made wherein the 2,3-diphenylquinoxaline scaffold was retained while changing the amino group. This resulted in a compound **2-27** (IC_{50} 290 nM against AKT1, 2090 nM against AKT2 and >50,000 nM against AKT3 & other kinases) which was more potent than **2-26**. But, this compound had poor solubility and no cellular activity.

Further analoging was done retaining the piperidinyl benzimidazolone scaffold (**Figure 21**). This resulted in AKT1 specific inhibitor **2-28** (IC_{50} s 760 nM; 24,000 nM and >50,000 nM against AKT1; AKT2 and AKT3 respectively) and AKT2 specific inhibitor **2-29** (IC_{50} s >20,000 nM; 325 nM and >20,000 nM against AKT1; AKT2 and AKT3 respectively). It was observed that in order to achieve maximum apoptotic response, both AKT1 and AKT2 had to be inhibited (caspase-3 assay was performed on human ovarian carcinoma cells A2780 using 1:1 mixture of **2-28** and **2-29**). This led to the development of dual AKT1/AKT2 inhibitor **2-30** (IC_{50} s 58 nM; 210 nM and 2,119 nM against AKT1; AKT2 and AKT3 respectively) which was potent and moderately cell-permeable. In cell-based assay, the IC_{50} values of **2-30** were 305 nM; 2086 nM and >25,000 nM against AKT1; AKT2 and AKT3 respectively. *In vivo* studies were done in mice using **2-30**, it was found to inhibit AKT1 and AKT2 but not AKT3 phosphorylation in lungs. The position of the allosteric binding site is not yet known. Merck has not published a crystal structure yet.

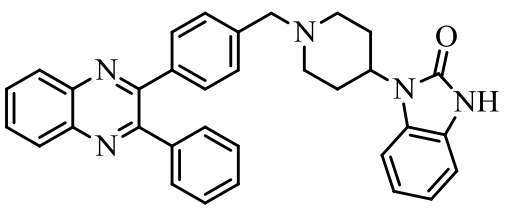

2-27
AKT1 IC_{50} = 290 nM
AKT2 IC_{50} = 2090 nM
AKT3 IC_{50} >50,000 nM

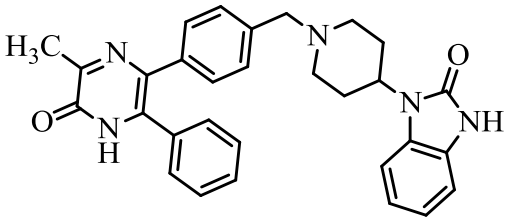

2-28
AKT1 IC_{50} = 760 nM
AKT2 IC_{50} = 24,000 nM
AKT3 IC_{50} >50,000 nM

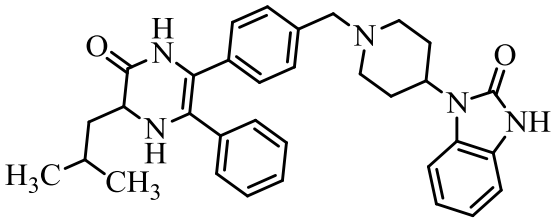

2-29
AKT1 IC_{50} > 20,000 nM
AKT2 IC_{50} = 325 nM
AKT3 IC_{50} > 20,000 nM

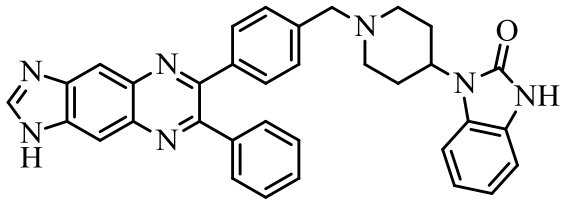

2-30

Biochemical
AKT1 IC_{50} = 58 nM
AKT2 IC_{50} = 210 nM
AKT3 IC_{50} > 2119 nM

Cellular
AKT1 IC_{50} = 305 nM
AKT2 IC_{50} = 2086 nM
AKT3 IC_{50} > 25,000 nM

Figure 21. Piperidinyl benzimidazolone analogs as allosteric AKT inhibitors

Using Microwave Assisted Organic Synthesis (MAOS), Diversity-Oriented Synthesis (DOS) was carried out to make compounds having the canthine alkaloid scaffold (**Figure 22**).[78] This resulted in the development of two unnatural canthine alkaloids **2-31** (IC_{50} s 1.3 µM; 1.6 µM and >50 µM against AKT1; AKT2 and AKT3 respectively) and **2-32** (IC_{50} s 1.5 µM; 2.3 µM and >50 µM) against AKT1; AKT2 and AKT3 respectively). These compounds were found to be dual AKT1/AKT2 selective allosteric inhibitors (**Figure 23**). They were active only against AKT having a PH domain and showed non-competitive inhibition towards AKT with respect to ATP.

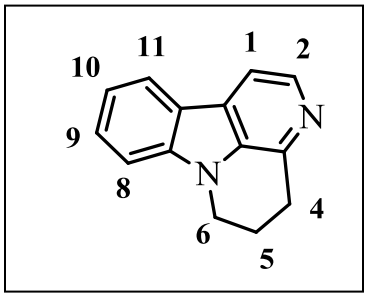

Figure 22. Canthine alkaloid scaffold

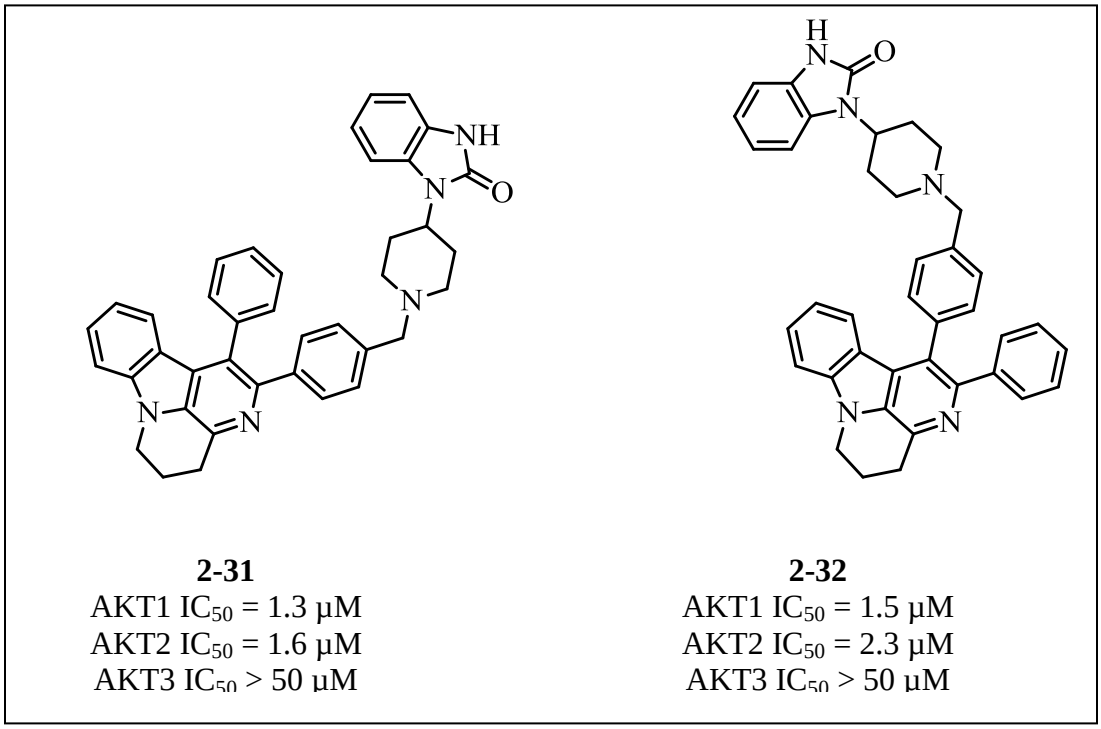

2-31
AKT1 IC_{50} = 1.3 µM
AKT2 IC_{50} = 1.6 µM
AKT3 IC_{50} > 50 µM

2-32
AKT1 IC_{50} = 1.5 µM
AKT2 IC_{50} = 2.3 µM
AKT3 IC_{50} > 50 µM

Figure 23. Unnatural canthine alkaloids

In order to improve the aqueous solubility and cell permeability, further analoging was done on **2-30**. This gave rise to compound **2-33** [IC_{50} s 138 nM; 212 nM; 7,200 nM (biochemical assay) and 253 nM; 276 nM; >10,000 nM (cellular assay) against AKT1; AKT2; AKT3 respectively] which was a potent allosteric inhibitor (**Figure 24**), inhibited phosphorylation *in vivo* (mice), but caused some behavioral effects.[79]

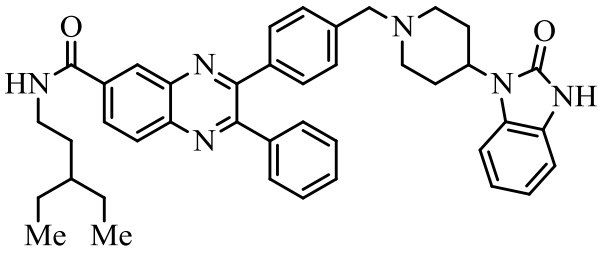

2-33

Biochemical	**Cellular**
AKT1 IC_{50} = 138 nM	AKT1 IC_{50} = 253nM
AKT2 IC_{50} = 212 nM	AKT2 IC_{50} = 276 nM
AKT3 IC_{50} = 7200 nM	AKT3 IC_{50} > 10,000 nM

Figure 24. Allosteric AKT inhibitor **2-33**

Attempts to improve both pharmacokinetics and tolerability *in vivo* resulted in the synthesis of several naphthyridines and naphthyridonones (**Figure 25**).[80]

Naphthyridine **2-34** had IC_{50} s of 44 nM; 280 nM (biochemical assay) and 149 nM; 995 nM (cellular assay) against AKT1 and AKT2 respectively. The naphthyridonone **2-35** had almost comparable activity both in biochemical and cellular assays [IC_{50} s 3.5 nM; 42 nM (biochemical assay) and 16 nM; 266 nM (cellular assay) against AKT1; AKT2 respectively]. *In vivo* studies were performed on mice using **2-35**. It was well tolerated. In tumor xenograft study (A2780), it

showed 95% and 54% inhibition against AKT1 and AKT2 respectively. A class of pyridopyrimidines were developed such as **2-36** [IC_{50} s 6 nM; 94 nM (biochemical assay) and 20.3 nM; 899 nM (cellular assay) against AKT1; AKT2 respectively].[81]

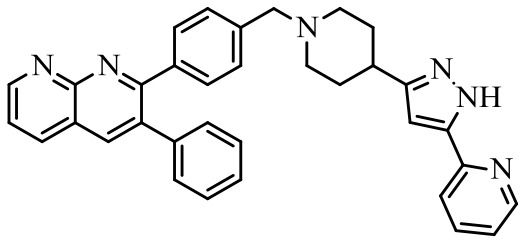

2-34

Biochemical	**Cellular**
AKT1 IC_{50} = 44 nM	AKT1 IC_{50} = 149 nM
AKT2 IC_{50} = 280 nM	AKT2 IC_{50} = 995 nM

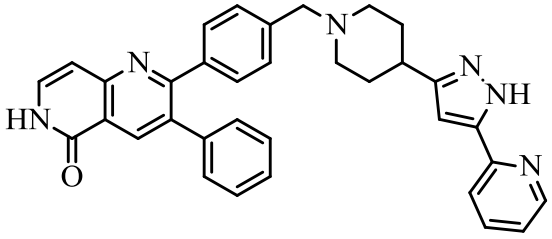

2-35

Biochemical	**Cellular**
AKT1 IC_{50} = 3.5 nM	AKT1 IC_{50} = 16 nM
AKT2 IC_{50} = 42 nM	AKT2 IC_{50} = 266 nM

Figure 25. Naphthyridine and naphthyridonones analogs

The major problem with some of the compounds discussed above is the off-target binding to a potassium channel I_{kr} hERG (human Ether-a-go-go-Related Gene), which produces cardiac

toxicity. In order to reduce this toxicity while maintaining potency towards AKT1 and AKT2, different analogs were made. As shown below, many heteroatoms were added to the ring

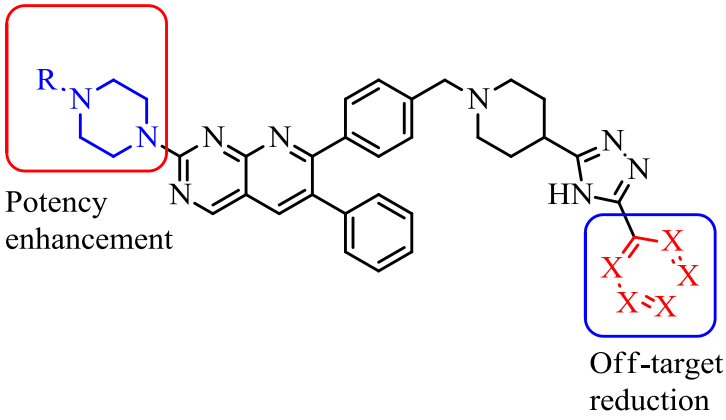

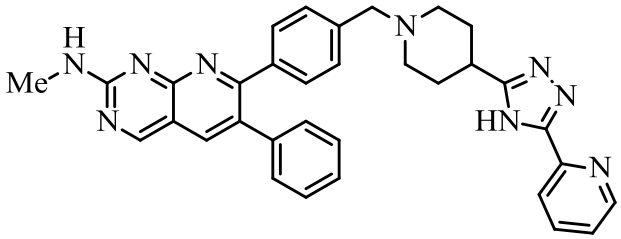

2-36

Biochemical	**Cellular**
AKT1 IC_{50} = 6 nM	AKT1 IC_{50} = 20.3 nM
AKT2 IC_{50} = 94 nM	AKT2 IC_{50} = 899 nM

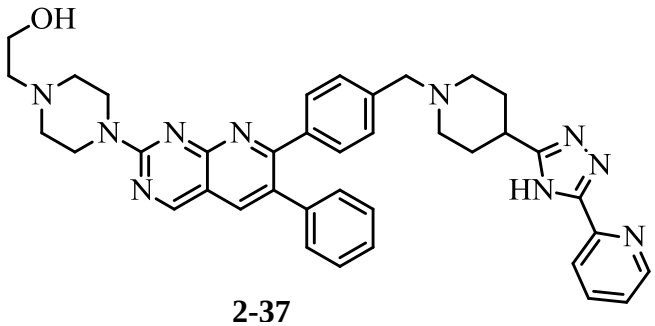

2-37

Biochemical

AKT1 IC_{50} = 13 nM

AKT2 IC_{50} = 48 nM

hERG IC_{50} > 10,000 nM

Figure 26. Pyridopyrimidine analogs

attached to the triazole (this reduced the lipophilicity and probably the π-interactions at hERG binding site reducing the off-target issues) and substituents which increased the hydrophilicity at the piperazine ring were used (to improve potency). This resulted in compound **2-37** [IC_{50} s 13 nM; 48 nM and >10,000 nM (biochemical assay) AKT1; AKT2 and hERG respectively] (**Figure 26**).[82]

Recently, compounds containing [1,2,4]triazolo[3,4-f][1,6]naphthyridines have been reported.[83] Compound **2-38** [IC_{50} s 4 nM, 10 nM (biochemical assay); 5 nM, 41 nM (cellular assay) against AKT1, AKT2 respectively] had good potency and no appreciable hERG binding (**Figure 27**). *In vivo* studies were done in mice. At 1.8 µM blood concentration, it was found to inhibit AKT1 phosphorylation by 92% and AKT2 phosphorylation by 41% in mouse lung and was well tolerated.

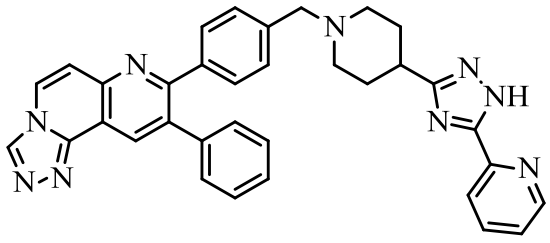

2-38

Biochemical	**Cellular**
AKT1 IC_{50} = 4 nM	AKT1 IC_{50} = 5 nM
AKT2 IC_{50} = 10 nM	AKT2 IC_{50} = 41 nM

Figure 27. [1,2,4]triazolo[3,4-f][1,6]naphthyridine analog

Clinical trials

Merck's compound MK-2206 (**2-39**) is a potent, allosteric, oral AKT inhibitor (**Figure 28**). The first clinical trials were done on 33 patients with advanced solid tumors (April 2008 - November 2009). It was well tolerated, caused minor adverse effects such as rash and was found to cause tumor shrinkage.[84]

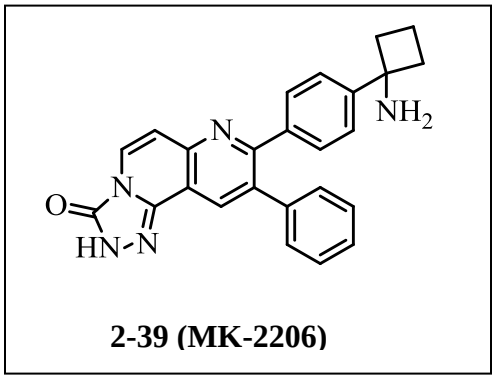

2-39 (MK-2206)

Figure 28. Oral AKT inhibitor **MK-2206**

CHAPTER 3

PYRANONAPHTHOQUINONE LACTONES AS AKT INHIBITORS

3.1 Discovery of PNQ lactones as AKT Inhibitors

In 2007, during a high-throughput screen to identify inhibitors of activated AKT1, Toral-Barza *et al* discovered the pyranonaphthoquinone lactones lactoquinomycin (IC_{50} 0.149 μM against commercially prepared AKT1) (**3-1**) and frenolicin B (IC_{50} 0.313 μM against commercially prepared AKT1) (**3-2**) to be potent and selective inhibitors of AKT (**Figure 29**).[85] Lactoquinomycin was not found to inhibit PKA (IC_{50} >200 μM). It weakly inhibited PKCα (~16% inhibition at 1 μM), HER2 (IC_{50} 2.42 μM), IKKβ (IC_{50} 3.9 μM) and did not inhibit closely related tyrosine and serine/threonine kinases (**Figure 30**). It was also tested against 45 different kinases at 1μM concentration (Invitrogen SelectScreen profiling), and was found to inhibit only AKT1 (92%) and AKT2 (99%) (**Table 5**).

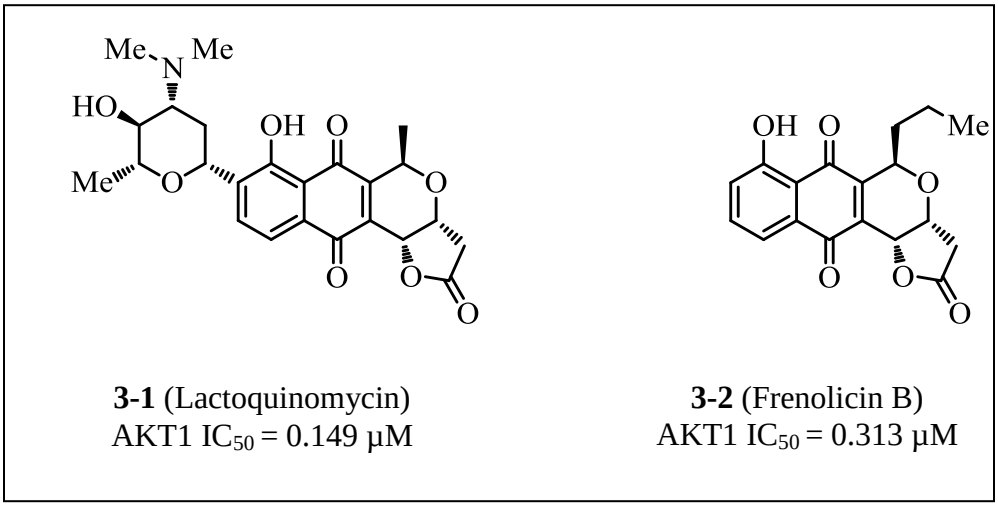

3-1 (Lactoquinomycin)
AKT1 IC_{50} = 0.149 μM

3-2 (Frenolicin B)
AKT1 IC_{50} = 0.313 μM

Figure 29. PNQ lactones – lactoquinomycin and frenolicin B

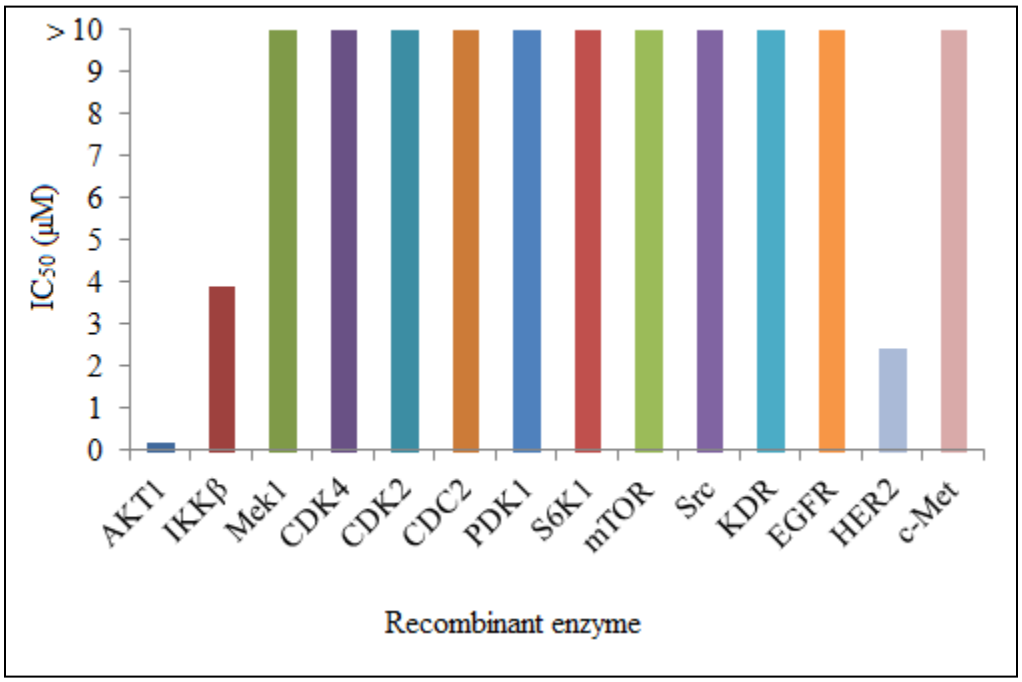

Figure 30. Lactoquinomycin IC_{50} values against 14 different kinases

3.2 Mechanism of inhibition

The inhibition of AKT1 by PNQ lactones was found to be non-competitive with respect to ATP. It did not require the presence of PH domain (as opposed to the other allosteric AKT inhibitors). The mechanism is thought to be an irreversible interaction between cysteines 296 and/or 310 present in the activation loop (T-loop) of AKT1 and the inhibitor.[85] The conformation of the T-loop region of the AKT family might be distinct from other AGC family members. Once lactoquinomycin binds to the T-loop cysteines, it could either directly inhibit the binding of substrate to AKT or cause a conformational change which inactivates AKT.

Table 5. Lactoquinomycin inhibition values against 45 kinases

Kinase tested	% Inhibition (1 µM)	Kinase tested	% Inhibition (1 µM)
ABL1	0	MAP2K1	0
AKT1	92	MAP4K5	34
AKT2	99	MAPK1	6
BTK	1	MAPK14	49
CDK1	2	MAPK3	7
CDK2	0	MET	14
CHEK1	10	NEK2	0
CSF1R	6	NTRK1	14
CSK	0	PDGFRA	15
EGFR	26	PDGFRB	32
EPHA1	8	PDK1	0
ERBB4 (HER4)	5	PLK1	0
FGFR1	38	PRKACA	0
FLT1 (VEGFR1)	29	PRKCA	16
FLT3	4	PRKCQ	22
FYN	17	PTK2	12
IGF1R	2	ROCK1	1
IKBKB	41	RPS6KB1	16
INSR	1	SGK	20
KDR	21	SRC	0
LCK	0	STK6	17
LYN A	3	SYK	2
		YES1	14

They have proposed the mechanism of action to be a bioreductive alkylation of the enzyme (**Figure 31**). AKT2 has four cysteine residues – C226, C297, C311 and C345. C226 and C345 are thought to be inaccessible while C297 and C311 are accessible and can covalently interact with the PNQ lactones. According to the above proposed mechanism, the quinone gets reduced *in vivo* and forms a quinone methide. This reacts with nucleophilic groups (like thiols) on the proteins. This mechanism is supported by the observation that C311 (in phosphorylated AKT2)

and both C297 and C311 (in unphosphorylated AKT2) formed a monoadduct with compound **3-4** (**Figure 32**). No disulfide formation was observed between C297 and C311. Hence, PNQ lactones are the first known inhibitors which act via a novel bioreductive alkylation mechanism of the T-loop cysteines in AKT.

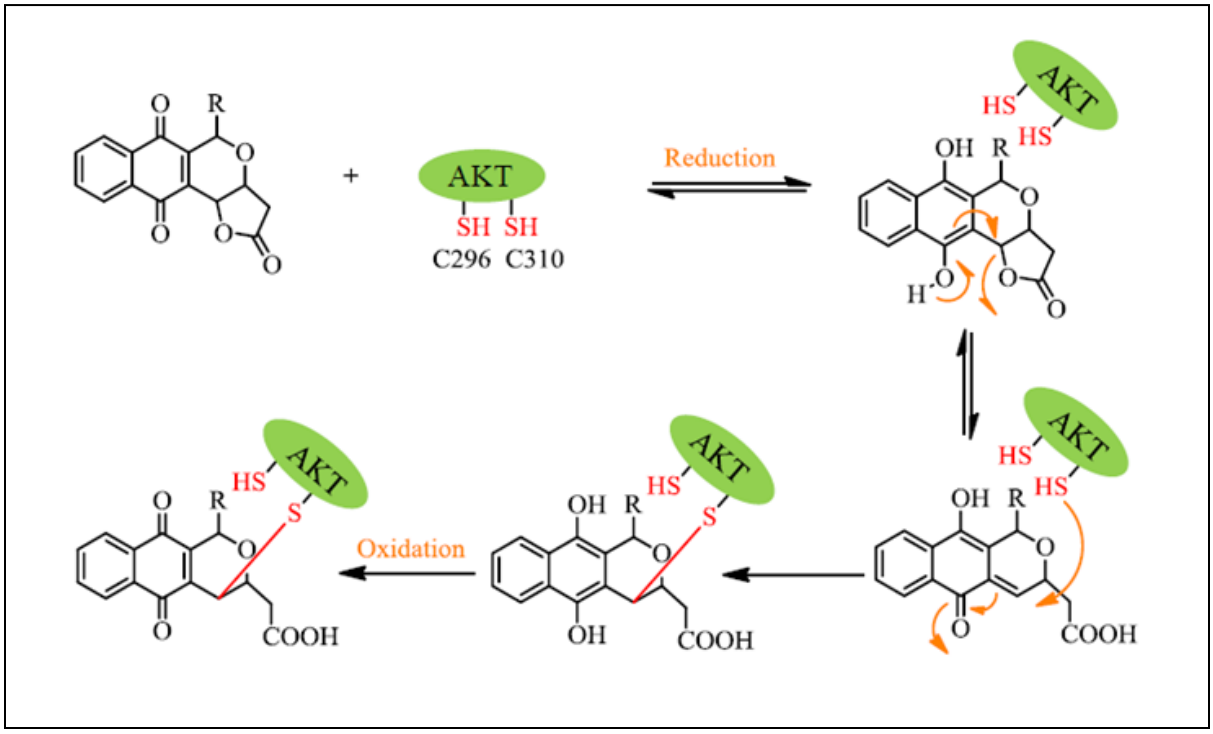

Figure 31. Proposed mechanism for the bioreductive alkylation by PNQ lactones[86]

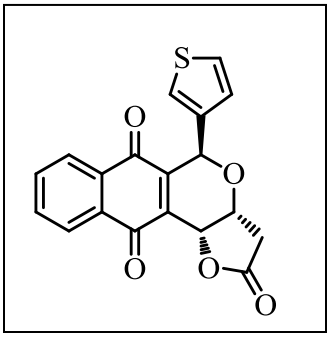

Figure 32. Thienyl compound **3-4**

3.2.1 *In vitro* experiments

To confirm the mechanism of action, mutants of C296 and C310 were prepared. In the single T-loop cysteine mutants of AKT1, C296A (IC_{50} 30.4 µM) and C310A (IC_{50} 38.5 µM), the inhibition by lactoquinomycin was reduced to a great extent and was completely lost in the double mutant C296A/C310A (IC_{50} > 40 µM) compared to wild-type AKT1 (IC_{50} 0.36 µM) obtained by expression in HEK293 cells. Whereas, Staurosporine (an ATP-competitive inhibitor) inhibited the three mutants and the wild-type AKT1 equally. This proved that the PNQ lactones did not bind to the ATP-binding site, but bind to the T-loop cysteines.

3.2.2 Effect on the downstream targets of AKT in tumor cells

Lactoquinomycin inhibited the phosphorylation of GSK3 in PTEN-negative U87MG cells (PTEN is a negative regulator of AKT). It also inhibited the phosphorylation of FKHRL1 induced by IGF-1 in Rat1 cells. It was observed that the phosphorylation of AKT at S473 and T308 was minimally affected by lactoquinomycin (suggesting that upstream kinases PDK1 and mTORC2 were not inhibited). In DU-AKT cells, lactoquinomycin inhibited the phosphorylation of S6K and 4EBP1 (substrates of mTORC1), suggesting that it inhibited mTORC1.

In 2009, Salaski *et al* determined the Structure-Activity Relationship (SAR) of the pyranonaphthoquinone lactones required to inhibit AKT:[86] the structure **3-3** (**Figure 33**) is the minimum scaffold required; amino sugar at position 8 and hydroxyl group at position 7 are not required; closed lactone ring is more potent compared to lactone formed *in situ*; bulky groups are tolerated at position 5; disubstitution at position 5 decreases the potency and the absolute configuration of the PNQ lactone has no effect on its inhibitory activity (**Table 6**).

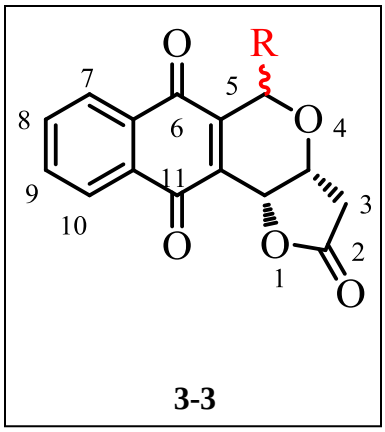

3-3

Figure 33. PNQ lactone scaffold

Table 6. SAR of PNQ lactones

R	Stereochemistry	AKT IC_{50} (μM)
H	(+)	0.044
2-thienyl	(+)-*anti*	0.057
CH_2OBn	(±)-*anti*	0.072
4-hydroxyphenyl	(±)-*syn*	0.08
3-thienyl	(-)-*anti*	0.099
3-thienyl	(+)-*anti*	0.122
methyl	(+)-*anti*	0.15
n-propyl	(±)-*anti*	0.163
$(CH_2)_4$	(±)	0.295
3-hydroxyphenyl	(±)-*syn*	0.35
n-propyl	(±)-*syn*	0.383
4-aminophenyl	(±)-*syn*	0.85
gem-dimethyl	(±)	1.44

CHAPTER 4

SYNTHESIS AND EVALUATION OF 7-DEOXYKALAFUNGIN AND ITS DECONSTRUCTION ANALOGS

4.1 Rationale

Wyeth researchers had reported the SAR of PNQ lactones necessary for inhibiting AKT in 2009.[86] We sought to further investigate the SAR in order to determine what structural features are required for AKT1 inhibition and what structural features are required for selectivity over the closely related kinase PKA. To achieve this, the synthesis of 7-deoxykalafungin and its deconstruction analogs was carried out.

4.2 Literature review

Several schemes for the syntheses of PNQ lactones have been reported to date, a few of which are highlighted below.

4.2.1 Enantiospecific total syntheses

In 1985, the first enatiospecific total syntheses of kalafungin and its enantiomers nanaomycin D was reported by Tatsuka *et al*.[87] Starting from L-rhamnose, compound **4-3** was synthesized in five steps. This was then condensed (Hauser annulation reaction) with compound **4-4** to give the pyranonaphthoquinone **4-5**. This was converted to the common "optically active intermediate" **4-8** in three steps (**Figure 34**).

Using “enantiodivergent” strategy, **4-8** was converted to **4-9** and **4-10** in a Wittig reaction using ethoxycarbonylmethylenetriphenylph-osphorane. **4-9** and **4-10** were converted to kalafungin (**4-11**) and nanaomycin D (**4-12**) respectively (**Figure 35**).

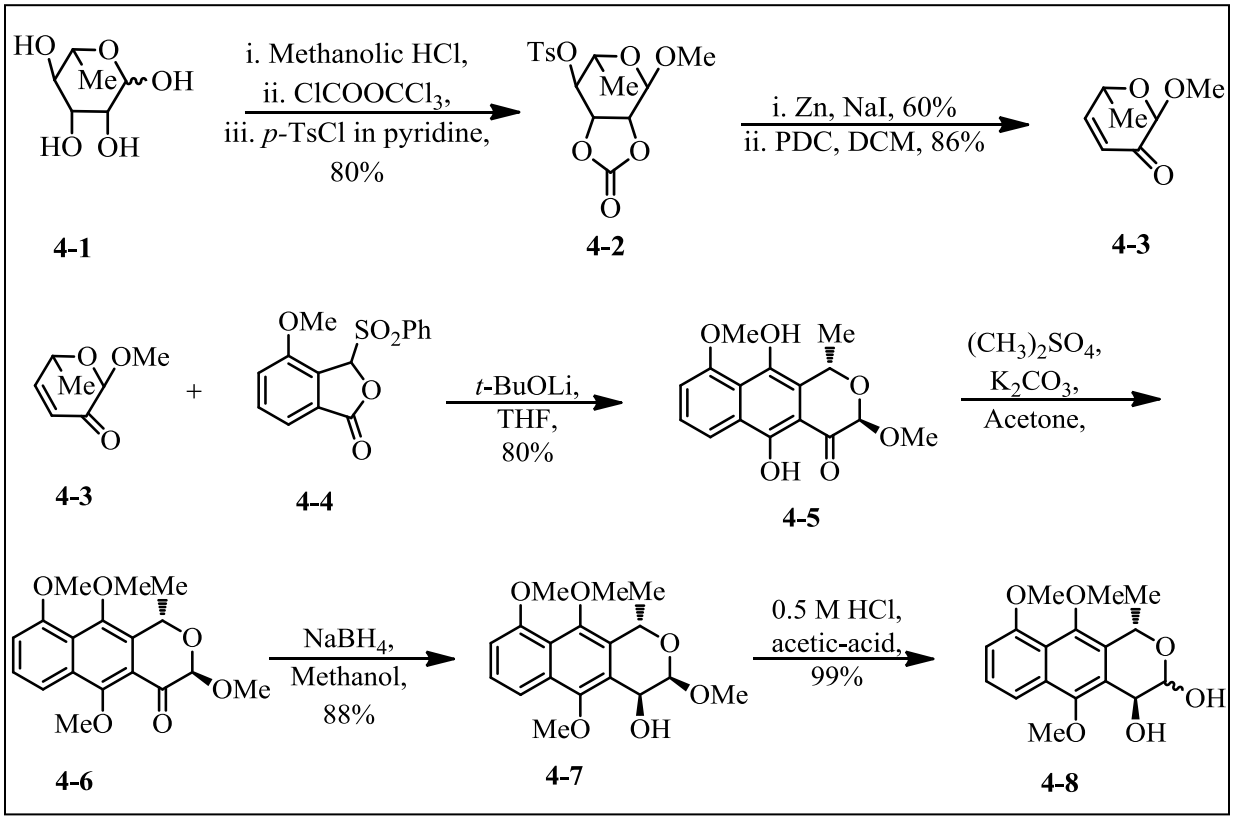

Figure 34. Synthesis of optically active intermediate **4-8**

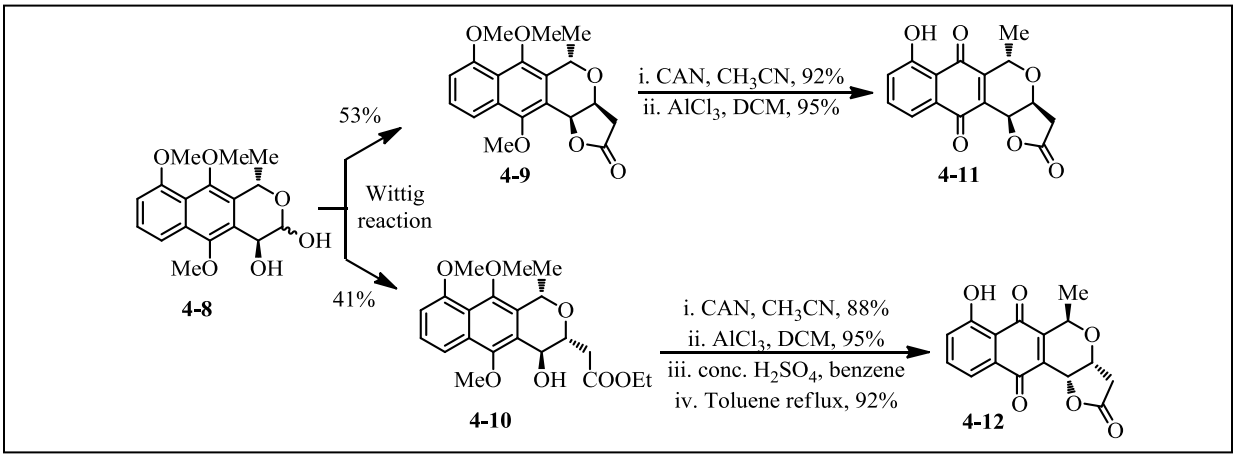

Figure 35. The first enantiodivergent total syntheses of kalafungin (**4-11**), nanaomycin D (**4-12**)

4.2.2 Regioselective Diels-Alder reactions

In 1995, Kraus *et al* reported the total syntheses of frenolicin B (**4-17**) and racemic kalafungin using regioselective Diels-Alder reactions (**Figure 36**).[88] Metalation on **4-13** followed by reaction with acrolein afforded **4-14**. Palladium catalyzed reaction in the presence of carbon monoxide yielded the tricyclic compound **4-15** which on treatment with silver oxide gave **4-16**. Regioselective Diels-Alder reaction on **4-16** followed by Jones oxidation afforded frenolicin B (**4-17**).

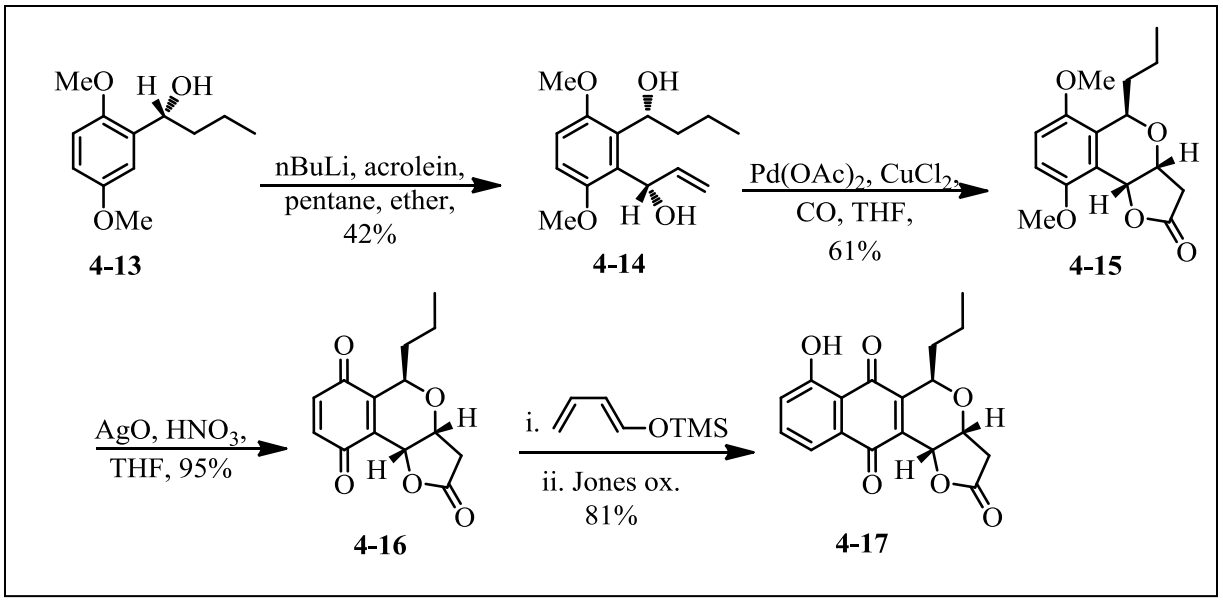

Figure 36. Total synthesis of frenolicin B (**4-17**) by regioselective Diels-Alder reaction

4.2.3 Furofuran annulation/Oxidative rearrangement

In 2000, Brimble reported the syntheses of kalafungin and other PNQ lactones using furofuran annulation/oxidative rearrangement strategy (**Figure 37**).[89] Starting from commercially available 1,5-dihydroxynaphthalene, **4-25** was synthesized in 6 steps. This underwent furofuran annulation with **4-26** to form the tetracyclic compound **4-27**. **4-27** underwent oxidative rearrangement in the

presence of CAN to give **4-28**. The *cis*-ether was reduced to give **4-29**, which was deprotected and epimerized to form kalafungin (**4-11**).

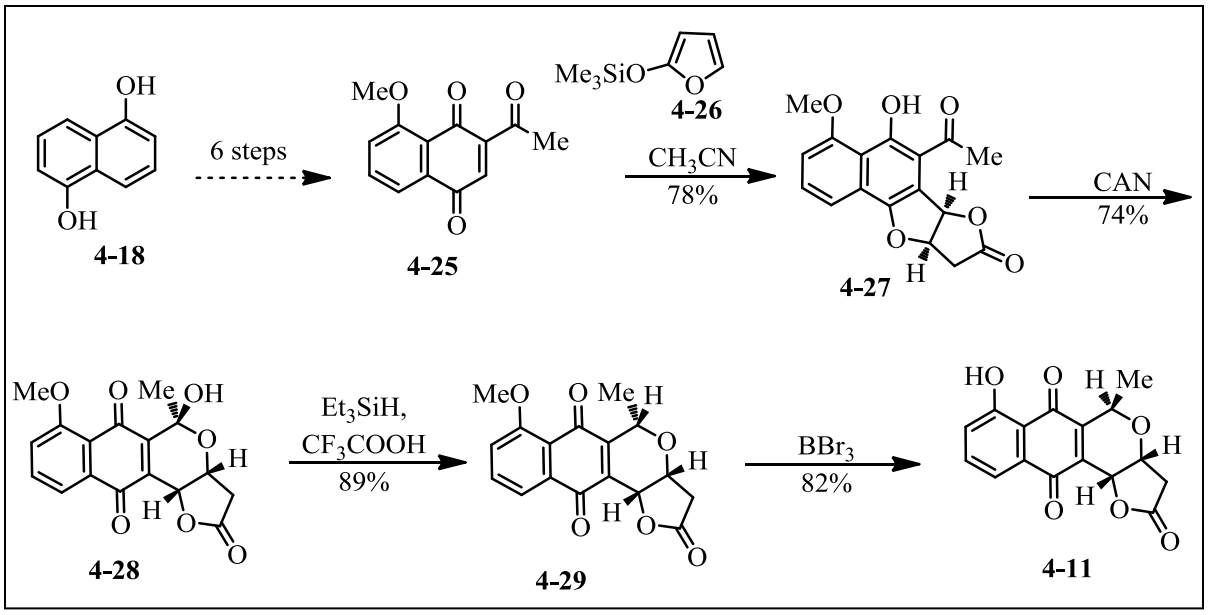

Figure 37. Synthesis of kalafungin (**4-11**) using furofuran annulation/oxidative rearrangement

4.2.4 Asymmetric Dihydroxylation, Oxa-Pictet Spengler cyclization in the synthesis of Kalafungin and Nanaomycin

In 2005, Fernandes and Bruckner reported the synthesis of kalafungin and its enantiomer nanaomycin by Asymmetric Dihydroxylation and Oxa-Pictet Spengler cyclization reactions as the key steps (**Figure 38**).[90] Starting from 1,5-dihydroxynaphthalene (**4-18**), the compound **4-30** was synthesized in five steps. **4-30** was converted to **4-31** utilising Palladium-catalyzed reaction. Sharpless Asymmetric Dihydroxylation (SAD) was carried out on **4-31** using $(DHQD)_2PHAL$ as the ligand to give **4-32**. This underwent Oxa-Pictet Spengler cyclization to form the pyranonaphthoquinone lactone **4-33**. Upon CAN oxidation, methoxy deprotection and epimerization, kalafungin (**4-11**) was formed. nanaomycin D was synthesized using the same

synthetic scheme, the only difference being the use of $(DHQ)_2PHAL$ as the ligand in the SAD reaction.

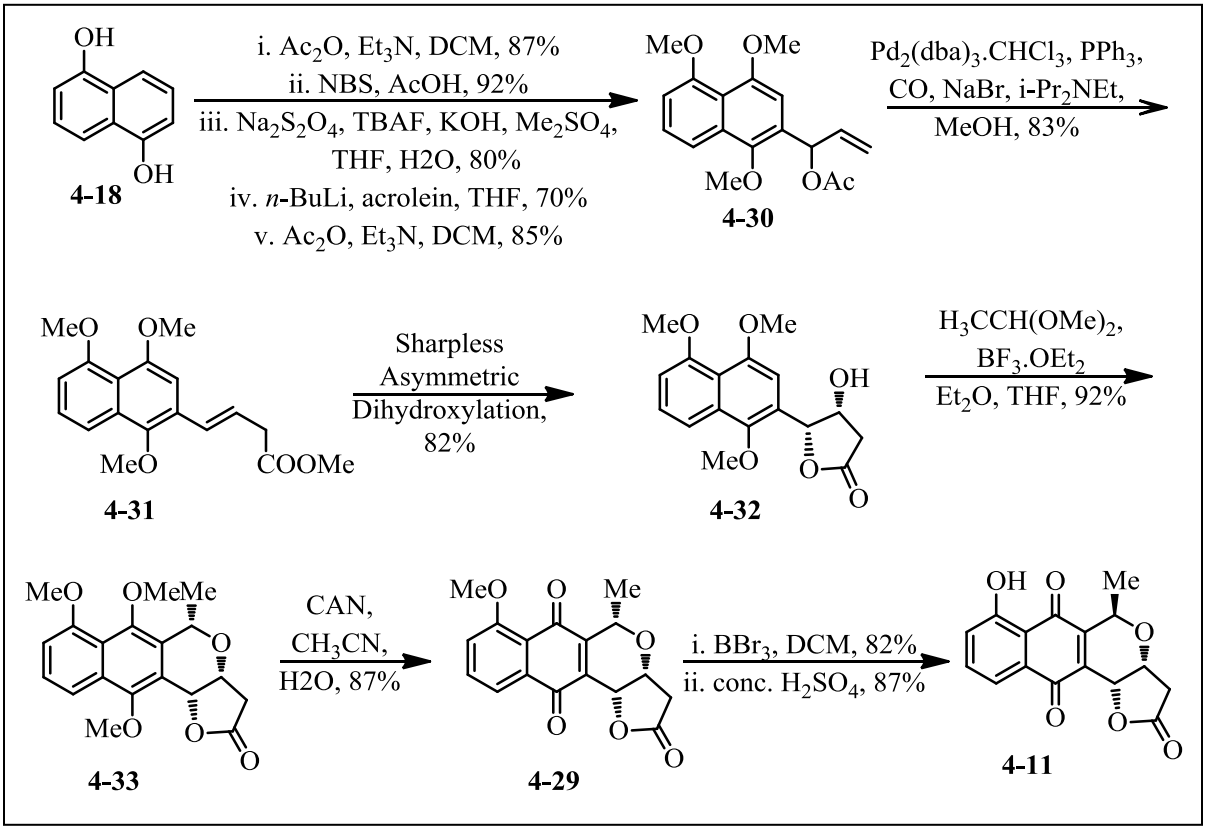

Figure 38. Kalafungin synthesis using SAD, Oxa-Pictet Spengler reactions

4.2.5 Michael-Dieckmann approach in the total synthesis of Kalafungin

In 2007, Donner reported the total synthesis of kalafungin using a tandem Michael-Dieckmann approach as shown below (**Figure 39**).[91] Starting from (*S*)-aspartic acid, compound **4-35** was formed in 5 steps. **4-34** reacted with **4-35** in a Michael-Dieckmann reaction to give the naphthopyranone **4-36**. This was subsequently converted to kalafungin **4-11**.

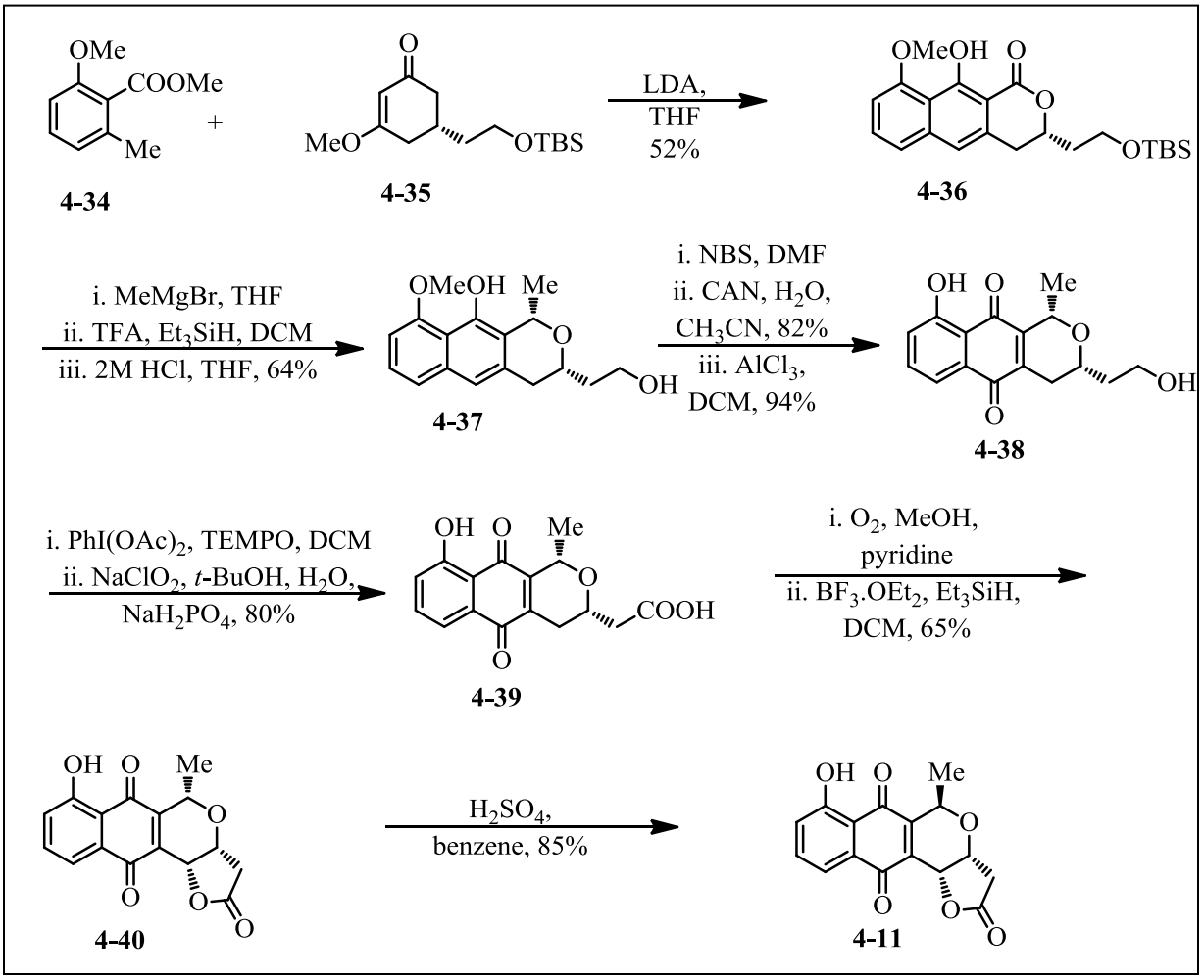

Figure 39. Total synthesis of kalafungin using Michael-Dieckmann reaction

4.3 Preparation of 7-deoxykalafungin and its deconstruction analogs

4.3.1 Synthesis of 7-deoxykalafungin (4-46)

We chose to synthesize 7-deoxykalafungin because of the ease of its synthetic accessibility and AKT (IC_{50} 0.044 μM)[86] inhibition data reported in the literature. The synthetic scheme (**Figure**

40) was chosen as it was a synthetically convenient route, had good literature precedent[92] and could be easily branched to make analogs.

Synthesis of 4-42

Starting from commercially available **4-41**, bromination was carried out using N-bromosuccinimide in dichloromethane to give **4-42** in 96% yield.

Synthesis of 4-43

Heck-coupling between **4-42** and iso-butyl vinyl acetate afforded **4-43** in 81% yield. This reaction required strict anhydrous and air-free conditions. The solvent toluene was dried over molecular sieves and degassed thoroughly using argon, prior to use. The catalyst used was bis(tri-*tert*-butylphosphine) palladium (0) which is highly air and moisture-sensitive. Using 2 mol% of the catalyst (as reported in the literature)[92] resulted in only ~10% conversion to the product. Optimization of this reaction (with *iso*-butylvinylacetate as the constant coupling partner) was previously carried out on very similar substrates (model substrates **4-47** and **4-49**) (**Figure 41**) using several other catalysts such as palladium acetate (II), palladium on carbon, etc (**Table 7**). Unfortunately, none of these catalysts worked. Finally, when the catalyst bis(tri-*tert*-butylphosphine) palladium (0) was increased from 2 mol% to 6 mol%, it resulted in ~70% conversion of the model substrate **4-47**. The same conditions were applied to **4-42**. Use of 6 mol% of the catalyst resulted in 81% of the product **4-43**. Thus, bis(tri-*tert*-butylphosphine) palladium (0) is a highly efficient catalyst for electron-rich aryl compounds.

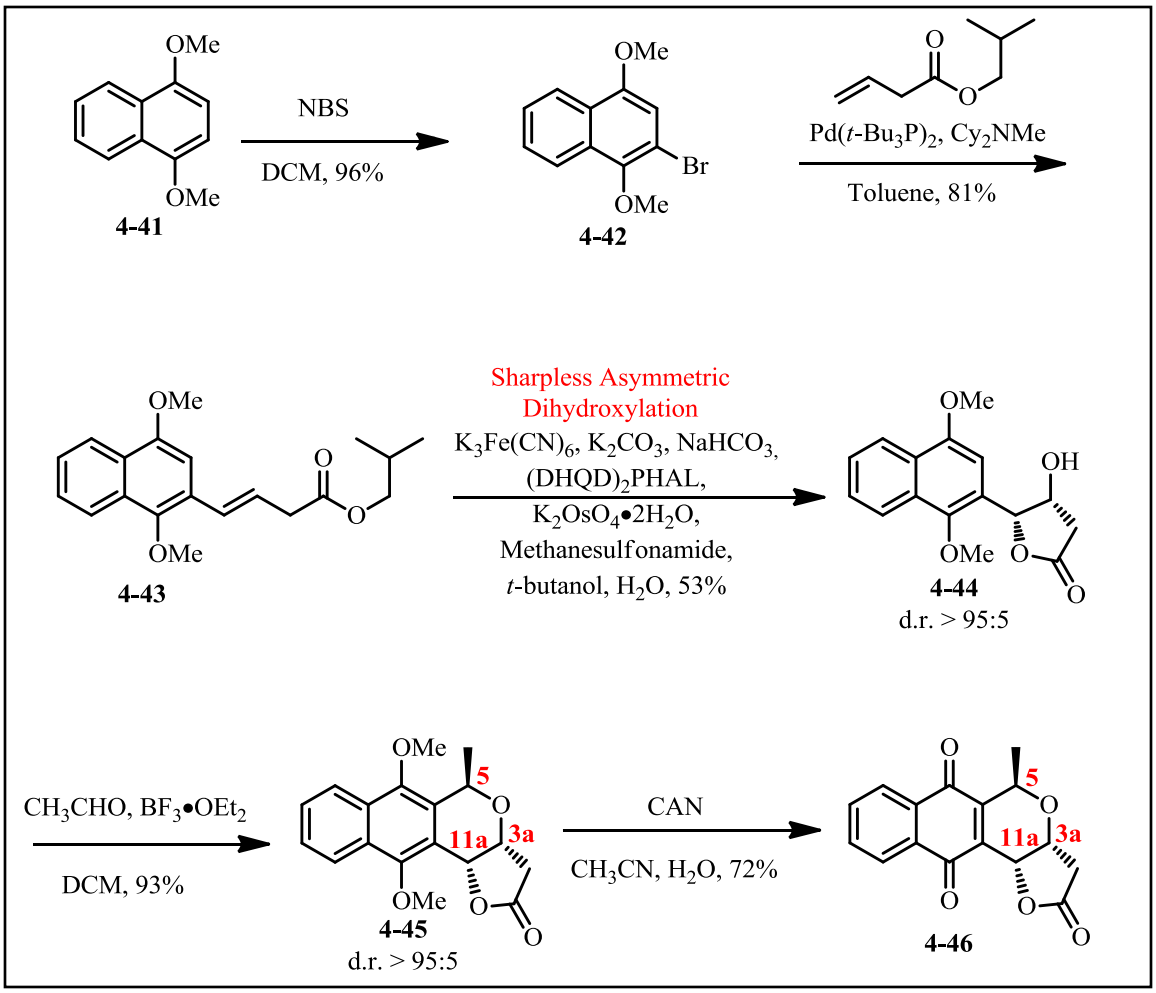

Figure 40. Synthesis of 7-deoxykalafungin

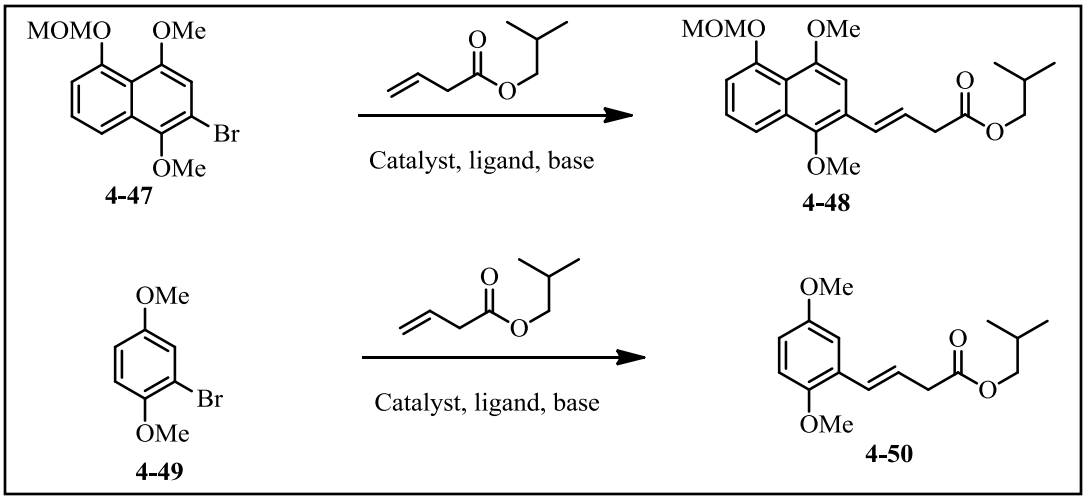

Figure 41. Optimization of Heck-coupling reaction on model substrates

Table 7. Optimization of Heck-coupling reaction using *iso*-butylvinylacetate

Substrate	Catalyst (w/wo ligand)	Base	# Eq. of catalyst	Solvent	Temp. (^oC)	Yield (%) **4-48**/**4-50**
4-47	Pd(*t*-$Bu_3P)_2$	Cy_2NMe	0.02	Toluene	111	<10
4-47	Pd(*t*-$Bu_3P)_2$	Cy_2NMe	0.02	DMF	154	0
4-47	Pd(*t*-$Bu_3P)_2$	Cy_2NMe	0.02	DMF	120	0
4-47	$Pd(OAc)_2$ + P(*o*-tolyl)$_3$	NaOAc	0.04	Toluene	111	0
4-47	Pd(*t*-$Bu_3P)_2$	Cy_2NMe	0.06	Toluene	111	70
4-49	Pd(*t*-$Bu_3P)_2$	Cy_2NMe	0.02	DMF	154	0
4-49	Pd(*t*-$Bu_3P)_2$	(*i*-$Pr)_2NEt$	0.02	Toluene	111	0
4-49	$Pd(OAc)_2$ + PPh_3	Cy_2NMe	0.02	DMF	95	0
4-49	$Pd(dba)_2$ + PPh_3	Cy_2NMe	0.02	DMF	95	0
4-49	Pd/C (10%)	Cy_2NMe	0.10	Toluene	111	0

Sharpless Asymmetric Dihydroxylation (SAD) on 4-43

Sharpless Asymmetric Dihydroxylation was carried out on **4-43** to give **4-44**. Use of commercially available AD-mixβ [$(DHQD)_2$PHAL - 0.0016 mole, potassium carbonate powder - 0.4988 mole, potassium ferricyanide - 0.4988 mole, potassium osmate dihydrate - 0.0007 mole] gave non-reproducible results. Hence, the reagents were added separately. The yield of this reaction was low (~50%). Sodium bicarbonate was added to buffer the reaction. This slightly improved the yield (53%). The reaction resulted in a mixture of lactonized and unlactonized products. In order to force the lactonization to proceed to completion, the mixture was treated

with sodium hydroxide to hydrolyze any isobutyl ester present in the dihydroxylated product to an acid. It was then acidified with hydrochloric acid and lactonized using *p*-toluene sulfonic acid (*p*-TsOH) as the catalyst. Unfortunately, the yield of this reaction could not be improved. Even after trying different conditions of temperature and time, around 35% of the starting material remained unreacted and the rest was converted to by-products which could not be characterized. The major advantage of this reaction is that the product formed is a single isomer [(*R, R*) in this case due to the ligand $(DHQD)_2PHAL$ used].

Synthesis of 4-45

Oxa-Pictet Spengler cyclization was carried out on **4-44** to give **4-45** in 93% yield. Use of acetaldehyde in dichloromethane in the presence of the Lewis acid - boron trifluoride diethyl etherate yielded exclusively the *trans* product **4-45** (*trans* relationship between positions 5 and 3a; 5 and 11a).

Synthesis of 4-46

4-45 was oxidized using ammonium cerium (IV) nitrate in water and acetonitrile mixture (1:1) to **4-46** in 72% yield. The stereochemistry of **4-46** was the same as that of **4-45**.

4.3.2 Deconstruction scheme for 7-deoxykalafungin

4-46 gets reduced *in vivo* to the **quinone methide** (**Figure 42**). This quinone methide is a very reactive Michael acceptor and it alkylates nucleophiles such as thiol groups in the proteins. In a similar manner to **4-46**, **4-61** would get reduced *in vivo* to **4-61B**.

To determine if the pyran ring is essential for activity, the compound **4-61** was synthesized. The naphthoquinone and the lactone rings were retained in **4-61**, which can still form a quinone methide. To find out if the lactone ring is essential for the activity, the compound **4-60** was synthesized, which does not have a lactone ring and cannot form a quinone methide.

In order to find out if just the Michael acceptor is sufficient to inhibit AKT1, **4-61C** was to be synthesized (the allylic oxidation reaction on **4-56** to form **4-61C** was unsuccessful). To know if the hydroxyl group in **4-61C** is essential, the compounds **4-59** (acid) and **4-56** (ester) were made, which lack the hydroxyl group, but retain the Michael acceptor.

To see if the length of the chain attached to phenyl ring had any influence on the activity of the compounds, **4-54** was made, which retained the Michael acceptor. **4-54** was further deconstructed to form **4-52** - the simplest deconstruction analog. The scheme is shown in **Figure 42**.

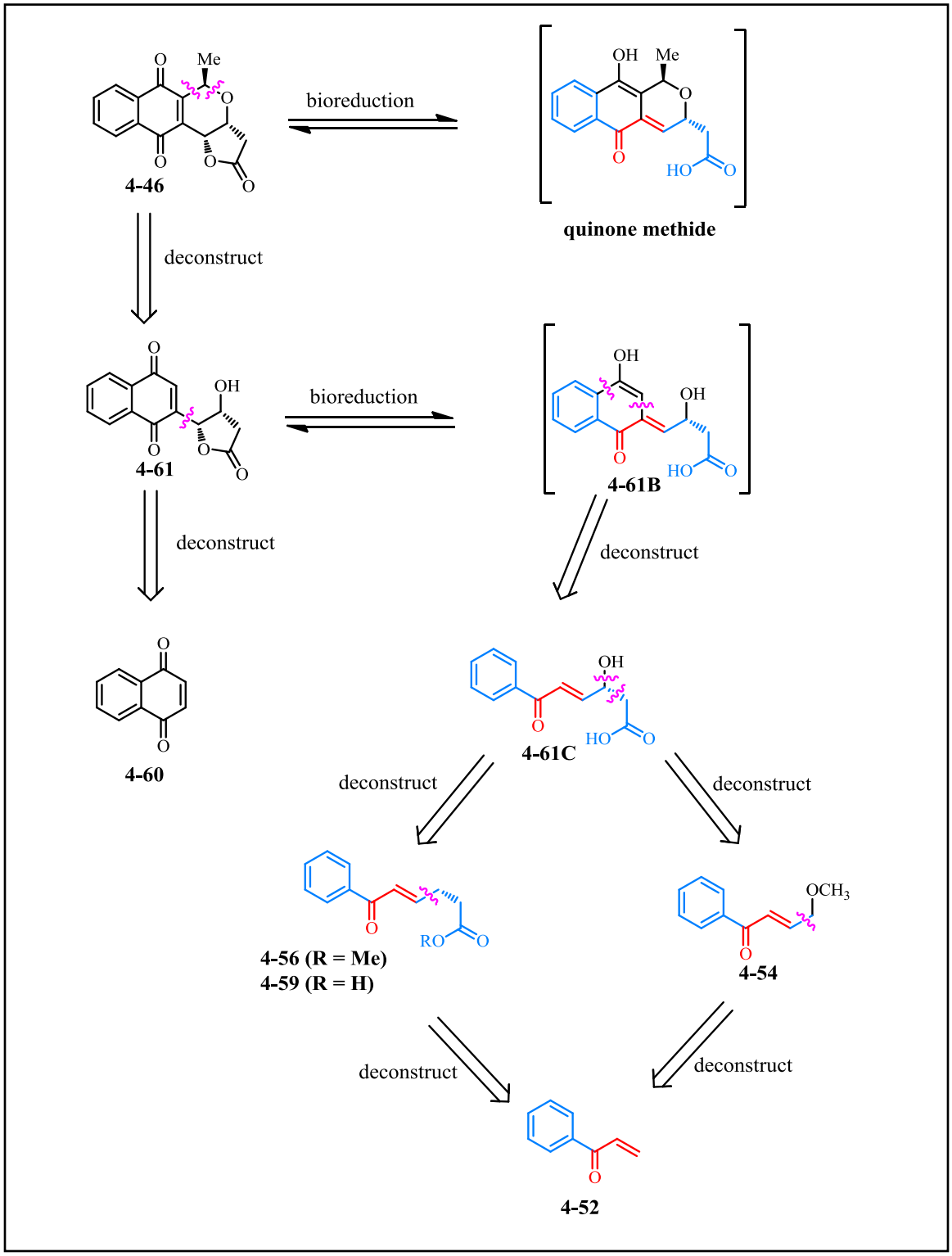

Figure 42. Deconstruction scheme for 7-deoxykalafungin

4.3.3 Synthesis of the deconstruction analogs of 7-deoxykalafungin: (figure 42)

Synthesis of 4-51

Benzoic acid was treated with *N,O*-Dimethylhydroxylamine hydrochloride in the presence of the coupling reagent EDC•HCl and base *N*-methyl morpholine to give the Weinreb amide **4-51** in 84% yield.

Synthesis of 4-52

Grignard reaction was carried out on **4-51** using vinylmagnesium bromide in dry diethyl ether. When THF was used as the solvent, the compound formed degraded during quenching of the reaction mixture. This reaction required strict anhydrous conditions and was performed under argon. The vinylmagnesium bromide solution had to be added very slowly over a period of 30 min. The product **4-52** was formed in 55% yield (**Figure 43**).

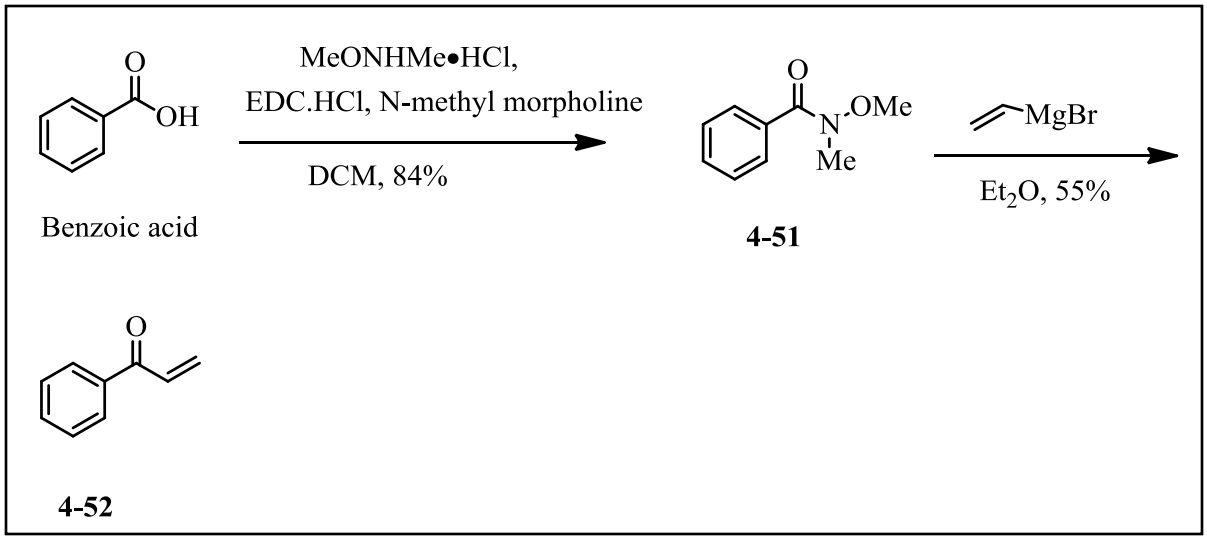

Figure 43. Synthesis of **4-51** and **4-52**

Synthesis of 4-54

The allyl methyl ether (3-metoxyprop-1-ene) was treated with **4-52** in the presence of the cross-metathesis (CM) catalyst (**4-53**) (**Figure 44**) in dichloromethane to afford **4-54** in 30% yield

(**Figure 45**). This reaction resulted in exclusively the *trans* compound. The yield was low due to the self-metathesis of the aliphatic partner. The phenyl vinyl ketone (**4-52**) underwent self-metathesis to a very low extent.

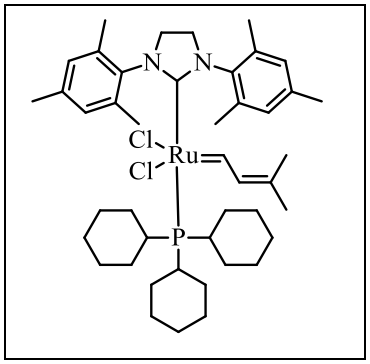

Figure 44. Cross Metathesis catalyst **4-53** (CAS number 253688-91-4)

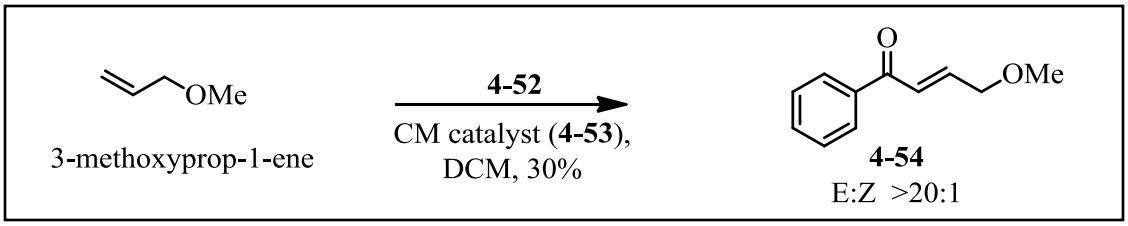

Figure 45. Synthesis of **4-54**

Synthesis of 4-55

Pent-4-enoic acid was treated with methyl iodide in the presence of potassium carbonate in acetone to afford **4-55** in 57% yield (**Figure 46**).

Synthesis of 4-56

Cross-metathesis between **4-55** and **4-52** was carried out in dichloromethane using the cross-metathesis catalyst to afford **4-56** in 41% yield (**Figure 46**). This reaction resulted in exclusively the *trans* compound. The yield was low due to the self-metathesis of the aliphatic partner. The phenyl vinyl ketone (**4-52**) underwent self-metathesis to a very low extent.

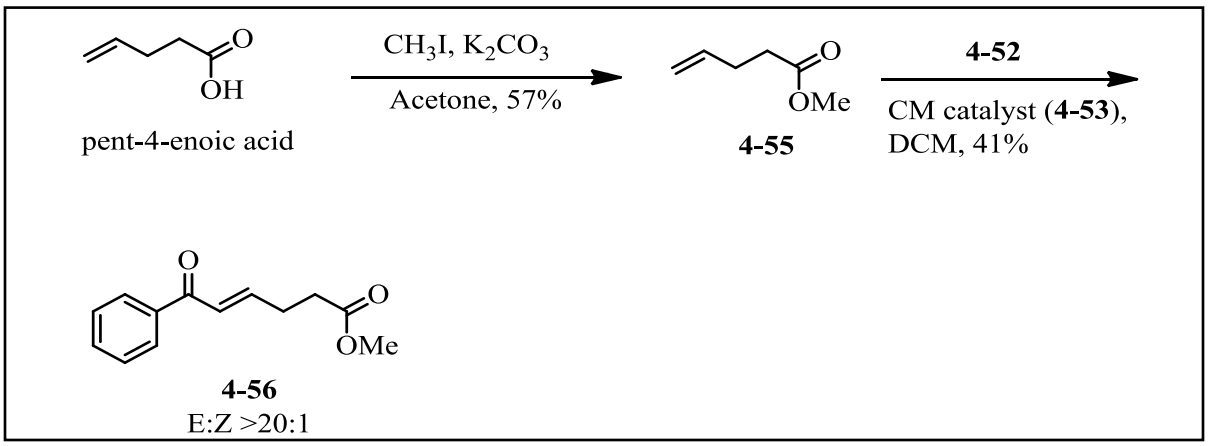

Figure 46. Synthesis of **4-55** and **4-56**

Synthesis of 4-57

Pent-4-enoic acid was protected as the *t*-butyl ester using *t*-butanol in the presence of the coupling reagent DCC and the catalyst 4-dimethyl amino pyridine (**Figure 47**). The product **4-57** was formed in 40% yield. A by-product was formed in ~40% yield which could not be characterized.

Synthesis of 4-58

Cross-metathesis between **4-57** and **4-52** was carried out in dichloromethane using the cross-metathesis catalyst to afford **4-58** in 46% yield. This reaction resulted in exclusively the *trans* compound. The yield was low due to the self-metathesis of the aliphatic partner. The phenyl vinyl ketone (**4-52**) underwent self-metathesis to a very low extent.

Synthesis of 4-59

The *t*-butyl ester of **4-58** was deprotected to give the acid **4-59** in 36% yield (**Figure 47**). Trifluoro acetic acid was used for the deprotection in the presence of the cation scavenger triethylsilane. Based on mass spectrum, **4-59** was found to exist mainly as dimers and trimers.

The yield was low due to the formation of by-products which could not be characterized by NMR spectra. Probably, lactone formation could have taken place as a result of closure of the acid group.

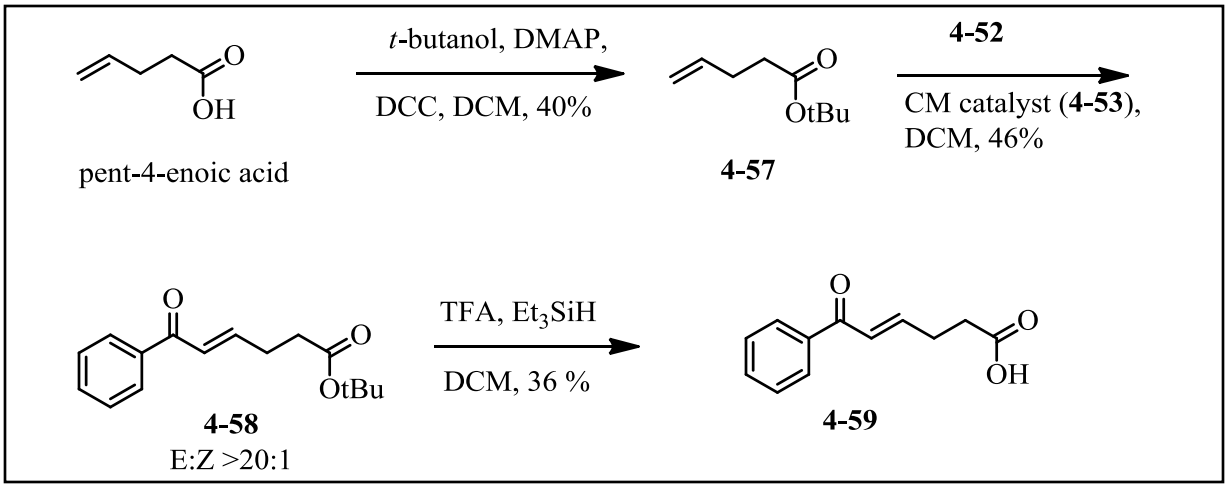

Figure 47. Synthesis of **4-57**, **4-58** and **4-59**

Synthesis of 4-60

1,4-dimethoxynaphthalene was oxidized using ammonium cerium (IV) nitrate in water and acetonitrile mixture (1:1) to **4-60** in 81% yield (**Figure 48**).

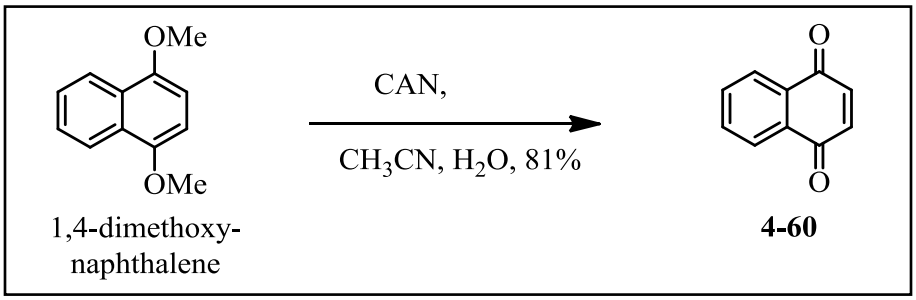

Figure 48. Synthesis of **4-60**

Synthesis of 4-61

4-44 was oxidized using ammonium cerium (IV) nitrate in water and acetonitrile mixture (1:1) to **4-61** in 65% yield (**Figure 49**). The stereochemistry of **4-61** was the same as that of **4-44**.

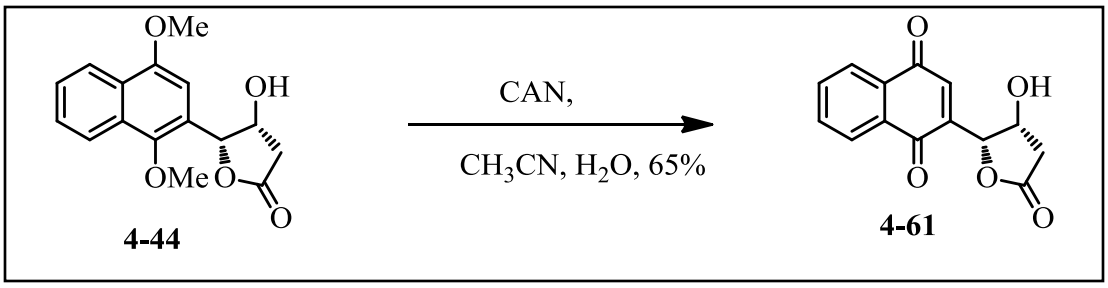

Figure 49. Synthesis of **4-61**

4.4 Evaluation of the kinase inhibition of the compounds

We chose the Z′-LYTE® kinase assay system to evaluate these compounds.

4.4.1 Z′-LYTE® assay principle

The Z′-LYTE® biochemical assay (Invitrogen, NY, USA) is used to measure the kinase (AKT1, PKA, etc.) inhibition. In a kinase (primary) reaction, the kinase transfers a phosphate group from ATP to a serine/threonine/tyrosine residue present in the FRET peptide. The FRET peptide is a synthetic peptide which has a coumarin fluorophore (donor) at one end and a fluoroscein fluorophore (acceptor) at the other end. In the development (secondary) reaction, a development reagent which contains a site-specific protease is added. This protease does not cleave the phosphorylated FRET peptide, but it cleaves the non-phosphorylated FRET peptide (**Figure 50**). The emission ratio is calculated after the donor fluorophore is excited at 410 nm.

Emission Ratio = Coumarin Emission (458 nm) / Fluoroscein Emission (522 nm)

Cleaved peptide has a higher Emission Ratio (as the FRET between donor and acceptor fluorophores is lost) indicating higher inhibition of the kinase whereas uncleaved peptide has a lower Emission Ration (as the FRET between donor and acceptor fluorophores is maintained) indication lower/no inhibition of the kinase.

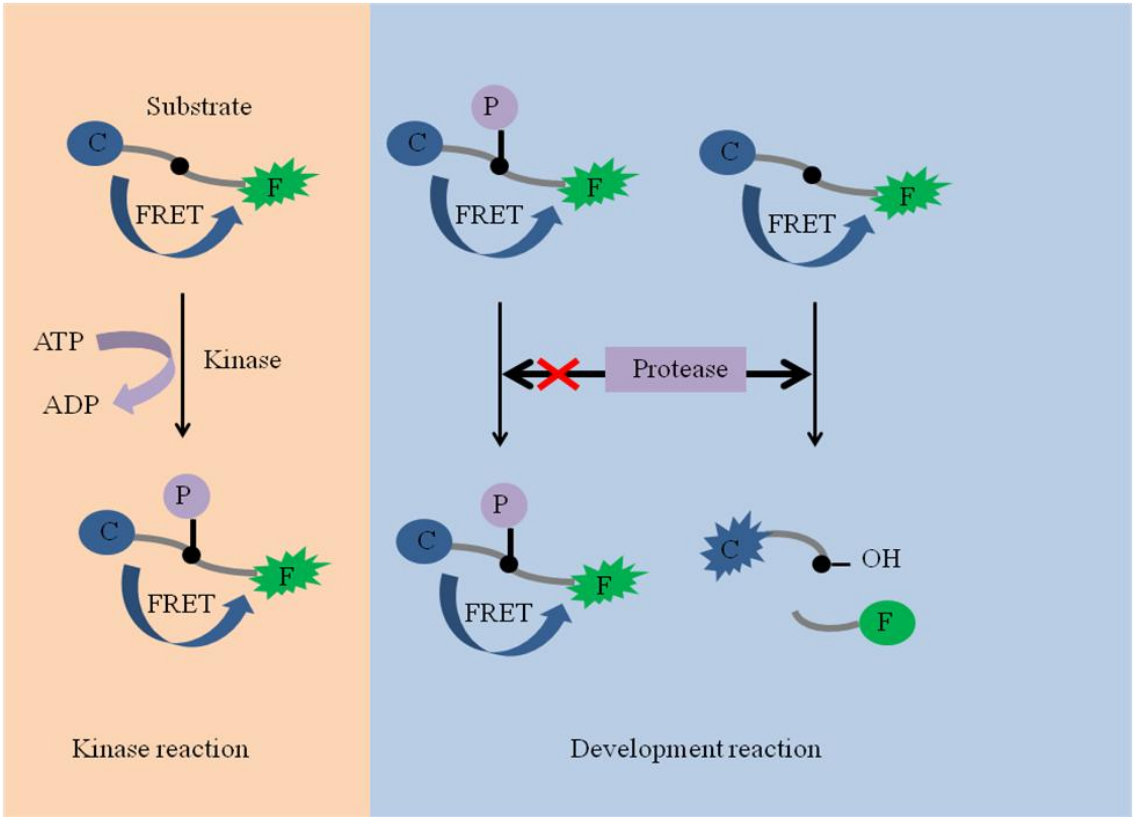

Figure 50. Z′-LYTE assay principle

4.4.2 AKT1 assay results

6 was the most potent one among the compounds tested (**Table 8**). This is assumed to be due to the pyran ring which confers rigidity to the molecule. Also, it has the Michael acceptor which could be alkylating the cysteine residue(s) present in the T-loop region of AKT1. A ten-fold loss of potency was observed in **4-61** compared to **4-46**. This is probably due to the flexibility of **4-61** which could be preventing it from making important interactions with AKT1 at its binding site. The compound **4-63** showed moderate potency though it was unstable in solution. The activity observed could be due to the rigidity of the molecule which does not get affected upon reduction. **4-56** was found to be about four times less potent than **4-61**. This could be due to the flexibility

of the aliphatic chain in **4-56** as compared to the closed rigid lactone ring in **4-61**. The potency of **4-52** was similar to **4-56**, probably because it cannot make the necessary interactions in AKT1 at its binding site. The IC_{50} value of **4-59** was >100 µM, this could be due to the flexibility or the hydrophilicity of the molecule which might be unfavorable for AKT1 interaction. Also, the compound mainly existed as dimers and trimers (based on mass spectrum); this could prevent the molecule(s) from entering the binding site of the enzyme. The IC_{50} value obtained for **4-60** might not be accurate as inhibition plateaus from 4-100 µM at 50% inhibition (**4-60** may exist as the reduced quinone in equilibrium with the oxidized form at higher concentrations). The IC_{50} value obtained for **4-54** might not be accurate as the inhibition curve does not cover the range of 0-100% inhibition.

4.4.3 Evaluation of the activity of the compounds against PKA

The 7-deoxykalafungin analogs were evaluated as PKA inhibitors to determine what features of the compounds confer selectivity to AKT1 over other closely related kinases. The compounds **4-46**, **4-52**, **4-54** and **4-56** had IC_{50} values >100 µM (**Table 8**). This is similar to the report of Wyeth researchers on PNQ lactones; they found PNQ lactones to selectively inhibit AKT1/AKT2 over PKA and PKC. **4-61** had an IC_{50} value of 0.43 µM. This is very surprising as the compound is not only the most potent one among the series against PKA, but also is a better inhibitor of PKA compared to AKT1. This could be due to the flexibility of the molecule which somehow makes it accessible to the binding site on PKA.

Table 8. AKT1 and PKA IC_{50} values of compounds

No.	Compound Structure	AKT1 IC_{50} (μM)	PKA IC_{50} (μM)
4-46	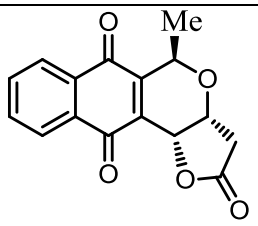	0.28	>100
4-61	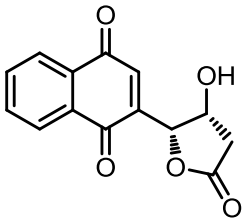	2.94	0.43
4-60	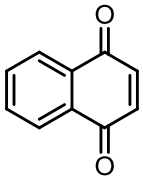	10.98	Not tested
4-56	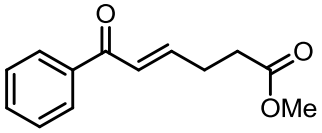	13.67	>100
4-59	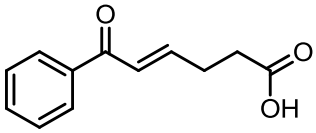	>100	Not tested
4-54	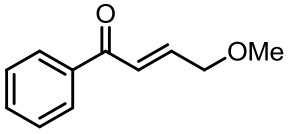	50.01	>100
4-52	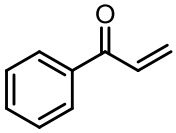	12.27	>100

4.5 Synthesis of 5-alkynyl analog of 7-deoxykalafungin (4-63)

4.5.1 Rationale

Based on the mechanism of inhibition of AKT by PNQ lactones, it can be hypothesized that, inside cells, 7-deoxykalafungin would bind covalently to AKT and other cellular targets (if any) to form covalent complex(es). Installing an alkyne handle in 7-deoxykalafungin could be used to perform a 'click reaction' *in situ* between the alkynyl 7-deoxykalafungin/cellular target covalent complex(es) and biotin-azide (**4-62**) to form adduct(s) (**4-64**) (**Figure 51**). This would allow the isolation of the covalent complexes by affinity purification using streptavidin or avidin columns (which bind biotin). The covalent complex(es) could be then characterized by mass spectrometry after purification on SDS gels.

According on the SAR studies on PNQ lactones inhibiting AKT, by Salaski *et al*, position 5 on the PNQ lactone tolerates a wide range of substituents. Hence, we decided to incorporate an alkyne functionality at position 5 in order to find out the cellular targets of PNQ lactones. Thus, we planned to synthesize the compound **4-63** (**Figure 51**).

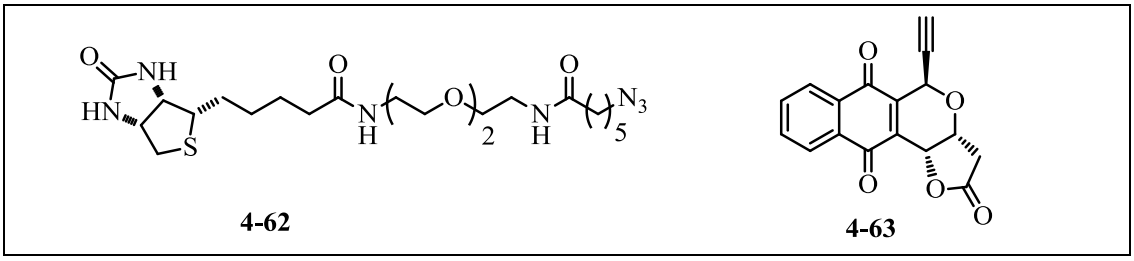

Figure 51. Biotin azide (**4-62**) and **4-63**

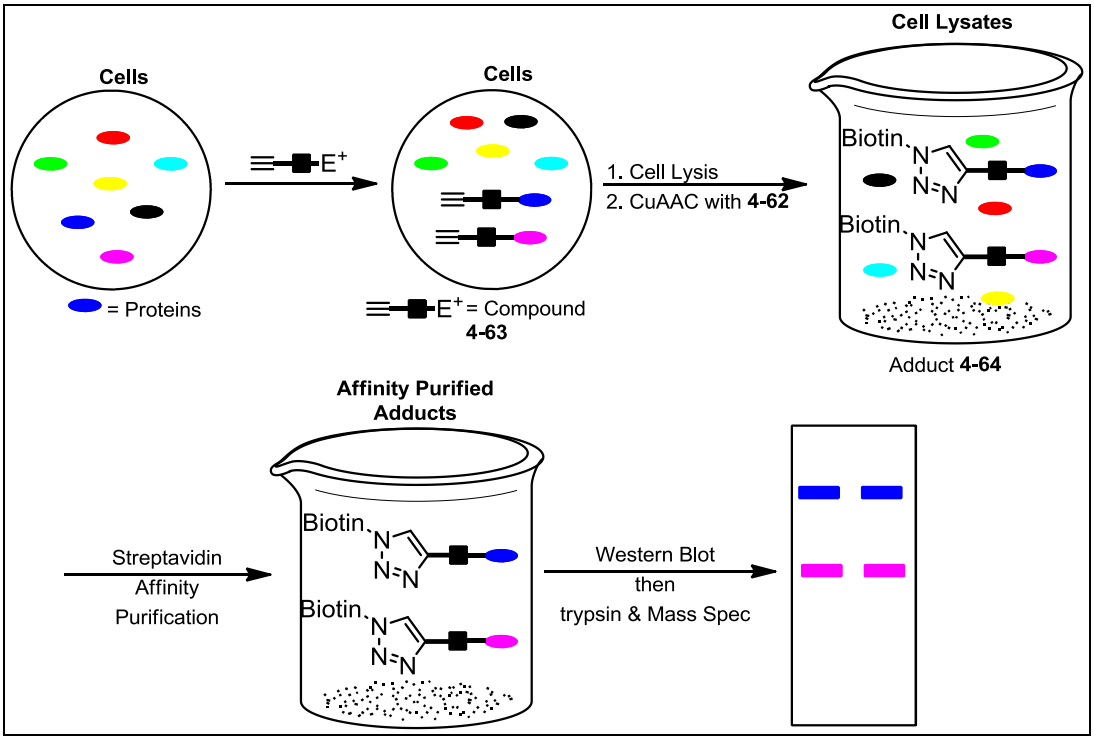

Figure 52. Schematic for the identification of cellular target(s) of PNQ lactones

Synthesis of 4-65

Oxa-Pictet Spengler cyclization was carried out on **4-44** using 3-(trimethylsilyl)-2-propynal in dichloromethane in the presence of the Lewis acid boron trifluoride diethyl etherate. It resulted in the desired product **4-65** (*trans* relationship between 5 and 3a; 5 and 11a) in 43% yield. Another diastereomer was formed in about 40% yield. This shows that the stereochemistry and the proportion of the products formed entirely depends upon the aldehyde used.

Synthesis of 4-66

The trimethylsilyl group of **4-65** was deprotected to give **4-66** using tetrabutyl ammonium fluoride solution. The yield was low due to some degradation of the compound during the

reaction. The by-products were not characterized. The stereochemistry of **4-66** was the same as that of **4-65**.

Synthesis of 4-63

4-66 was oxidized using ammonium cerium (IV) nitrate in water and acetonitrile mixture (1:1) to **4-63** in 60% yield (**Figure 52**). The stereochemistry of **4-63** was the same as that of **4-66**. The product **4-63** was very unstable. Within 10 min of purification on silica gel, the color of the product in solution changed from yellow to dark red. Due the color change, we hypothesize that the compound is auto-reduced in a redox reaction. Based on the NMR spectra, there were two compounds, whose ratio changed as a function of time. In order to find out if the compound is getting degraded due to the purification on silica, the reaction was repeated and the product was extracted with ethyl acetate and no purification was performed. Even in this case, the compound turned from yellow color (oxidized) to a dark red color (reduced). Thus, it was concluded that the product is unstable by its own nature. Upon treating the reduced product with ammonium cerium (IV) nitrate, it was getting re-oxidised during the course of the reaction; but again after extraction it was getting auto-reduced i.e. the product was stable only in the presence of ammonium cerium (IV) nitrate. It could be getting degraded to **4-67**, **4-68** or **4-69 (Figure 53)**. Due to the inherent unstable nature of this compound (**4-63**), it could not be used as a cellular probe. This work would be continued in the near future by making similar alkynyl analogs. The IC_{50} of **4-63** against AKT1 was 3.89 µM.

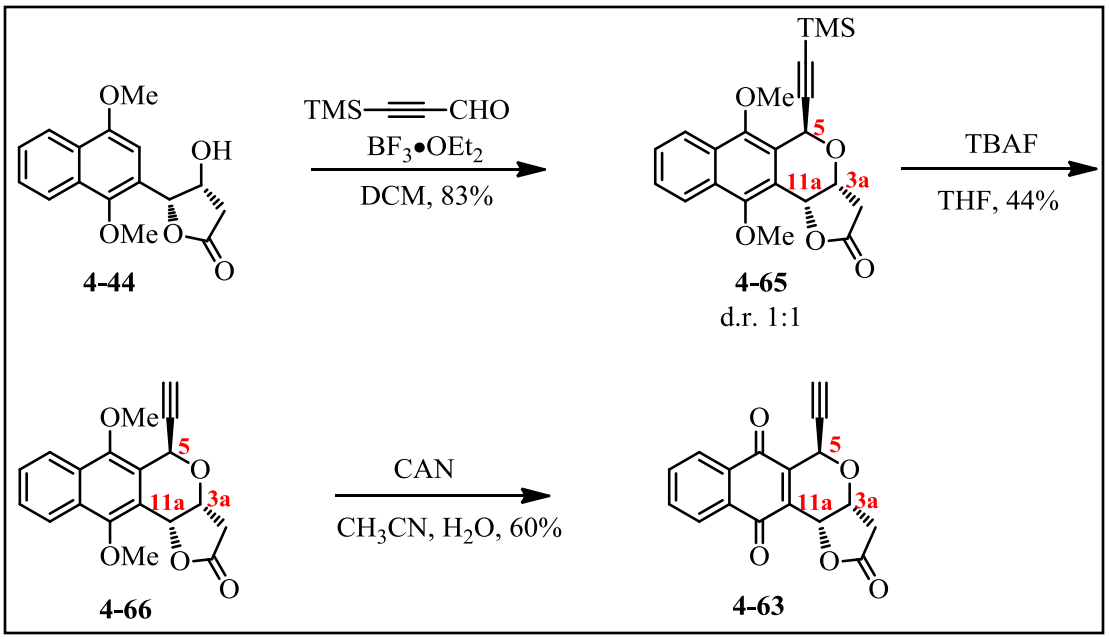

Figure 53. Synthesis of 5-alkynyl analog of 7-deoxykalafungin **4-63**

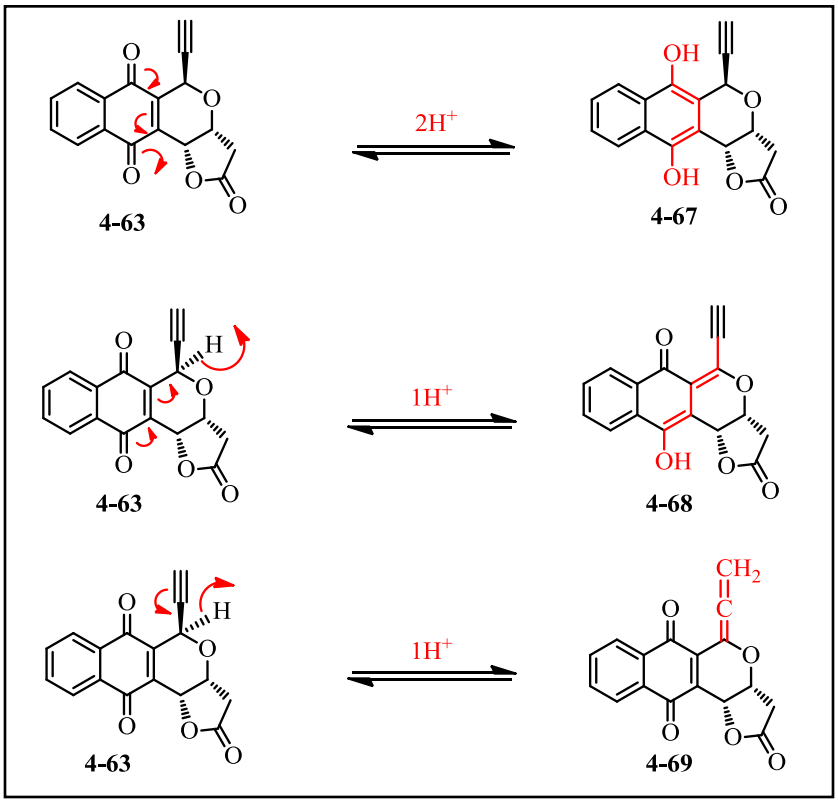

Figure 54. Proposed mechanisms for the degradation of **4-63**

4.6 Future direction

The future work on the compounds synthesized would be:

- To determine the inhibition mechanism of AKT1 (allosteric/ATP competitive/peptide substrate competitive, etc.)
- To find out the specific residues alkylated
- To determine the specificity of inhibition of AKT1 over AKT2 and AKT3
- To perform cell-based assays on cancer cell lines (for potency determination) and normal cell lines (for toxicity determination)
- To synthesize an alkynyl probe (handle for 7-deoxykalafungin) to find the cellular targets of PNQ lactones

4.7 Summary

In summary, we successfully synthesized 7-deoxykalafungin and its deconstruction analogs. We hypothesize that the pyran ring is essential for AKT1 inhibition probably due to the rigidity it confers to the molecule. The role of the Michael acceptor in the molecules could not be determined for sure. Flexible compounds were found to have lower potency probably due to the failure to make important interactions at the binding site of AKT1. Surprisingly, compound **4-61** was found to be a very potent inhibitor of PKA; the flexibility of this compound probably makes it more accessible to the binding site of PKA.

EXPERIMENTAL SECTION

1. Biology experimentals

a. AKT1 Assay

The assay of AKT1 was performed using Z′-LYTE Kinase Assay Kit – Ser/Thr 6 Peptide (Invitrogen, NY, USA) in non-binding low-volume 384-well plates (Cat. No 3676, Corning, NY, USA). The compounds were tested in 0.8% DMSO (final concentration) in the well. 10 different concentrations of the compounds were tested using 3-fold serial dilutions. AKT1 was diluted in the kinase buffer (50 mM HEPES pH 7.5, 0.01% BRIJ-35, 10 mM $MgCl_2$, 1 mM EGTA) and added to the wells. The test compounds (diluted in kinase buffer) were then added into these wells. The kinase reaction was then started by adding a mixture containing ATP, peptide substrate (serine/threonine 06) and kinase buffer to the above solution. The final reaction volume of 10 µL contained 6 ng of AKT1 (600 ng/ml), 75 µM ATP and 2 µM peptide substrate in kinase buffer. The assays were incubated at room temperature for 1 h. Then 5 µL of development reagent was added. This mixture was incubated at room temperature for further 1 h and then terminated by the addition of 5 µL of stop reagent. The Relative Fluorescence Units (RFU) was measured using Flexstation 3 microplate reader (Molecular Devices, CA, USA) using an excitation wavelength of 410 nm and emission wavelengths of 458 nm and 522 nm. Staurosporine was used as a standard compound (**Figure 54**). The graphs in **figures 55-57** were used to calculate the IC_{50} values against AKT1.

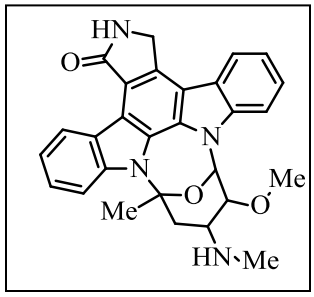

Figure 55. Staurosporine

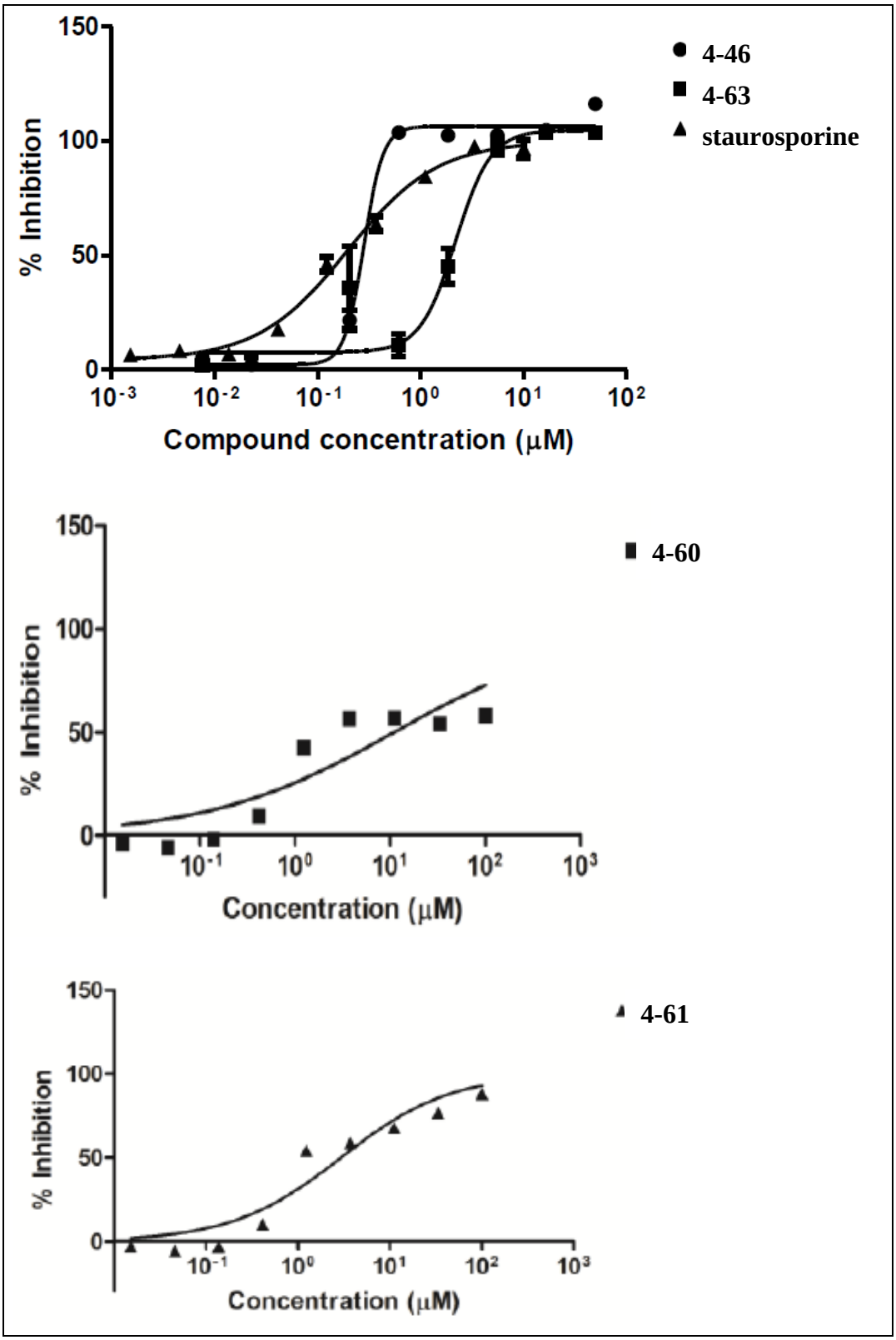

Figure 56. AKT1 inhibition graphs of **4-46**, **4-63**, **staurosporine**, **4-60** and **4-61**

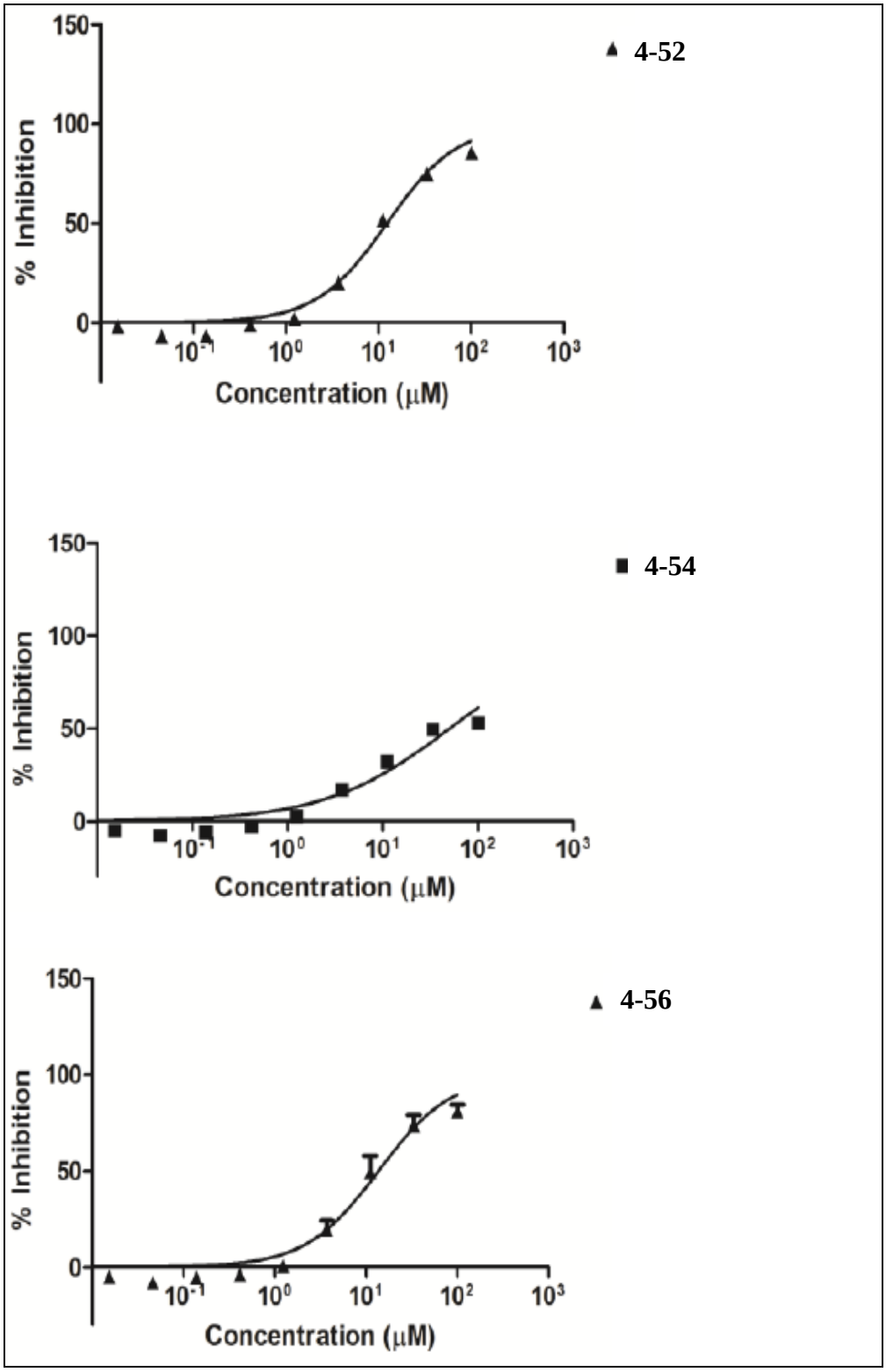

Figure 57. AKT1 inhibition graphs of **4-52**, **4-54** and **4-56**

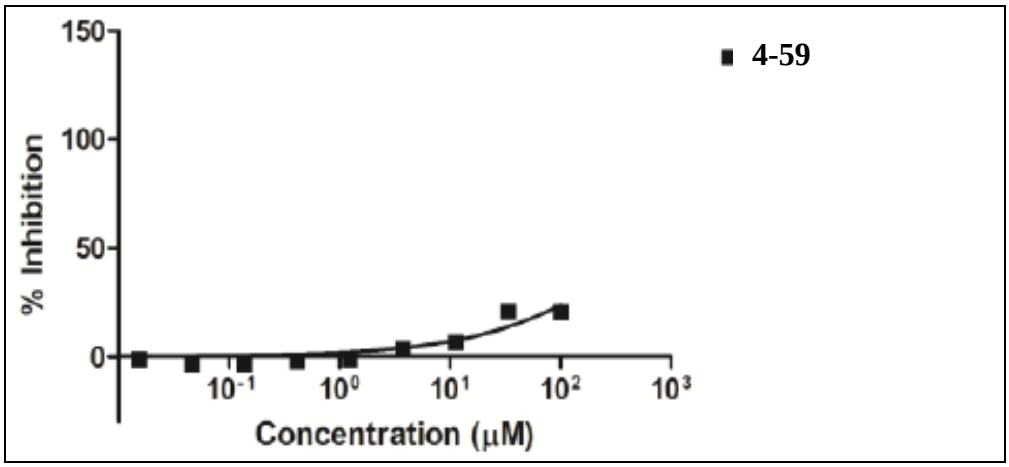

Figure 58. AKT1 inhibition graph of **4-59**

Table 9. IC_{50} values of the compounds against AKT1

Compound	IC_{50} (µM)	95% Confidence Interval
4-46	0.28	0.23-0.34
4-63	3.89	3.26-4.65
Staurosporine	0.011	0.007-0.017
4-60	10.98[a]	5.52-21.82
4-61	2.94	2.02-4.08
4-52	12.27	10.48-14.37
4-54	50.01[b]	35.62-70.21
4-56	13.67	10.60-17.63
4-59	>100	-

[a] This value might not be meaningful as inhibition seems to plateau at 50% inhibition from around 4-100µM

[b] This value might not be accurate as the inhibition curve does not span the range of 0-100% inhibition

b. PKA Assay

The assay of PKAα was performed using Z′-LYTE Kinase Assay Kit – Ser/Thr 1 Peptide (Invitrogen, NY, USA) in non-binding low-volume 384-well plates (Cat. No 3676, Corning, NY, USA). The compounds were tested in 0.8% DMSO (final concentration) in the well. 10 different concentrations of the compounds were tested using 3-fold serial dilutions. PKAα was diluted in the kinase buffer (50 mM HEPES pH 7.5, 0.01% BRIJ-35, 10 mM $MgCl_2$, 1 mM EGTA) and added to the wells. The test compounds (diluted in kinase buffer) were then added into these wells. The kinase reaction was then started by adding a mixture containing ATP, peptide substrate (serine/threonine 01) and kinase buffer to the above solution. The final reaction volume of 10 µL contained 0.3 ng of PKAα (30 ng/ml), 4 µM ATP and 2 µM peptide substrate in kinase buffer. The assays were incubated at room temperature for 1 h. Then 5 µL of development reagent A was added. This mixture was incubated at room temperature for further 1 h and then terminated by the addition of 5 µL of stop reagent. The Relative Fluorescence Units (RFU) was measured using Flexstation 3 microplate reader (Molecular Devices, CA, USA) using an excitation wavelength of 410 nm and emission wavelengths of 458 nm and 522 nm.

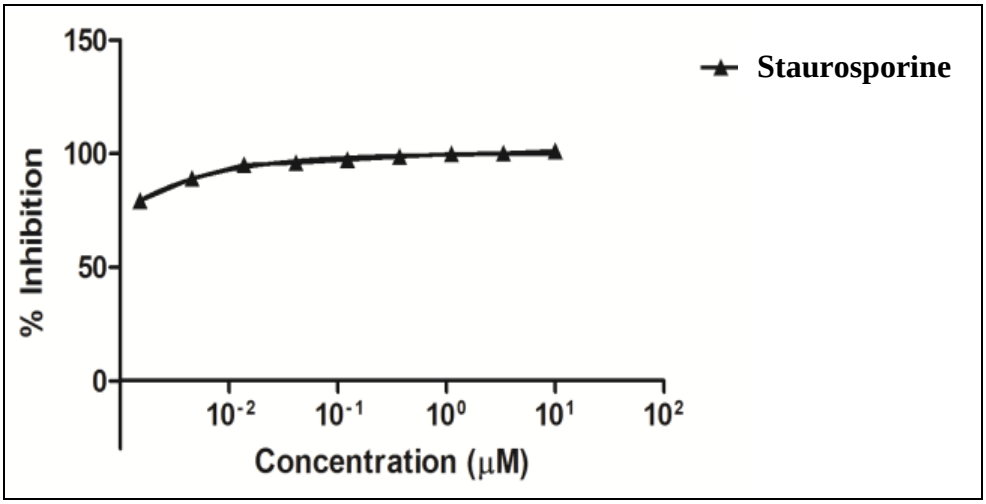

Figure 59. PKA inhibition graph of **staurosporine**

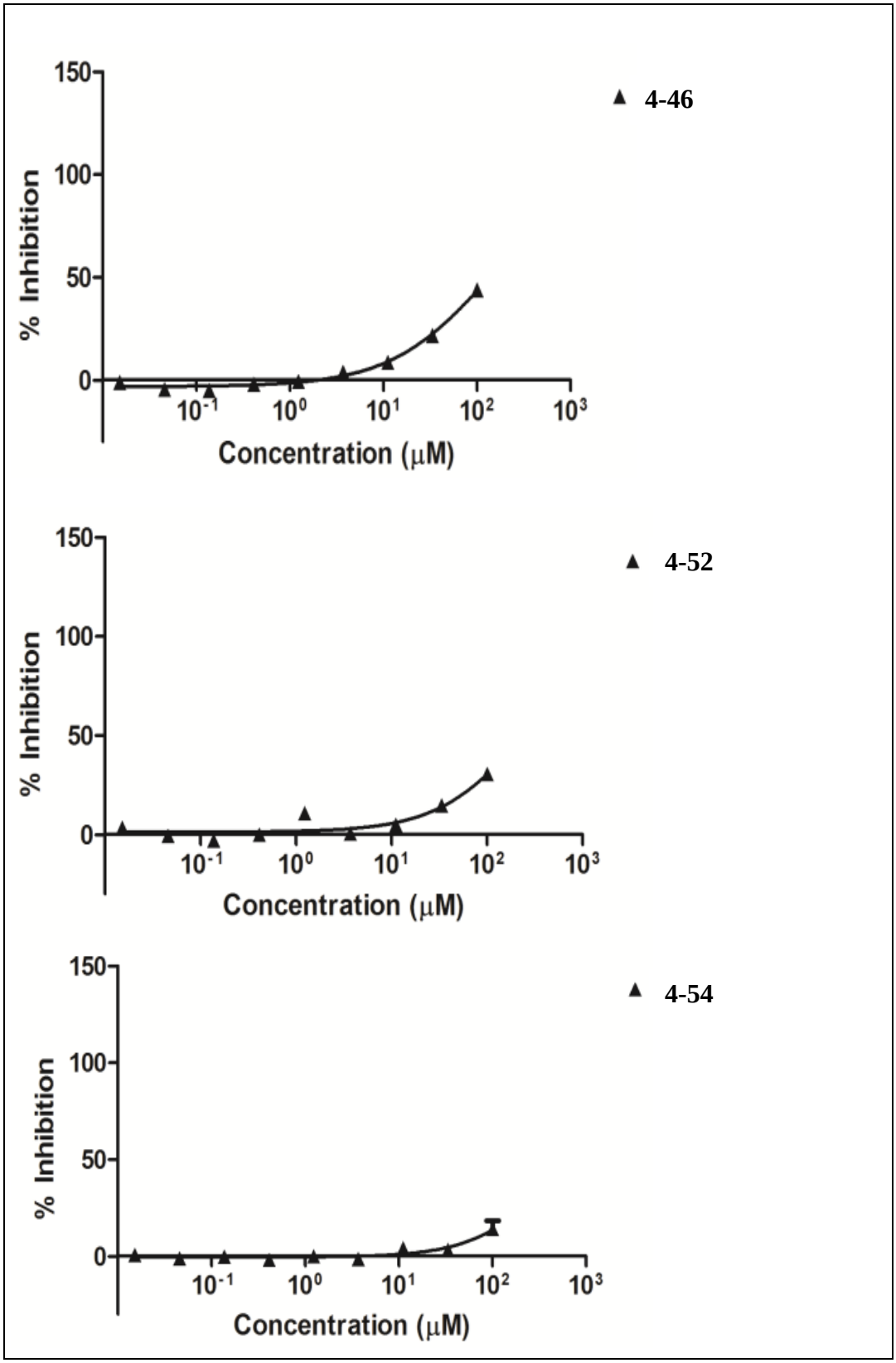

Figure 60. PKA inhibition graphs of **4-46**, **4-52** and **4-54**

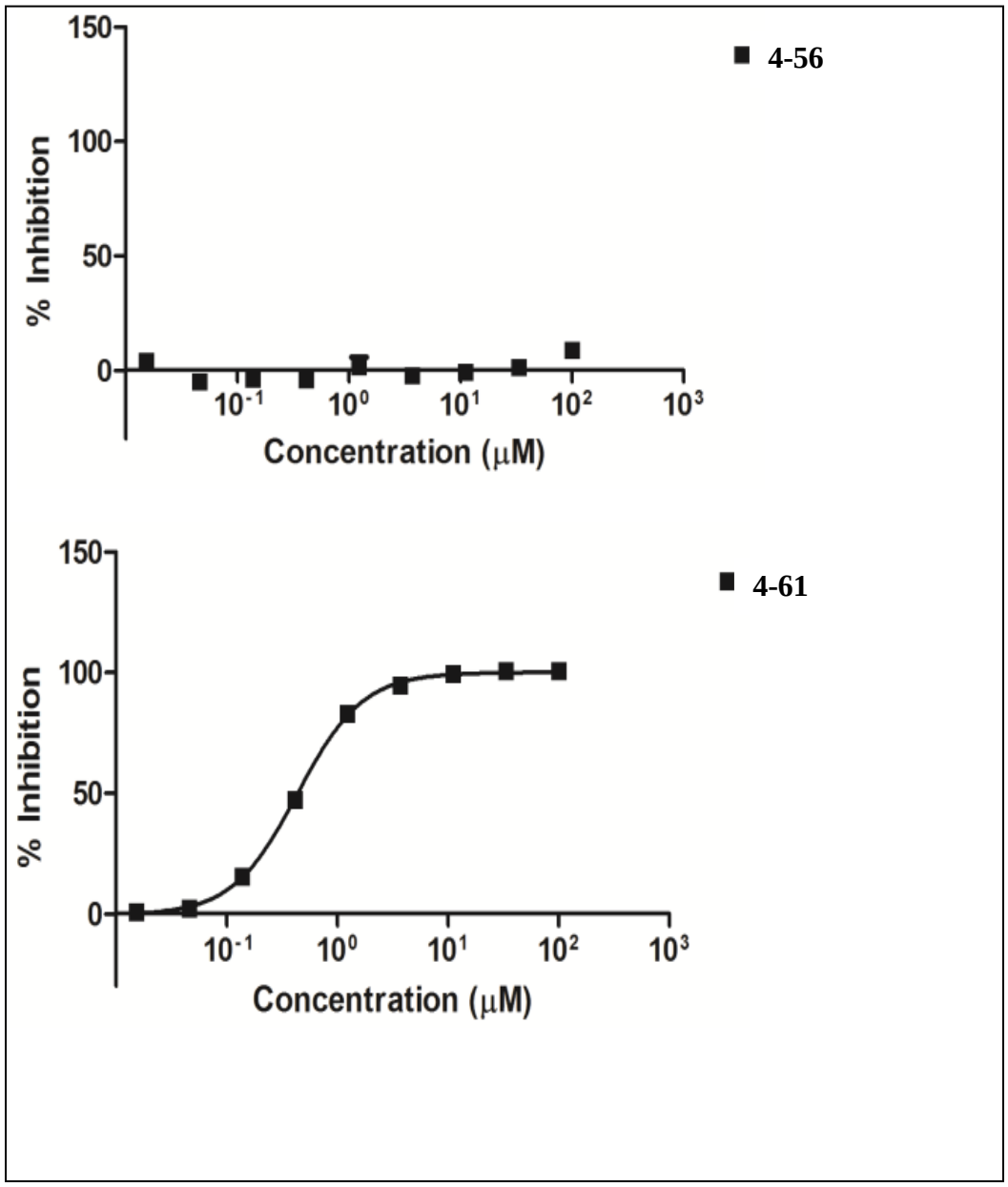

Figure 61. PKA inhibition graphs of **4-56** and **4-61**

Table 10. IC_{50} values of the compounds against PKA

Compound	IC_{50} (μM)	95% Confidence Interval
Staurosporine	<0.0015	-
4-46	>100	-
4-52	>100	-
4-54	>100	-
4-56	>100	-
4-61	0.43	0.41-0.46

(Staurosporine was used as a standard compound)

The graphs in **figures 58-60** were used to calculate the IC_{50} values against PKA.

2. Chemistry experimentals

General methods:

Reagents/chemicals, catalysts, solvents were purchased from Sigma-Aldrich, Fisher and Alfa-Aesar.

Analytical Thin Layer Chromatography (TLC) was performed using silica gel GHLF plates (Analtech Inc.)

Flash chromatography was performed on TELEDYNE ISCO CombiFlash® Rf instrument using RediSep Rf Normal-phase Flash Columns (4-gm, 12-gm, 24-gm or 40-gm).

^{1}H NMR and ^{13}C NMR experiments were recorded on BRUKER 400MHz NMR instrument in deuterated solvents - chloroform ($CDCl_{3)}$ or methanol (CD_3OD). All chemical shifts are reported in parts per million (ppm) with reference to chloroform and methanol residual peaks at 7.26 and 3.31 respectively (^{1}H NMR spectra); 77.16 and 49.00 respectively (^{13}C NMR spectra). The data is reported as: chemical shifts (ppm), multiplicity (s = singlet, d = doublet, dd = doublet of doublets, t = triplet, dt = doublet of triplets, td = triplet of doublets, tt = triplet of triplets, q = quartet, m = multiplet), coupling constant(s) (Hz) and integral values.

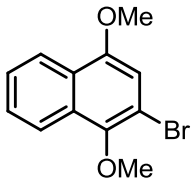

2-bromo-1,4-dimethoxynaphthalene (4-42): 1,4-dimethoxynaphthalene (1.00 g, 5.31 mmol) was dissolved in anhydrous DCM (7.48 ml). To this solution, N-bromosuccinimide (0.95 g, 5.34 mmol) was added. The reaction mixture was stirred at room temperature for 18 h. It was then

diluted with DCM. The organic layer was washed with saturated sodium sulfite solution, dried over Na_2SO4, concentrated in vacuo and purified on silica gel (3:1 hexanes/EtOAc) to afford 1.37 g of **4-42** (96%) as a colorless oil. ^{1}H NMR (400 MHz, $CDCl_3$) δ 8.20 (d, J = 8.2 Hz, 1H), 8.08 (d, J = 8.2 Hz, 1H), 7.59-7.48 (m, 2H), 6.88 (s, 1H), 3.98 (s, 3H), 3.96 (s, 3H).

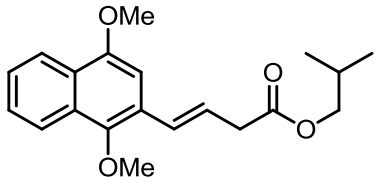

(E)-isobutyl 4-(1,4-dimethoxynaphthalen-2-yl)but-3-enoate (4-43): Under an atmosphere of argon, compound **4-42** (1.32 g, 4.96 mmol) was dissolved in 5.69 ml of anhydrous toluene (which was passed over molecular sieves and degassed prior to use). To this solution, isobutyl vinylacetate (1.80 ml, 11.26 mmol), dicyclohexylmethylamine (1.64 ml, 7.66 mmol) and bis(tri-*tert*-butylphosphine)palladium (0.14 g, 0.28 mmol) were added. The reaction mixture was heated at 110 ^{o}C under argon for 16 h. It was then quenched with aqueous $NaHCO_3$ solution and extracted with EtOAc. The organic layer was dried over Na_2SO_4 and evaporated. Purification of the residue on silica gel (5:1 hexanes/EtOAc) afforded 1.32 g (81%) of **4-43** as a brown viscous liquid. ^{1}H NMR (400 MHz, $CDCl_3$) δ 8.20 (d, J = 8.6 Hz, 1H), 8.05 (d, J = 8.1 Hz, 1H), 7.56-7.42 (m, 2H), 7.04-6.98 (dt, J = 16.2 Hz, 1H), 6.89 (s, 1H), 6.45-6.37 (m, 1H), 4.01 (s, 3H), 4.0-3.9 (m, 2H), 3.88 (s, 3H), 3.40-3.36 (dd, J = 7.3 Hz, 2H), 2.00 (m, 1H), 0.96 (s, 3H), 0.95 (s, 3H); ^{13}C NMR (125 MHz, $CDCl_3$) δ 128.9, 128.2, 126.9, 125.7, 124.9, 122.8, 122.6, 122.3, 100.8, 71.0, 62.6, 55.8, 38.9, 27.9, 19.2.

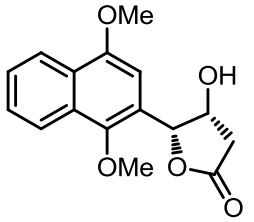

(4R,5R)-5-(1,4-dimethoxynaphthalen-2-yl)-4-hydroxydihydrofuran-2(3H)-one (4-44): A round bottom flask was charged with potassium ferricyanide (III) (4.53 g, 13.74 mmol), potassium carbonate (1.86 g, 13.47 mmol), hydroquinidine 1,4-phthalazinediyl diether (0.03 g, 0.04 mmol), potassium osmate dihydrate (9.00 mg, 0.02 mmol), methanesulfonamide (0.44 g, 4.67 mmol), sodium bicarbonate (1.03 g, 12.27 mmol), water (24.00 ml) and *tert*-butanol (9.00 ml). This mixture was stirred at room temperature till all the solids dissolved. It was then cooled to 0 °C. To this mixture was added a solution of **4-43** (1.34 g, 4.09 mmol) in *tert*-butanol (15.00 ml) in one portion. The resulting turbid mixture was stirred at 0 °C for 24 h and then room temperature for 3 days. The reaction was quenched by the addition of sodium sulfite (4.27 g, 33.90 mmol) in one portion and was allowed to stir for 1 hr at room temperature. It was extracted with EtOAc and concentrated in vacuo. It was observed that under these conditions, the lactonization was not fully completed. In order to facilitate complete lactonization, the crude product obtained above was treated with 40 ml of 0.1 N NaOH solution and stirred at room temperature for 2 h. This resulted in the cleavage of the isobutyl ester to form the acid. The reaction mixture was then acidified with 14 ml of 3 N hydrochloric acid. To this mixture, p-toluenesulfonic acid monohydrate (0.08 g, 0.40 mmol) in DCM (14.00 ml) was added and allowed to stir at room temperature for 24 h. The reaction mixture was then extracted with DCM, washed with brine and aqueous $NaHCO_3$ solution. The organic layer was dried over Na_2SO_4 and

evaporated. Purification of the residue on silica gel (1:3 hexanes/EtOAc) afforded 0.62 g (53%) of **4-44** as a white solid (d.r. >95:5). ^{1}H NMR (400 MHz, $CDCl_3$) δ 8.28 (d, J = 8.7 Hz, 1H), 8.01 (d, J = 8.3 Hz, 1H), 7.60-7.46 (m, 2H), 6.88 (s, 1H), 5.90 (d, J = 3.7 Hz, 1H), 4.84 (t, J = 4.3 Hz, 1H), 4.0 (s, 3H), 3.92 (s, 3H), 2.98-2.90 (dd, J = 18.1 Hz, 1H), 2.77-2.71 (d, J = 18.1 Hz, 1H); ^{13}C NMR (125 MHz, $CDCl_3$) δ 175.5, 152.7, 146.4, 128.1, 127.2, 127.0, 126.3, 122.9, 121.8, 102.0, 82.1, 70.0, 62.4, 56.1, 38.4.

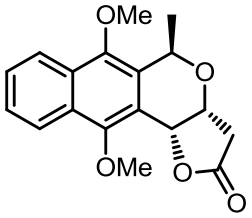

(3aR,5R,11bR)-6,11-dimethoxy-5-methyl-3,3a,5,11b-tetrahydro-2H-benzo[g]furo[3,2-c]isochromen-2-one (4-45): Compound **4-44** (0.10 g, 0.34 mmol) was dissolved in anhydrous DCM (3.45 ml). To this solution, acetaldehyde (0.02 ml, 0.38 mmol) was added. The reaction mixture was cooled to 0 ^{o}C. To it, boron trifluoride diethyl etherate (0.04 ml, 0.36 mmol) was added drop wise. The reaction was allowed to warm to room temperature overnight. It was then quenched with saturated aqueous sodium bicarbonate solution, extracted with DCM. The organic layer was dried over Na_2SO_4, concentrated in vacuo and purified on silica gel (3:1 hexanes/EtOAc) to yield 0.10 g (d.r. >95:5) of **4-45** (93%). ^{1}H NMR (400 MHz, $CDCl_3$) δ 8.10 (d, J = 8.6 Hz, 1H), 8.03 (d, J = 8.3 Hz, 1H), 7.58-7.50 (m, 2H), 5.60 (d, J = 2.6 Hz, 1H), 5.35 (q, J = 6.8 Hz, 1H), 4.7 (q, J = 2.8, 2.0 Hz, 1H), 4.08 (s, 3H), 3.93 (s, 3H), 3.00 (dd, J = 17.8, 1H), 2.70 (d, J = 17.5 Hz, 1H), 1.53 (d, J = 6.7 Hz, 3H).

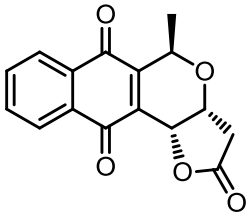

(3aR,5R,11bR)-5-methyl-3,3a-dihydro-2H-benzo[g]furo[3,2-c]isochromene-2,6,11(5H,11bH)-trione (4-46): Compound **4-45** (0.10 g, 0.32 mmol) was dissolved in acetonitrile (6.8 ml). This solution was cooled to 0 ^{o}C. To this, a solution of cerium ammonium nitrate (0.41 g, 0.74 mmol) in water (6.8 ml) was added at once. The reaction mixture was stirred at 0 ^{o}C for 30 min. It was then quenched with ethyl acetate and water. The organic phase was washed several times till it was free from the cerium salt. It was then dried over Na_2SO_4, concentrated in vacuo and purified on silica gel (3:1 hexanes/EtOAc) to afford 0.07 g of **4-46** (71%) as a yellow solid. ^{1}H NMR (400 MHz, $CDCl_3$) δ 8.18-8.15 (m, 1H), 8.13-8.10 (m, 1H), 7.82-7.76 (m, 2H), 5.29 (d, J = 3.0 Hz, 1H), 5.12-5.06 (q, J = 7.0 Hz, 1H), 4.70-4.68 (q, J = 3.0 Hz, 2.1 Hz, 1H), 3.00-2.92 (dd, J = 17.6 Hz, 1H), 2.70 (d, J = 17.6, 1H), 1.54 (d, J = 6.7 Hz, 3H); ^{13}C NMR (125 MHz, $CDCl_3$) δ 183.2, 182.4, 174.0, 149.6, 134.6, 134.4, 134.3, 132.0, 131.9, 127.0, 126.7, 68.9, 66.7, 66.6, 37.1, 18.7.

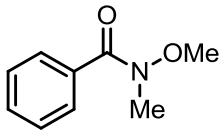

N-methoxy-N-methylbenzamide (4-51):[93] Benzoic acid (1.2 g, 9.81 mmol) was dissolved in DCM (24.54 ml). To this 1-ethyl-3-(3-dimethylaminopropyl) carbodiimide hydrochloride (2.25 g, 11.79 mmol) and N-methyl morpholine (1.08 ml, 9.81 mmol) followed by *N*,*O*-Dimethylhydroxylamine hydrochloride (1.05 g, 10.8 mmol) were added. The reaction mixture was stirred at room temperature for 4 h. It was diluted with diethyl ether. The organic layer was washed with water and brine, dried over Na_2SO_4, concentrated in vacuo and purified on silica gel (3:1 hexanes/EtOAc) to afford 1.36 g of **4-51** (84%) as a colorless oil. ^{1}H NMR (400 MHz, $CDCl_3$) δ 7.67-7.64 (d, J = 7.7 Hz, 2H), 7.45-7.35 (m, 3H), 3.55 (s, 3H), 3.35 (s, 3H); ^{13}C NMR (125 MHz, $CDCl_3$) δ 170.0, 134.3, 130.6, 128.2, 128.1, 61.1, 33.9.

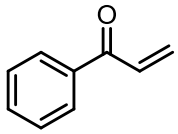

1-phenylprop-2-en-1-one (4-52):[94] N-methoxy-N-methylbenzamide (0.1 g, 0.60 mmol) was dissolved in anhydrous diethyl ether (2.01 ml). The solution was cooled to 0 ^{o}C. To this, vinyl magnesium bromide solution (0.91 ml, 1.0 M in THF) was added drop wise over 30 min at 0 ^{o}C. After the completion of addition, the reaction mixture was stirred for a further 60 min at 0 ^{o}C and for 30 min at room temperature. It was then quenched with 1M HCl at 0 ^{o}C. The reaction mixture was diluted with diethyl ether. The organic layer was washed with brine, dried over Na_2SO_4, concentrated in vacuo, purified on silica gel (3:1 hexanes/EtOAc) to afford 0.04 g of **4-52** (55%)

as a colorless oil. ^{1}H NMR (400 MHz, $CDCl_3$) δ 7.96-7.93 (d, J = 8.3 Hz, 2H), 7.60-7.55 (tt, J = 7.4 Hz, 1H), 7.51-7.46 (t, J = 8.0 Hz, 2H), 7.20-7.10 (q, J = 10.5 Hz, 6.6 Hz, 1H), 6.40 (dd, J = 17.1 Hz, 1H), 5.90 (dd, J = 10.6 Hz, 1H); ^{13}C NMR (125 MHz, $CDCl_3$) δ 191.2, 137.5, 133.1, 132.6, 130.2, 128.8, 128.7.

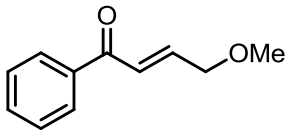

(E)-4-methoxy-1-phenylbut-2-en-1-one (4-54):[95] 1-phenylprop-2-en-1-one (0.23 g, 1.73 mmol) and 3-methoxyprop-1-ene (0.05 g, 0.69 mmol) were dissolved in anhydrous DCM (3.46 ml) under argon. To this solution, the cross-metathesis catalyst [CAS number 253688-91-4 (0.02 g, 0.02 mmol)] was added. The reaction mixture was refluxed overnight (maintaining the temperature below 42 ^{o}C) under argon. It was then cooled to room temperature, concentrated in vacuo and purified on silica gel (3:1 hexanes/EtOAc) to afford 0.04 g of **4-54** (30%) as a brown oil (E:Z >20:1). ^{1}H NMR (400 MHz, $CDCl_3$) δ 7.99-7.95 (d, J = 8.3 Hz, 2H), 7.59-7.54 (tt, J = 7.4 Hz, 1H), 7.50-7.45 (tt, J = 7.7 Hz, 2H), 7.20-7.14 (dt, J = 15.5, 1H), 7.08-7.01(dt, J = 15.5 Hz, 1H), 4.20 (q, J = 2.0 Hz, 1.8 Hz, 2H), 3.46 (s, 3H); ^{13}C NMR (125 MHz, $CDCl_3$) δ 190.4, 144.4, 137.8, 133.0, 128.8, 128.7, 124.9, 71.8, 58.9.

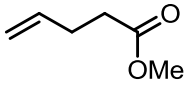

Methyl pent-4-enoate (4-55):[96] Pent-4-enoic acid (0.83 g, 8.29 mmol) and potassium carbonate (5.69 g, 41.17 mmol) were dissolved in acetone (8.16 ml). To this suspension, iodomethane (2.55 ml, 40.96 mmol) was added drop wise at room temperature. This suspension was refluxed at 60 ^{o}C overnight. The reaction mixture was cooled to room temperature, diluted with diethyl ether. The organic layer was washed with ammonium chloride solution, dried over Na_2SO_4, concentrated at reduced pressure to afford 0.54 g of **4-55** (57%) as a colorless oil. ^{1}H NMR (400 MHz, $CDCl_3$) δ 5.86-5.76 (m, 1H), 5.08-4.95 (m, 2H), 3.67 (s, 3H), 2.43-2.36 (m, 4H); ^{13}C NMR (125 MHz, $CDCl_3$) δ 173.6, 136.8, 115.6, 51.6, 33.5, 28.9.

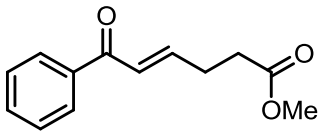

(E)-methyl 6-oxo-6-phenylhex-4-enoate (4-56):[95] 1-phenylprop-2-en-1-one (0.28 g, 2.18 mmol) and Methyl pent-4-enoate (0.10 g, 0.88 mmol) were dissolved in anhydrous DCM (4.38 ml) under argon. To this solution, the cross-metathesis catalyst [CAS number 253688-91-4 (30 mg, 0.04 mmol)] was added. The reaction mixture was refluxed overnight under argon. It was then cooled to room temperature, concentrated in vacuo and purified on silica gel (3:1 hexanes/EtOAc) to afford 0.08 g of **4-56** (41%) as a brown oil (E:Z >20:1). ^{1}H NMR (400 MHz, $CDCl_3$) δ 7.9 (d, J = 8.3 Hz, 2H), 7.55 (t, J = 7.3 Hz, 1H), 7.45 (t, J = 7.8 Hz, 7.3 Hz, 2H), 7.0 (m, 1H), 6.9 (dt, J = 15.5 Hz, 1H), 3.7 (s, 3H), 2.6 (q, J = 7.0 Hz, 2H), 2.5 (t, J = 7.0 Hz, 2H); ^{13}C NMR (125 MHz, $CDCl_3$) δ 190.6, 172.8, 146.8, 137.9, 132.8, 128.6, 126.8, 51.8, 32.6, 27.9.

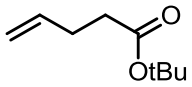

tert-butyl pent-4-enoate (4-57):[97] Pent-4-enoic acid (0.10 g, 0.99 mmol) was dissolved in DCM (0.49 ml). To this solution, t-butanol (0.38 ml, 0.29 mmol) and 4-DMAP (1.95 mg, 0.01 mmol) were added. This mixture was cooled to 0 ^{o}C. Then, *N,N'*-Dicyclohexylcarbodiimide (0.22 g, 1.09 mmol) was added. The reaction mixture was stirred at 0 ^{o}C for 15 min and at room temperature for 20 h. The reaction mixture was filtered through celite. The organic layer was washed with 0.1 M HCl, saturated aqueous sodium bicarbonate solution and water. It was dried over Na_2SO_4, concentrated in vacuo and purified on silica gel (3:1 hexanes/EtOAc) to afford 0.06 g of **4-57** (40%) as a colorless oil. ^{1}H NMR (400 MHz, $CDCl_3$) δ 5.86-5.76 (m, 1H), 5.08-4.96 (m, 2H), 2.36-2.27 (m, 4H), 1.44 (s, 9H); ^{13}C NMR(125 MHz, $CDCl_3$) δ 172.5, 137.1, 115.3, 80.3, 55.9, 34.9, 29.2, 28.3, 25.6, 24.8, 21.9.

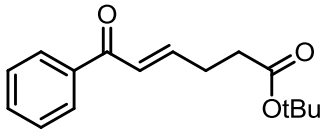

(E)-tert-butyl 6-oxo-6-phenylhex-4-enoate (4-58):[95] 1-phenylprop-2-en-1-one (0.11 g, 0.80 mmol) and tert-butyl pent-4-enoate (0.05 g, 0.32 mmol) were dissolved in anhydrous DCM (1.6 ml) under argon. To this solution, the cross-metathesis catalyst [CAS number 253688-91-4 (0.01 g, 0.01 mmol)] was added. The reaction mixture was refluxed overnight under argon. It was then cooled to room temperature, concentrated in vacuo and purified on silica gel (EtOAc : hexanes = 1 : 3) to afford 0.04 g of **4-58** (46%) as a brown oil (E:Z >20:1). ^{1}H NMR (400 MHz, $CDCl_3$) δ 7.9 (d, *J* = 8.4 Hz, 2H), 7.57-7.52 (tt, *J* = 7.4 Hz, 1H), 7.48-7.42 (tt, *J* = 7.7 Hz, 2H), 7.06-6.99 (m, 1H), 6.94-6.88 (dt, J = 15.5 Hz, 1H), 2.63-2.57 (q, *J* = 6.9 Hz, 2H), 2.48-2.42 (t, *J*

= 7.3 Hz, 2H), 1.47 (s, 9H); ^{13}C NMR (125 MHz, $CDCl_3$) δ 190.7, 171.7, 147.5, 138.0, 132.8, 128.7, 126.7, 80.9, 53.5, 34.0, 28.2.

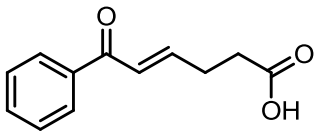

(E)-6-oxo-6-phenylhex-4-enoic acid (4-59):[98] (E)-tert-butyl 6-oxo-6-phenylhex-4-enoate (0.03 g, 0.13 mmol) was dissolved in anhydrous DCM (1.26 ml). To this solution, triethylsilane (0.05 ml, 0.31 mmol) was added followed by the drop wise addition of trifluoroacetic acid (0.09 ml, 1.18 mmol). The reaction mixture was stirred at room temperature for 6 h. The solvent was concentrated in vacuo and the crude product was purified on silica gel (1:20 methanol/DCM) to afford 0.01 g of **4-59** (36%) as a white solid. There was another product formed during this reaction which tailed on TLC plate in 40% EtOAc-hexanes (R_f = 0.3) solvent system, but it could not be characterized by NMR data. Based on the mass spectrum, a majority of this compound **4-59** was found to exist as dimers, and the minor portion consisted of trimers and monomers. ^{1}H NMR (400 MHz, $CDCl_3$) δ 8.00 (d, J = 8.3 Hz, 2H), 7.68-7.62 (tt, J = 7.3 Hz, 1H), 7.52 (t, J = 7.9 Hz, 7.4 Hz, 2H), 5.16-5.08 (m, 1H), 3.65-3.57 (dd, J = 17.4 Hz, 1H), 3.42-3.35 (dd, J = 17.5 Hz, 1H), 2.65-2.50 (m, 3H), 2.09-1.98 (m, 1H); ^{13}C NMR (125 MHz, $CDCl_3$) δ 134.6, 129.8, 129.2, 78.7, 44.7, 29.4.

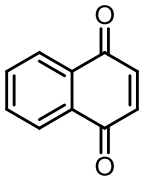

Naphthalene-1,4-dione (4-60): 1,4-dimethoxynaphthalene (0.05 g, 0.26 mmol) was dissolved in acetonitrile (5.3 ml). This solution was cooled to 0 ^{o}C. To this, a solution of cerium ammonium nitrate (0.34 g, 0.61 mmol) in water (5.3 ml) was added at once. The reaction mixture was stirred at 0 ^{o}C for 30 min. It was then quenched with ethyl acetate and water. The organic phase was washed several times till it was free from the cerium salt. It was then dried over Na_2SO_4, concentrated in vacuo and purified on silica gel (3:1 hexanes/EtOAc) to afford 0.03 g of **4-60** (81%) as a yellow solid. ^{1}H NMR (400 MHz, $CDCl_3$) δ 8.12-8.07 (m, 2H), 7.79-7.74 (m, 2H), 7.00 (s, 2H); ^{13}C NMR (125 MHz, $CDCl_3$) δ 138.8, 134.1, 132.1, 126.6.

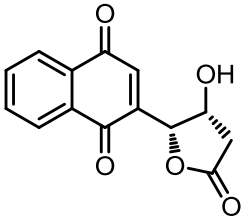

2-((2R,3R)-3-hydroxy-5-oxotetrahydrofuran-2-yl)naphthalene-1,4-dione (4-61): (4R,5R)-5-(1,4-dimethoxynaphthalen-2-yl)-4-hydroxydihydrofuran-2(3H)-one (0.04 g, 0.12 mmol) was dissolved in acetonitrile (2.4 ml). This solution was cooled to 0 ^{o}C. To this, a solution of cerium ammonium nitrate (0.15 g, 0.28 mmol) in water (2.4 ml) was added at once. The reaction mixture was stirred at 0 ^{o}C for 30 min. It was then quenched with ethyl acetate and water. The organic phase was washed several times till it was free from the cerium salt. It was then dried

over Na_2SO_4, concentrated in vacuo and purified on silica gel (1:1 hexanes/EtOAc) to afford 0.02 g of **4-61** (65%) as a yellowish-brown solid. ^{1}H NMR (400 MHz, $CDCl_3$) δ 8.13-8.08 (td, 6.87 Hz,7.0 Hz, 2H), 7.82-7.76 (m, 2H), 7.17 (d, *J* = 1.9 Hz, 1H), 5.60 (dd, *J* = 4.2 Hz, 1H), 5.07 (t, *J* = 5.1 Hz, 1H), 3.02-2.95 (dd, *J* = 18 Hz, 1H), 2.72-2.66 (d, *J* = 17.8 Hz, 1H); ^{13}C NMR (125 MHz, $CDCl_3$) δ 184.8, 184.1, 173.8, 143.8, 135.6, 134.6, 134.1, 132.2, 131.8, 126.7, 126.5, 80.6, 69.5, 38.6.

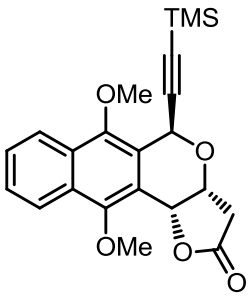

(3aR,5S,11bR)-6,11-dimethoxy-5-((trimethylsilyl)ethynyl)-3,3a,5,11b-tetrahydro-2H-benzo[g]furo[3,2-c]isochromen-2-one (4-65): Compound **4-46** (0.30 g, 1.04 mmol) was dissolved in anhydrous DCM (10.34 ml). To this solution, 3-(trimethylsilyl)propiolaldehyde (0.17 ml, 1.14 mmol) was added. The reaction mixture was cooled to 0 ^{o}C. To it, boron trifluoride diethyl etherate (0.13 ml, 1.05 mmol) was added drop wise. The reaction was allowed to warm to room temperature overnight. It was then quenched with saturated aqueous sodium bicarbonate solution, extracted with DCM. The organic layer was dried over Na_2SO_4, concentrated in vacuo and purified on silica gel (3:1 hexanes/EtOAc) to yield 0.18 g (d.r. 1:1) of **4-65** (43%),. About 40% of another diastereomer was formed. ^{1}H NMR (400 MHz, $CDCl_3$) δ 8.16-8.13 (dd, *J* = 8.0 Hz, 1H), 8.10-8.07 (dd, *J* = 6.8 Hz, 1H), 7.62-7.54 (m, 2H), 6.05 (s, 1H), 5.63 (d, *J* = 2.8 Hz, 1H), 5.07-5.04 (q, *J* = 2.9 Hz, 2.3 Hz, 1H), 4.15 (s, 3H), 4.05 (s, 3H), 3.08-3.00 (dd, *J* = 17.7, 1H), 2.80 (d, *J* = 17.9 Hz, 1H), 0.13 (s, 9H); ^{13}C NMR (125 MHz, $CDCl_3$) δ

174.9, 153.8, 148.1, 129.3, 128.5, 127.4, 126.6, 123.7, 123.3, 122.8, 117.5, 102.4, 92.9, 72.3, 68.8, 64.4, 62.4, 62.3, 37.5.

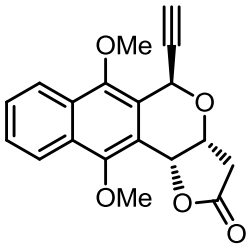

(3aR,5R,11bR)-5-ethynyl-6,11-dimethoxy-3,3a,5,11b-tetrahydro-2H-benzo[g]furo[3,2-c]isochromen-2-one (4-66): Compound **4-65** (0.18 g, 0.45 mmol) was dissolved in tetrahydrofuan (4.02 ml). To this solution, tetrabutylammoniumflouride solution (0.49 ml, 1.0 M in THF) was added. The reaction mixture was stirred at room temperature for 1 h. The organic layer was washed with saturated aqueous ammonium chloride solution, extracted with DCM. The DCM layer was dried over Na_2SO_4, concentrated in vacuo and purified on silica gel (3:1 hexanes/EtOAc to yield 0.07 g of **4-66** (44%). A major quantity of the starting material was degraded during the reaction resulting in low yield of the desired product. ^{1}H NMR (400 MHz, $CDCl_3$) δ 8.16-8.13 (dd, J = 7.9 Hz, 1H), 8.11-8.07 (dd, J = 8.0 Hz, 1H), 7.63-7.55 (m, 2H), 6.03 (d, J = 2.3 Hz, 1H), 5.64 (d, J = 2.8 Hz, 1H), 5.09-5.06 (q, J = 3.0 Hz, 2.4 Hz, 1H), 4.12 (s, 3H), 4.05 (s, 3H), 3.08-3.01 (dd, J = 17.9, 1H), 2.82-2.77 (d, J = 17.8 Hz, 1H), 2.61 (d, J = 2.3 Hz, 1H).

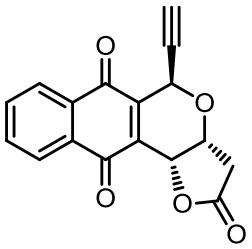

(3aR,5R,11bR)-5-ethynyl-3,3a-dihydro-2H-benzo[g]furo[3,2-c]isochromene-2,6,11(5H,11bH)-trione (4-63): Compound **4-66** (0.07 g, 0.20 mmol) was dissolved in acetonitrile (4.26 ml). This solution was cooled to 0 ^{o}C. To this, a solution of cerium ammonium nitrate (0.25 g, 0.46 mmol) in water (4.26 ml) was added at once. The reaction mixture was stirred at 0 ^{o}C for 30 min. It was then quenched with ethyl acetate and water. The organic phase was washed several times till it was free from the cerium salt. It was then dried over Na_2SO_4, concentrated in vacuo and purified on silica gel (3:1 hexanes/EtOAc) to afford 0.03 g of **4-63** (60%) as a yellow unstable solid. ^{1}H NMR (400 MHz, $CDCl_3$) δ 8.20-8.13 (m, 2H), 7.85-7.80 (m, 2H), 5.69 (d, J = 2.4 Hz, 1H), 5.29 (d, J = 3.1 Hz, 1H), 4.96-4.93 (q, J = 3.3 Hz, 3.1 Hz, 2.1 Hz, 1H), 3.05-2.99 (dd, J = 18.0 Hz, 1H), 2.80-2.76 (d, J = 17.9, 1H), 2.64 (d, J = 2.3 Hz, 1H).

List of References

List of References

1. Khoury, G. A.; Baliban, R. C.; Floudas, C. A. Proteome-wide post-translational modification statistics: frequency analysis and curation of the swiss-prot database. *Sci. Rep.* **2011**, *1*, 1-5.

2. Manning, G.; Whyte, D. B.; Martinez, R.; Hunter, T.; Sudarsanam, S. The protein kinase complement of the human genome. *Science* **2002**, *298*, 1912-1916.

3. Hanks, S. K.; Hunter, T. Protein kinases 6. The eukaryotic protein kinase superfamily: kinase (catalytic) domain structure and classification. *FASEB. J.* **1995**, *9*, 576-596.

4. Hauge, C.; Antal, T. L.; Hirschberg, D.; Doehn, U.; Thorup, K.; Idrissova, L.; Hansen, K.; Jensen, O. N.; Jørgensen, T. J.; Biondi, R. M.; Frödin, M. Mechanism for activation of the growth factor-activated AGC kinases by turn motif phosphorylation. *EMBO. J.* **2007**, *26*, 2251-2261.

5. Knighton, D. R.; Zheng, J.; Eyck, L. T.; Ashford, V. A.; Xuong, N. H.; Taylor, S. S.; Sowadski, J. M. Crystal structure of the catalytic subunit of cyclic adenosine monophosphate-dependent protein kinase. *Science* **1991**, *253*, 407-414.

6. Staal, S. P.; Hartley, J. W.; Rowe, W. P. Molecular cloning of the akt oncogene and its human homologues AKT1and AKT2: Amplification of AKT1 in a primary human gastric adenocarcinoma. *P. Natl. Acad. Sci. USA.* **1987**, *84*, 5034-5037.

7. Chen, W. S.; Xu, P. Z.; Gottlob, K.; Chen, M. L.; Sokol, K.; Shiyanova, T.; Roninson, I.; Weng, W.; Suzuki, R.; Tobe, K.; Kadowaki, T.; Hay, N. Growth retardation and increased apoptosis in mice with homozygous disruption of the Akt1 gene. *Genes. Dev.* **2001**, *15*, 2203-2208.

8. Garofalo, R. S.; Orena, S. J.; Rafidi, K.; Torchia, A. J.; Stock, J. L.; Hildebrandt, A. L.; Coskran, T.; Black, S. C.; Brees, D. J.; Wicks, J. R.; McNeish, J. D.; Coleman, K. G. Severe diabetes, age-dependent loss of adipose tissue, and mild growth deficiency in mice lacking Akt2/PKBβ. *J. Clin. Invest.* **2003**, *112*, 197-208.

9. Kumar, C. C.; Madison, V. AKT crystal structure and AKT-specific inhibitors. *Oncogene* **2005**, *24,* 7493-7501.

10. Nicholson, K. M.; Anderson, N. G. The protein kinase B/Akt signalling pathway in human malignancy. *Cell. Signal.* **2002**, *14,* 381-395.

11. Thomas, C. C.; Deak, M.; Alessi, D. R.; Aalten, D. F. High-resolution structure of the pleckstrinhomology domain of protein kinase B/Akt boundto phosphatidylinositol (3,4,5)-trisphosphate. *Curr. Biol.* **2002**, *12,* 1256-1262.

12. Yang, J.; Cron, P.; Good, V. M.; Thompson, V.; Hemmings, B. A.; Barford, D. Crystal structure of an activated Akt/protein kinase B ternary complex with GSK3-peptide and AMP-PNP. *Nat. Struct. Biol.* **2002**, *9,* 940-944.

13. Franke, T. F.; Yang, S.; Chan, T. O.; Datta, K.; Kazlauskas, A.; Morrison, D. K.; Kaplan, D. R.; Tsichlis, P. N. The protein kinase encoded by the Akt proto-oncogene is a target of the PDGF-activated Phosphatidylinositol 3-Kinase. *Cell* **1995**, *81,* 721-736.

14. Heldin, C. H. Dimerization of cell surface receptors in signal transduction. *Cell* **1995**, *80,* 213-223.

15. Bellacosa, A.; Chan, T. O.; Ahmed, N. N.; Datta, K.; Malstrom, S.; Stokoe, D.; McCormick, F.; Feng, J.; Tsichlis, P. Akt activation by growth factors is a multiple-step process: the role of the PH domain. *Oncogene* **1998**, *17,* 313-325.

16. Alessi, D. R.; James, S. R.; Downes, C. P.; Holmes, A. B.; Gaffney, P. J.; Reese, C. B.; Cohen, P. Characterization of a 3-phosphoinositide-dependent protein kinase which phosphorylates and activates protein kinase Bα. *Curr. Biol.* **1997**, *7,* 261-269.

17. Anderson, K. E.; Coadwell, J.; Stephens, L. R.; Hawkins, P. T. Translocation of PDK-1 to the plasma membrane is important in allowing PDK-1 to activate protein kinase B. *Curr. Biol.* **1998**, *8,* 684-691.

18. Currie, R. A.; Walker, K. S.; Gray, A.; Deak, M.; Casamayor, A.; Downes, C. P.; Cohen, P.; Alessi, D. R.; Lucocq, J. Role of phosphatidylinositol 3,4,5-trisphosphate in regulating the activity and localization of 3-phosphoinositide-dependent protein kinase-1. *Biochem. J.* **1999**, *337,* 575-583.

19. Stokoe, D.; Stephens, L. R.; Copeland, T.; Gaffney, P. J.; Reese, C. B.; Painter, G. F.; Holmes, A. B.; McCormick, F.; Hawkins, P. T. Dual role of phosphatidylinositol-3,4,5-trisphosphate in the activation of protein kinase B. *Science* **1997**, *277,* 567-570.

20. Delcommenne, M.; Tan, C.; Gray, V.; Rue, L.; Woodgett, J.; Dedhar, S. Phosphoinositide-3-OH kinase-dependent regulation of glycogen synthase kinase 3 and protein kinase B/AKT by the integrin-linked kinase. *P. Natl. Acad. Sci. USA.* **1998**, *95,* 11211-11216.

21. Balendran, A.; Casamayor, A.; Deak, M.; Paterson, A.; Gaffney, P.; Currie, R.; Downes, C. P.; Alessi, D. R. PDK1 acquires PDK2 activity in the presence of a synthetic peptide derived from the carboxyl terminus of PRK2. *Curr. Biol.* **1999**, *9*, 393-404.

22. Sarbassov, D. D.; Guertin, D. A.; Ali, S. M.; Sabatini, D. M. Phosphorylation and regulation of Akt/PKB by the rictor-mTOR Complex. *Science* **2005**, *307*, 1098-1101.

23. Bozulic, L.; Surucu, B.; Hynx, D.; Hemmings, B. A. PKBα/Akt1 Acts Downstream of DNA-PK in the DNA Double-Strand Break Response and Promotes Survival. *Mol. Cell* **2008**, *30*, 203-213.

24. King, W. G.; Mattaliano, M. D.; Chan, T. O.; Tsichlis, P. N.; Brugge, J. S. Phosphatidylinositol 3-kinase is required for integrin-stimulated AKT and Raf-1/mitogen-activated protein kinase pathway activation. *Mol. Cell Biol.* **1997**, *17*, 4406-4418.

25. Chen, H. C.; Guan, J. L. Association of focal adhesion kinase with its potential substrate phosphatidylinositol 3-kinase. *P. Natl. Acad. Sci. USA.* **1994**, *91*, 10148-10152.

26. Gold, M. R.; Scheid, M. P.; Santos, L.; Lawson, M. D.; Roth, R. A.; Matsuuchi, L.; Duronio, V.; Krebs, D. L. The B cell antigen receptor activates the Akt (protein kinase B)/glycogen synthase kinase-3 signaling pathway via phosphatidylinositol 3-kinase. *J. Immunol.* **1999**, *163*, 1894-1905.

27. Takahashi, T.; Taniguchi, T.; Konishi, H.; Kikkawa, U.; Ishikawa, Y.; Yokoyama, M. Activation of Akt/protein kinase B after stimulation with angiotensin II in vascular smooth muscle cells. *Am. J. Physiol-Heart C.* **1999**, *276*, H1927-H1934.

28. Fukai, M. U.; Alexander, R. W.; Akers, M.; Yin, Q. Q.; Fujio, Y.; Walsh, K.; Griendling, K. K. Reactive oxygen species mediate the activation of Akt/protein kinase B by angiotensin II in vascular smooth muscle cells. *J. Biol. Chem.* **1999**, *274*, 22699-22704.

29. Steck, P. A.; Pershouse, M. A.; Jasser, S. A.; Yung, W. A.; Lin, H.; Ligon, A. H.; Langford, L. A.; Baumgard, M. L.; Hattier, T.; Davis, T.; Frye, C.; Hu, R.; Swedlund, B.; Teng, D. F.; Tavtigian, S. V. Identification of a candidate tumour suppressor gene, MMAC1, at chromosome 10q23.3 that is mutated in multiple advanced cancers. *Nat. Genet.* **1997**, *15*, 356-362.

30. Myers, M. P.; Pass, I.; Batty, I. H.; Kaay, J. D.; Stolarov, J. P.; Hemmings, B. A.; Wigler, M. H.; Downes, C. P.; Tonks, N. K. The lipid phosphatase activity of PTEN is critical for its tumor supressor function. *P. Natl. Acad. Sci. USA.* **1998**, *95*, 13513-13518.

31. Wu, X.; Senechal, K.; Neshat, M. S.; Whang, Y. E.; Sawyers, C. L. The PTEN/MMAC1 tumor suppressor phosphatase functions as a negative regulator of the phosphoinositide 3-kinase/AKT pathway. *P. Natl. Acad. Sci. USA.* **1998**, *95*, 15587-15591.

32. Tamura, M.; Gu, J.; Matsumoto, K.; Aota, S.; Parsons, R.; Yamada, K. M. Inhibition of cell migration, spreading, and focal adhesions by tumor suppressor PTEN. *Science* **1998**, *280,* 1614-1617.

33. Liu, Q.; Sasaki, T.; Kozieradzki, I.; Wakeham, A.; Itie, A.; Dumont, D. J.; Penninger, J. M. SHIP is a negative regulator of growth factor receptor-mediated PKB/Akt activation and myeloid cell survival. *Gene. Dev.* **1999**, *13,* 786-791.

34. Aman, M. J.; Lamkin, T. D.; Okada, H.; Kurosaki, T.; Ravichandran, K. S. The inositol phosphatase SHIP inhibits Akt/PKB activation in B cells. *J. Biol. Chem.* **1998**, *273,* 33922-33928.

35. Calleja, V.; Laguerre, M.; Parker, P. J.; Larijani, B. Role of a novel PH-kinase domain interface in PKB/Akt regulation: structural mechanism for allosteric inhibition. *PLOS. Biol.* **2009**, *7,* 0189-0200.

36. Alessi, D. R.; Caudwell, B. F.; Andjelkovic, M.; Hemmings, B. A.; Cohen, P. Molecular basis for the substrate specificity of protein kinase B; comparison with MAPKAP kinase-1 and p70 S6 kinase. *FEBS. Lett.* **1996**, *399,* 333-338.

37. Welsh, G. I.; Proud, C. G. Glycogen synthase kinase-3 is rapidly inactivated in response to insulin and phosphorylates eukaryotic initiation factor elF-2B. *Biochemical. J.* **1993**, *294,* 625-629.

38. Saito, Y.; Vandenheedet, J. R.; Cohen, P. The mechanism by which epidermal growth factor inhibits glycogen synthase kinase 3 in A431 cells. *Biochemical J.* **1994**, *303,* 27-31.

39. Woodgett, J. R. A common denominator linking glycogen metabolism, nuclear oncogenes and development. *Trends Biochem. Sci.* **1991**, *16,* 177-181.

40. Burgering, B. M. T.; Medema, R. H. Decisions on life and death: FOXO Forkhead transcription factors are in command when PKB/Akt is off duty. *J. Leucocyte. Biol.* **2003**, *73,* 689-701.

41. Brunet, A.; Bonni, A.; Zigmond, M. J.; Lin, M. Z.; Juo, P.; Hu, L. S.; Anderson, M. J.; Arden, K. C.; Blenis, J.; Greenberg, M. E. Akt promotes cell survival by phosphorylating and inhibiting a forkhead transcription factor. *Cell* **1999**, *96,* 857-868.

42. Datta, S. R.; Dudek, H.; Tao, X.; Masters, S.; Fu, H.; Gotoh, Y.; Greenberg, M. E. Akt Phosphorylation of BAD Couples Survival Signals to the Cell-Intrinsic Death Machinery. *Cell* **1997**, *91,* 231-241.

43. Datta, S. R.; Katsov, A.; Hu, L.; Petros, A.; Fesik, S. W.; Yaffe, M. B.; Greenberg, M. E. 14-3-3 Proteins and Survival Kinases Cooperate to Inactivate BAD by BH3 Domain Phosphorylation. *Mol. Cell* **2000**, *6,* 41-51.

44. Manning, B. D.; Tee, A. R.; Logsdon, M. N.; Blenis, J.; Cantley, L. C. Identification of the Tuberous Sclerosis Complex-2 Tumor Suppressor Gene Product Tuberin as a Target of the Phosphoinositide 3-Kinase/Akt Pathway. *Mol. Cell* **2002**, *10*, 151-162.

45. Huang, J.; Manning, B. D. A complex interplay between Akt, TSC2 and the two mTOR complexes. *Biochem. Soc. Trans.* **2009**, *37*, 217-222.

46. Manning, B. D.; Cantley, L. C. AKT/PKB Signaling: Navigating Downstream. *Cell* **2007**, *129*, 1261-1274.

47. Cheng, J. Q.; Godwin, A. K.; Bellacosa, A.; Taguchi, T.; Franke, T. F.; Hamilton, T. C.; Tsichlis, P. N.; Testa, J. R. AKT2, a putative oncogene encoding a member of a subfamily of protein-serine/threonine kinases, is amplified in human ovarian carcinomas. *P. Natl. Acad. Sci. USA.* **1992**, *89*, 9267-9271.

48. Bellacosa, A.; De Feo, D.; Godwin, A. K.; Bell, D. W.; Cheng, J. Q.; Altomare, D. A.; Wan, M.; Dubeau, L.; Scambia, G.; Masciullo, V.; Ferrandina, G.; Panici, P. B.; Mancuso, S.; Neri, G.; Testa, J. R. Molecular alterations of the AKT2 oncogene in ovarian and breast carcinomas. *Int. J. Cancer* **1995**, *64*, 280-285.

49. Testa, J. R.; Bellacosa, A. AKT plays a central role in tumorigenesis. *P. Natl. Acad. Sci. USA.* **2001**, *98*, 10983-10985.

50. Ruggeri, B. A.; Huang, L.; Wood, M.; Cheng, J. Q.; Testa, J. R. Amplification and overexpression of the AKT2 oncogene in a subset of human pancreatic ductal adenocarcinomas. *Mol. Carcinog.* **1998**, *21*, 81-86.

51. Xu, X.; Sakon, M.; Nagano, H.; Hiraoka, N.; Yamamoto, H.; Hayashi, N.; Dono, K.; Nakamori, S.; Umeshita, K.; Ito, Y.; Matsuura, N.; Monden, M. Akt2 expression correlates with prognosis of human hepatocellular carcinoma. *Oncol. Rep.* **2004**, *11*, 25-32.

52. Arboleda, M. J.; Lyons, F.; Kabbinavar, F. F.; Bray, M. R.; Snow, B. E.; Ayala, R.; Danino, M.; Karlan, B. Y.; Slamon, D. J.; Lee, S. H.; Kim, H. S.; Park, W. S.; Kim, S. Y.; Lee, K. Y.; Kim, S. H.; Lee, J. Y.; Yoo, N. J. Overexpression of AKT2/protein kinase Bβ leads to up-regulation of β1 integrins, increased invasion, and metastasis of human breast and ovarian cancer cells. *Cancer Res.* **2003**, *63*, 193-206.

53. Altomare, D. A.; Testa, J. R. Perturbations of the AKT signaling pathway in human cancer. *Oncogene* **2005**, *24*, 7455-7464.

54. Bellacosa, A.; Kumar, C. C.; Cristofano, A. D.; Testa, J. R. Activation of AKT kinases in cancer: implications for therapeutic targeting. *Adv. Cancer Res.* **2005**, *94*, 29-86.

55. Sun, M.; Wang, G.; Paciga, J. E.; Feldman, R. I.; Yuan, Z.; Ma, X.; Shelley, S. A.; Jove, R.; Tsichlis, P. N.; Nicosia, S. V.; Cheng, J. Q. AKT1/PKBα kinase is frequently elevated in

human cancers and its constitutive activation is required for oncogenic transformation in NIH3T3 cells. *Am. J. Pathol.* **2001**, *159*, 431-437.

56. Altomare, D. A.; Tanno, S.; De Rienzo, A.; Klein-Szanto, A. J.; Tanno, S.; Skele, K. L.; Hoffman, J. P.; Testa, J. R. Frequent activation of AKT2 kinase in human pancreatic carcinomas. *J. Cell. Biochem.* **2002**, *87*, 470-476.

57. Hanahan, D.; Weinberg, R. A. The hallmarks of cancer. *Cell* **2000**, *100*, 57-70.

58. Sordella, R.; Bell, D. W.; Haber, D. A.; Settleman, J. Gefitinib-sensitizing EGFR mutations in lung cancer activate anti-apoptotic pathways. *Science* **2004**, *305*, 1163-1167.

59. Philp, A. J.; Campbell, I. G.; Leet, C.; Vincan, E.; Rockman, S. P.; Whitehead, R. H.; Thomas, R. J.; Phillips, W. A. The phosphatidylinositol 3'-kinase p85α gene is an oncogene in human ovarian and colon tumors. *Cancer Res.* **2001**, *61*, 7426-7429.

60. Sansal, I.; Sellers, W. R. The biology and clinical relevance of the *PTEN* tumor suppressor pathway. *J. Clin. Oncol.* **2004**, *22*, 2954-2963.

61. Breitenlechner, C. B.; Wegge, T.; Berillon, L.; Graul, K.; Marzenell, K.; Friebe, W. G.; Thomas, U.; Schumacher, R.; Huber, R.; Engh, R. A.; Masjost, B. Structure-based optimization of novel azepane derivatives as PKB inhibitors. *J. Med. Chem.* **2004**, *47*, 1375-1390.

62. Reuveni, H.; Livnah, N.; Geiger, T.; Klem, S.; Ohne, O.; Cohen, I.; Benhar, M.; Gellerman, G.; Levitzki, A. Toward a PKB inhibitor: modification of a selective PKA inhibitor by rational design. *Biochemistry* **2002**, *41*, 10304-10314.

63. Li, Q.; Li, T.; Zhu, G. D.; Gong, J.; Claibone, A.; Dalton, C.; Luo, Y.; Johnson, E. F.; Shi, Y.; Liu, X.; Klinghofer, V.; Bauch, J. L.; Marsh, K. C.; Bouska, J. J.; Arries, S.; De Jong, R.; Oltersdorf, T.; Stoll, V. S.; Jakob, C. G.; Rosenberg, S. H.; Giranda, V. L. Discovery of trans-3,4'-bispyridinylethylenes as potent and novel inhibitors of protein kinase B (PKB/Akt) for the treatment of cancer: Synthesis and biological evaluation. *Bioorg. Med. Chem. Lett.* **2006**, *16*, 1679-1685.

64. Thomas, S. A.; Li, T.; Woods, K. W.; Song, X.; Packard, G.; Fischer, J. P.; Diebold, R. B.; Liu, X.; Shi, Y.; Klinghofer, V.; Johnson, E. F.; Bouska, J. J.; Olson, A.; Guan, R.; Magnone, S. R.; Marsh, K.; Luo, Y.; Rosenberg, S. H.; Giranda, V. L.; Li, Q. Identification of a novel 3,5-disubstituted pyridine as a potent, selective, and orally active inhibitor of Aktl kinase. *Bioorg. Med. Chem. Lett.* **2006**, *16*, 3740-3744.

65. Heerding, D. A.; Rhodes, N.; Leber, J. D.; Clark, T. J.; Keenan, R. M.; Lafrance, L. V.; Li, M.; Safonov, I. G.; Takata, D. T.; Venslavsky, J. W.; Yamashita, D. S.; Choudhry, A. E.; Copeland, R. A.; Lai, Z.; Schaber, M. D.; Tummino, P. J.; Strum, S. L.; Wood, E. R.; Duckett, D. R.; Eberwein, D.; Knick, V. B.; Lansing, T. J.; McConnell, R. T.; Zhang, S. Y.; Minthorn, E. A.; Concha, N. O.; Warren, G. L.; Kumar, R. Identification of 4-(2-(4-Amino-

I,2,5-oxadiazol-3-yl)-I-ethyl-7-{ [(3S)- 3-piperidinylmethyl]oxy }-I *H*imidazo[4,5-c]pyridin-4-yl)-2-methyl-3-butyn-2-01 (GSK690693), a Novel Inhibitor of AKT Kinase. *J. Med. Chem.* **2008**, *51,* 5663-5679.

66. Lippa, B.; Pan, G.; Corbett, M.; Li, C.; Kauffmam, G. S.; Pandit, J.; Robinson, S.; Wei, L.; Kozina, E.; Marr, E. S.; Borzillo, G.; Knauth, E.; Barbacci-Tobin, E. G.; Vincent, P.; Troutman, M.; Baker, D.; Rajamohan, F.; Kakar, S.; Clark, T.; Morris, J. Synthesis and structure based optimization of novel Akt inhibitors. *Bioorg. Med. Chem. Lett.* **2008**, *18,* 3359-3363.

67. Powis, G.; Aksoy, I. A.; Melder, D. C.; Aksoy, S.; Eichinger, H.; Fauq, A. H.; Kozikowski, A. P. D-3-deoxy-3-substituted myoinositol analogues as inhibitors of cell growth. *Cancer Chemother. Pharmacol.* **1991**, *29,* 95-104.

68. Kozikowski, A. P.; Kiddle, J. J.; Frew, T.; Berggren, M.; Powis, G. Synthesis and biology of 1 D-3-deoxyphosphatidylinositol: a putative antimetabolite of phosphatidylinositol-3-phosphate and an inhibitor of cancer cell colony formation. *J. Med. Chem.* **1995**, *38,* 1053-1056.

69. Qiao, L.; Nan, F.; Kunkel, M.; Gallegos, A.; Powis, G.; Kozikowski, A. P. 3-Deoxy-D-myo-inositol 1-phosphate,1I-phosphonate, and ether lipid analogues as inhibitors of phosphatidylinositol-3-kinase signaling and cancer cell growth. *J. Med. Chem.* **1998**, *41,* 3303-3306.

70. Castillo, S. S.; Brognard, J.; Petukhov, P. A.; Zhang, C. Y.; Tsurutani, J.; Granville, C. A.; Li, M.; Jung, M.; West, K. A.; Gills, J. G.; Kozikowski, A. P.; Dennis, P. A. Preferential inhibition of Akt and killing of Akt-dependent cancer cells by rationally designed phosphatidylinositol ether lipid analogues. *Cancer Res.* **2004**, *64,* 2782-2792.

71. Obata, T.; Yaffe, M. B.; Leparc, G. G.; Piro, E. T.; Maegawa, H.; Kashiwagi, A.; Kikkawa, R.; Cantley, L. C. Peptide and protein library screening defines optimal substratemotifs for AKT/PKB. *J. Biol. Chem.* **2000**, *275,* 36108-36115.

72. Luo, Y.; Smith, R. A.; Guan, R.; Liu, X. S.; Klinghofer, V.; Shen, J. W.; Hutchins, C.; Richardson, P.; Holzman, T.; Rosenberg, S. H.; Giranda, V. L. Pseudosubstrate peptides inhibit Akt and induce cell growth inhibition. *Biochemistry* **2004**, *43,* 1254-1263.

73. Kayser, K. J.; Glenn, M. P.; Sebti, S. M.; Cheng, J. Q.; Hamilton, A. D. Modifications of the GSK3b substrate sequence to producesubstrate-mimetic inhibitors of Akt as potential anti-cancer therapeutics. *Bioorg. Med. Chem. Lett.* **2007**, *17,* 2068-2073.

74. Kayser-Bricker, K. J.; Glenn, M. P.; Lee, S. H.; Sebti, S. M.; Cheng, J. Q.; Hamilton, A. D. Non-peptidic substrate-mimetic inhibitors of Akt as potential anti-cancer agents. *Bioorg. Med. Chem.* **2009**, *17,* 1764-1771.

75. Barnett, S. F.; Defeo-Jones, D.; Fu, S.; Hancock, P. J.; Haskell, K. M.; Jones, R. E.; Kahana, J. A.; Kral, A. M.; Leander, K.; Lee, L. L.; Malinowski, J.; McAvoy, E. M.; Nahas, D. D.; Robinson, R.; Huber, H. E. Identification and characterization of pleckstrin homology domain dependent and isozyme specific Akt inhibitors. *Biochem. J.* **2004**, *385*, 399-408.

76. Lindsley, C. W. The Akt/PKB family of protein kinases: a review of small molecule inhibitors and progress towards target validation: a 2009 update. *Curr. Top. Med. Chem.* **2010**, *10*, 458-477.

77. Lindsley, C. W.; Zhao, Z.; Duggan, M. E.; Barnett, S. F.; DefeoJones, D.; Huber, H. E.; Huff, J. R.; Hartman, G. D.; Leister, W.; Kral, A.; Fu, S.; Hancock, P. J.; Haskell, K. A.; Jones, R. E.; Robinson, R. Allosteric Akt (PKB) kinase inhibitors. Discovery and SAR of isozyme selective inhibitors. *Bioorg. Med. Chem. Lett.* **2005**, *15*, 761-764.

78. Lindsley, C. W.; Bogusky, M. J.; Leister, W. H.; McClain, R. T.; Robinson, R.; Barnett, S. F.; Defeo-Jones, D.; Ross, C. W.; Hartman, G. D. Synthesis and biological evaluation of unnatural canthine alkaloids. *Tetrahedron Lett.* **2005**, *46*, 2779-2782.

79. Zhao, Z.; Robinson, R. G.; Barnett, S. F.; Defeo-Jones, D.; Jones, R. J.; Hartman, G. D.; Huber, M. E.; Lindsley, C. W. Development of potent, allosteric Aktl and Akt2 dual inhibitors with improved physical properties and cell activity. *Bioorg. Med. Chem. Lett.* **2008**, *18*, 49-53.

80. Bilodeau, M. T.; Balitza, A. E.; Hoffman, J. M.; Manley, P. J.; Barnett, S. F.; Defeo-Jones, D.; Haskell, K.; Jones, R. J.; Leander, K.; Robinson, R. G.; Smith, A. E.; Huber, M. E.; Hartman, G. D. Allosteric inhibitors of Aktl and Akt2: A naphthyridinone with efficacy in an A2780 tumor xenograft model. *Bioorg. Med. Chem. Lett.* **2008**, *18*, 3178-3182.

81. Wu, Z.; Hartnett, J. C.; Neilson, L. A.; Robinson, R. G.; Fu, S.; Barnett, S. F.; Defeo-Jones, D.; Jones, R. J.; Kral, A. M.; Huber, M. E.; Kohl, N. E.; Hartman, G. D.; Bilodeau, M. T. Development of pyridopyrimidines as potent Aktl/2 inhibitors. *Bioorg. Med. Chem. Lett.* **2008**, *18*, 1274-1279.

82. Sui, T.; Li, Y.; Nagasawa, J.; Liang, J.; Tehrani, L.; Jones, R. J.; Defeo-Jones, D.; Barnett, S. F.; Robinson, R. G. The design and synthesis of potent and cell-active allosteric dual Akt 1 and 2 inhibitors devoid of hERG activity. *Bioorg. Med. Chem. Lett.* **2008**, *18*, 4191-4194.

83. Li, Y.; Liang, J.; Sui, T.; Hu, E.; Rossi, M. A.; Barnett, S. F.; Jones, R. J.; Defeo-Jones, D.; Robinson, R. G.; Leander, K.; Huber, H. A.; Mittal, S.; Cosford, N.; Prasit, P. Allosteric inhibitors of Akt 1 and Akt2: Discovery of [1,2,4]triazolo[3,4-f][1,6]naphthyridines with potent and balanced activity. *Bioorg. Med. Chem. Lett.* **2009**, *19*, 834-836.

84. Yap, T. A.; Yan, Y.; Patnaik, A.; Fearen, I.; Olmos, D.; Papadopoulos, K.; Baird, R. D.; Delgado, L.; Taylor, A.; Lupinacci, L.; Riisnaes, R.; Pope, L. L.; Heaton, S. P.; Thomas, G.; Garrett, M. D.; Sullivan, D. M.; de Bono, J. S.; Tolch, A. W. First-in-man clinical trial of the

oral pan-AKT inhibitor MK-2206 in patients with advanced solid tumors. *J. Clin. Oncol.* **2011**, *29*, 4688-4695.

85. Toral-Barza, L.; Zhang, W. G.; Huang, X.; McDonald, L. A.; Salaski, E. J.; Barbieri, L. R.; Ding, W. D.; Krishnamurthy, G.; Hu, Y. B.; Lucas, J.; Bernan, V. S.; Cai, P.; Levin, J. I.; Mansour, T. S.; Gibbons, J. J.; Abraham, R. T.; Yu, K. Discovery of lactoquinomycin and related pyranonaphthoquinones as potent and allosteric inhibitors of AKT/PKB: mechanistic involvement of AKT catalytic activation loop cysteines. *Mol. Cancer Ther.* **2007**, *6*, 3028-3038.

86. Salaski, E. J.; Krishnamurthy, G.; Ding, W.; Yu, K.; Insaf, S. S.; Eid, C.; Shim, J.; Levin, J. I.; Tabei, K.; Toral-Barza, L.; Zhang, W. G.; McDonald, L. A.; Honores, E.; Hanna, C.; Yamashita, A.; Johnson, B.; Li, Z.; Laakso, L.; Powell, D.; Mansour, T. S. Pyranonaphthoquinone lactones: A new class of AKT selective kinase inhibitors alkylate a regulatory kinase loop cysteine. *J. Med. Chem.* **2009**, *52*, 2181-2184.

87. Tatsuta, K.; Akimoto, K.; Annaka, M.; Ohno, Y.; Kinoshita, M. Enantiodivergent total syntheses of Nanaomycins and their enantiomers Kalafungins. *Bull. Chem. Soc. Jpn.* **1985**, *58*, 1699-1706.

88. Kraus, G. A.; Li, J.; Gordon, M. S.; Jensen, J. H. Direct total syntheses of Frenolicin B and Kalafungin via highly regioselective Diels-Alder reactions. *J. Org. Chem.* **1995**, *60*, 1154-1159.

89. Brimble, M. A. Synthetic studies toward pyranonaphthoquinone antibiotics. *Pure Appl. Chem.* **2000**, *72*, 1635-1639.

90. Fernandes, R. A.; Bruckner, R. Efficient synthesis of (+)-Kalafungin and (-)-Nanaomycin D by asymmetric dihydroxylation, Oxa-pictet-spengler cyclization, and H_2SO_4-mediated isomerization. *Synlett* **2005**, *8*, 1281-1285.

91. Donner, C. D. Total synthesis of (+)-Kalafungin using a tandem Michael–Dieckmann approach. *Tetrahedron Lett.* **2007**, *48*, 8888-8890.

92. Eid, C. N.; Shim, J.; Bikker, J.; Lin, M. Direct Oxa-Pictet-Spengler cyclization to the natural (3a,5)-*trans*-stereochemistry in the syntheses of (+)-7-deoxyfrenolicin B and(+)-7-deoxykalafungin. *J. Org. Chem.* **2009**, *74*, 423-426.

93. Badiger, S.; Behnke, D.; Betschart, C.; Chaudhari, V.; Chebrolu, M.; Costesta, S.; Hintermann, S.; Pandit, C. WO Patent 2011076744, 2011.

94. Uehara, K.; Wagner, C. B.; Vogler, T.; Luftmann, H.; Studer, A. poly(vinyl ketone)s by controlled boron group transfer polymerization (BGTP). *Angew. Chem. Int. Ed.* **2010**, *49*, 3073-3076.

95. Chatterjee, A. K.; Morgan, J. P.; Scholl, M.; Grubbs, R. H. Synthesis of functionalized olefins by cross and ring-closing metatheses. *J. Am. Chem. Soc.* **2000**, *122*, 3783-3784.

96. Falck, J. R.; Kumar, P. S.; Reddy, Y. K.; Zou, G.; Capdevila, J. H. Stereospecific synthesis of EET metabolites via Suzuki–Miyaura coupling. *Tetrahedron Lett.* **2001**, *42*, 7211-7212.

97. Sanie`re, L.; Leman, L.; Bourguignon, J. J.; Daubana, P.; Dodd, R. H. Iminoiodane mediated aziridination of *α*-allylglycine: access to a novel rigid arginine derivative and to the natural amino acid enduracididine. *Tetrahedron* **2004**, *60*, 5889-5897.

98. Mehta, A.; Jaouhari, R.; Benson, T. J.; Douglas, K. T. Improved efficiency and selectivity in peptide synthesis: use of triethylsilane as a carbocation scavenger in deprotection of t-butylesters and *t*-butoxycarbonyl protected sites. *Tetrahedron Lett.* **1992**, *33*, 5441-5444.

Appendix

NMR spectra

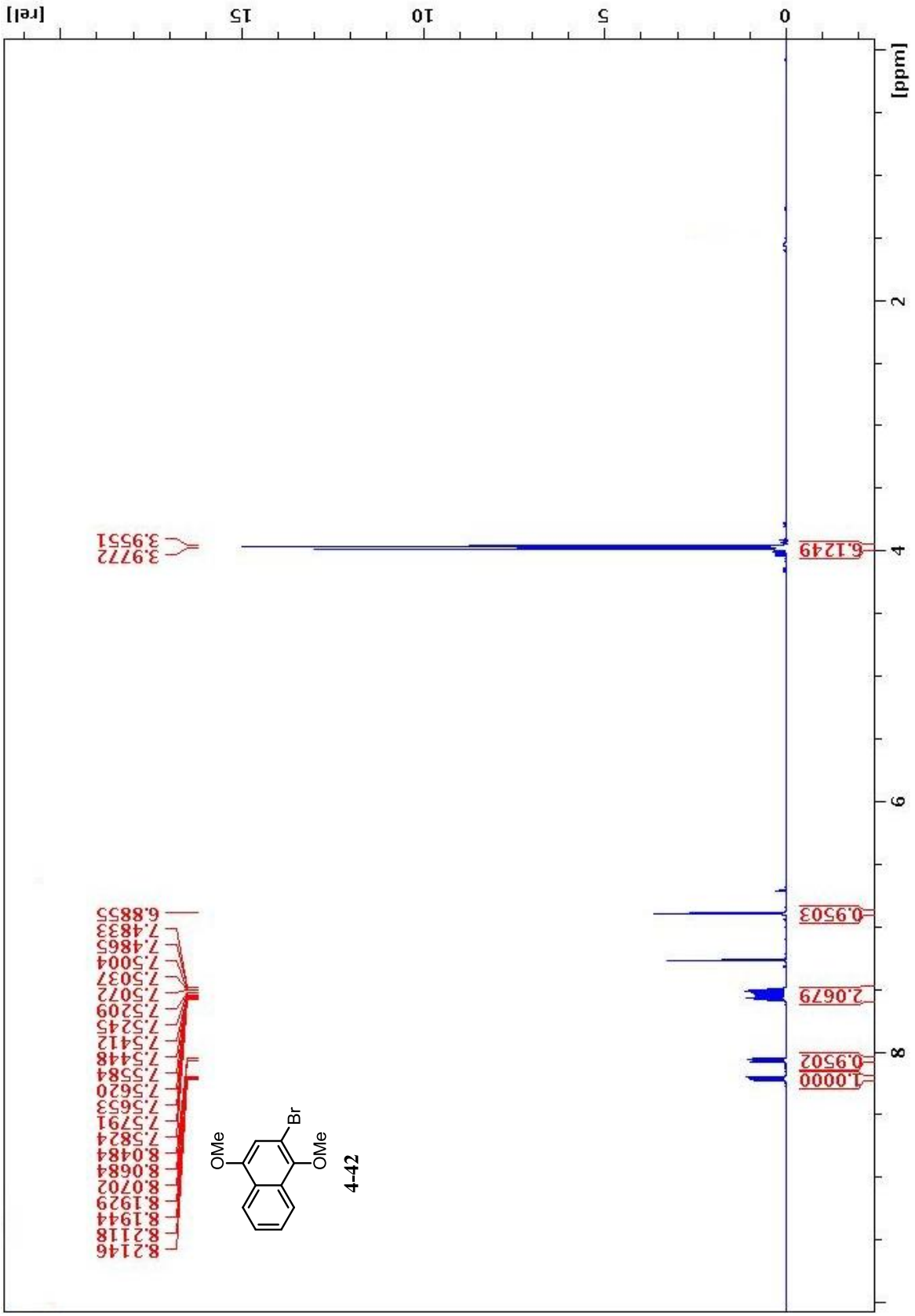
[rel]
15
10
5
0
[ppm]
2
4
6
8
3.9772
3.9551
6.1249
0.9503
2.0679
1.0000
0.9502
8.2146
8.2118
8.1944
8.1929
8.0702
8.0684
8.0484
7.5824
7.5791
7.5653
7.5620
7.5584
7.5448
7.5412
7.5245
7.5209
7.5072
7.5037
7.5004
7.4865
7.4833
6.8855
Br
OMe
OMe
4-42

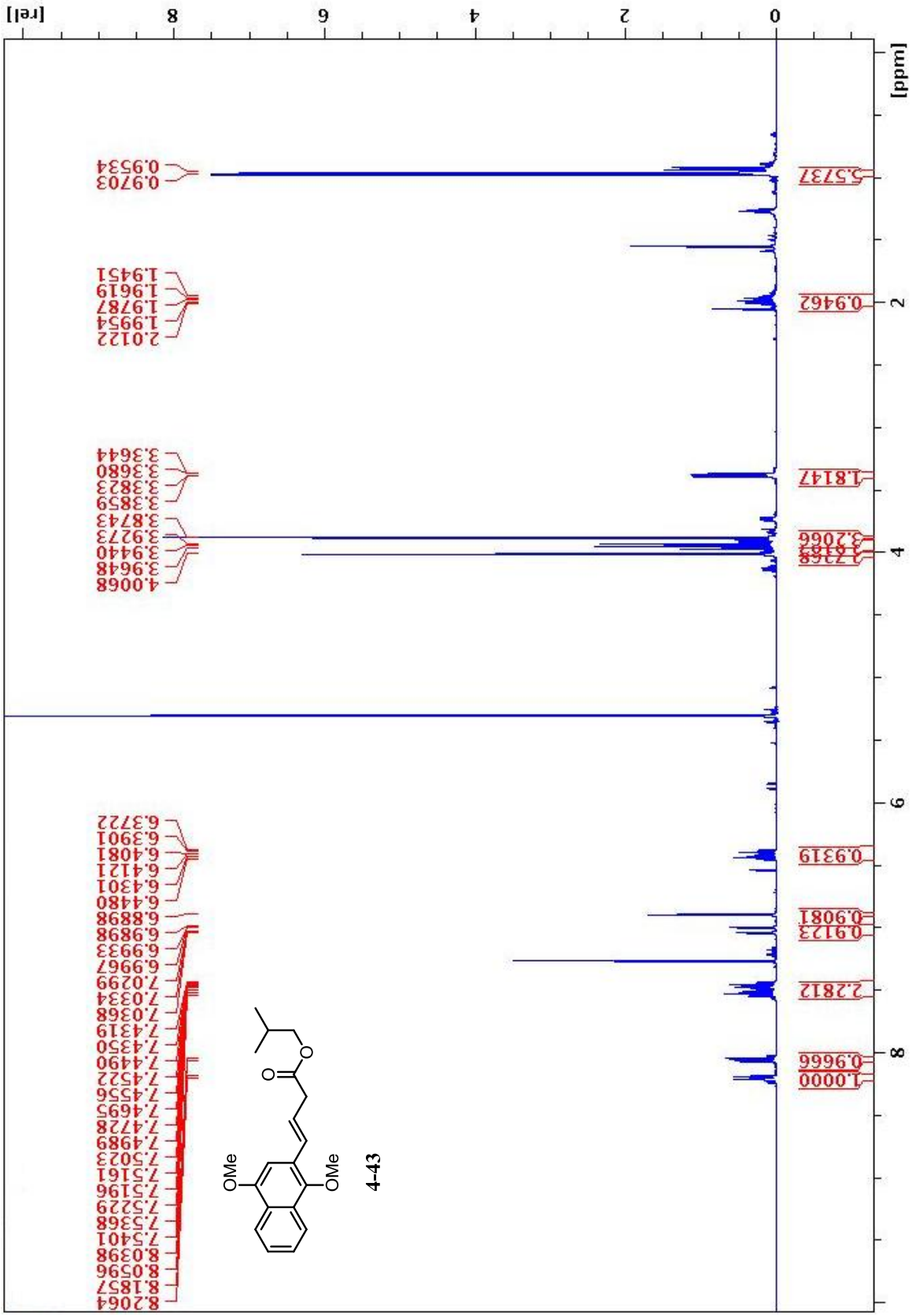
OMe
OMe
O
O
4-43

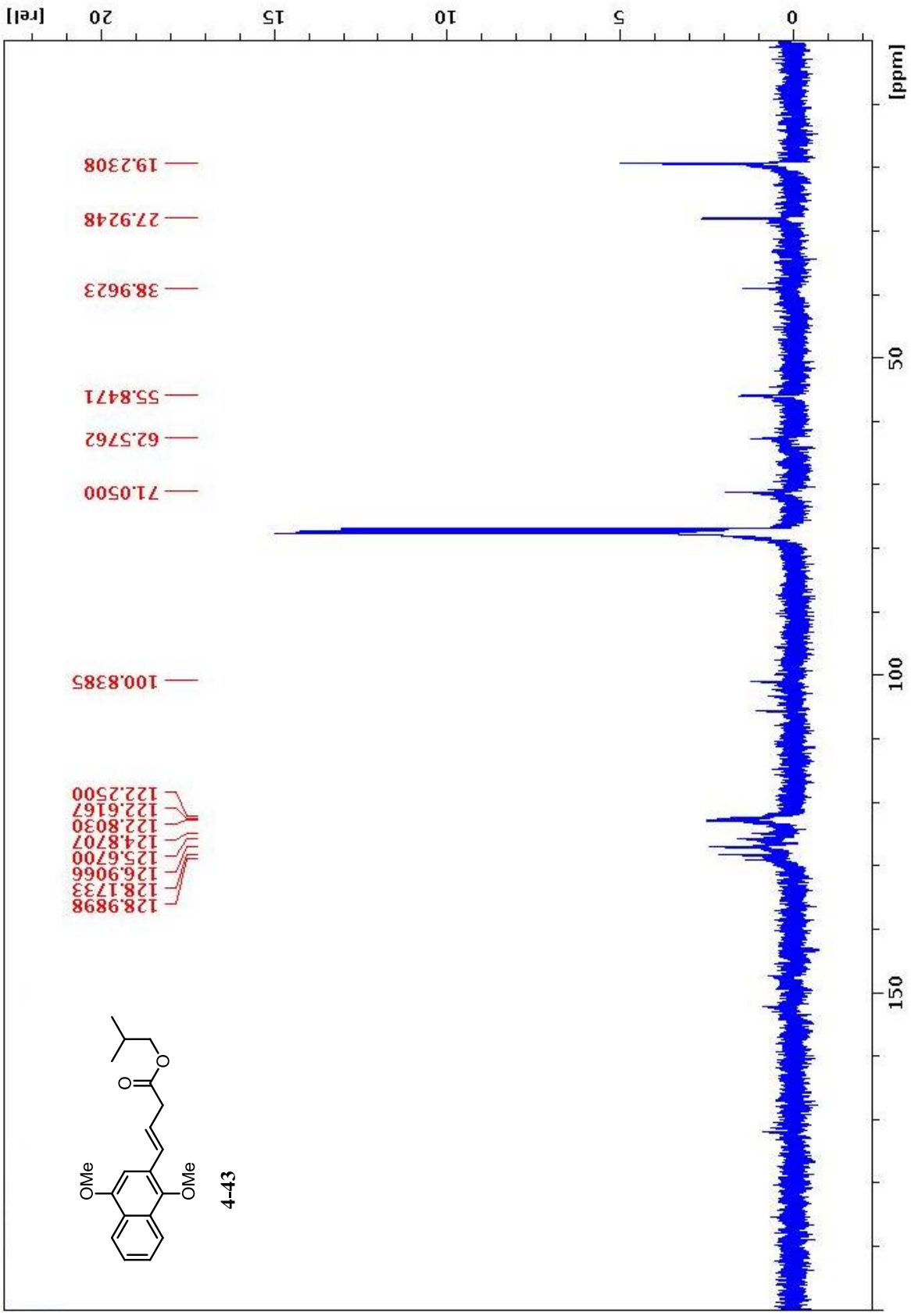
[rel]
20
15
10
5
0
[ppm]
150
100
50
19.2308
27.9248
38.9623
55.8471
62.5762
71.0500
100.8385
122.2500
122.6167
122.8030
124.8707
125.6700
126.9066
128.1733
128.9898
OMe
OMe
O
O

4-43

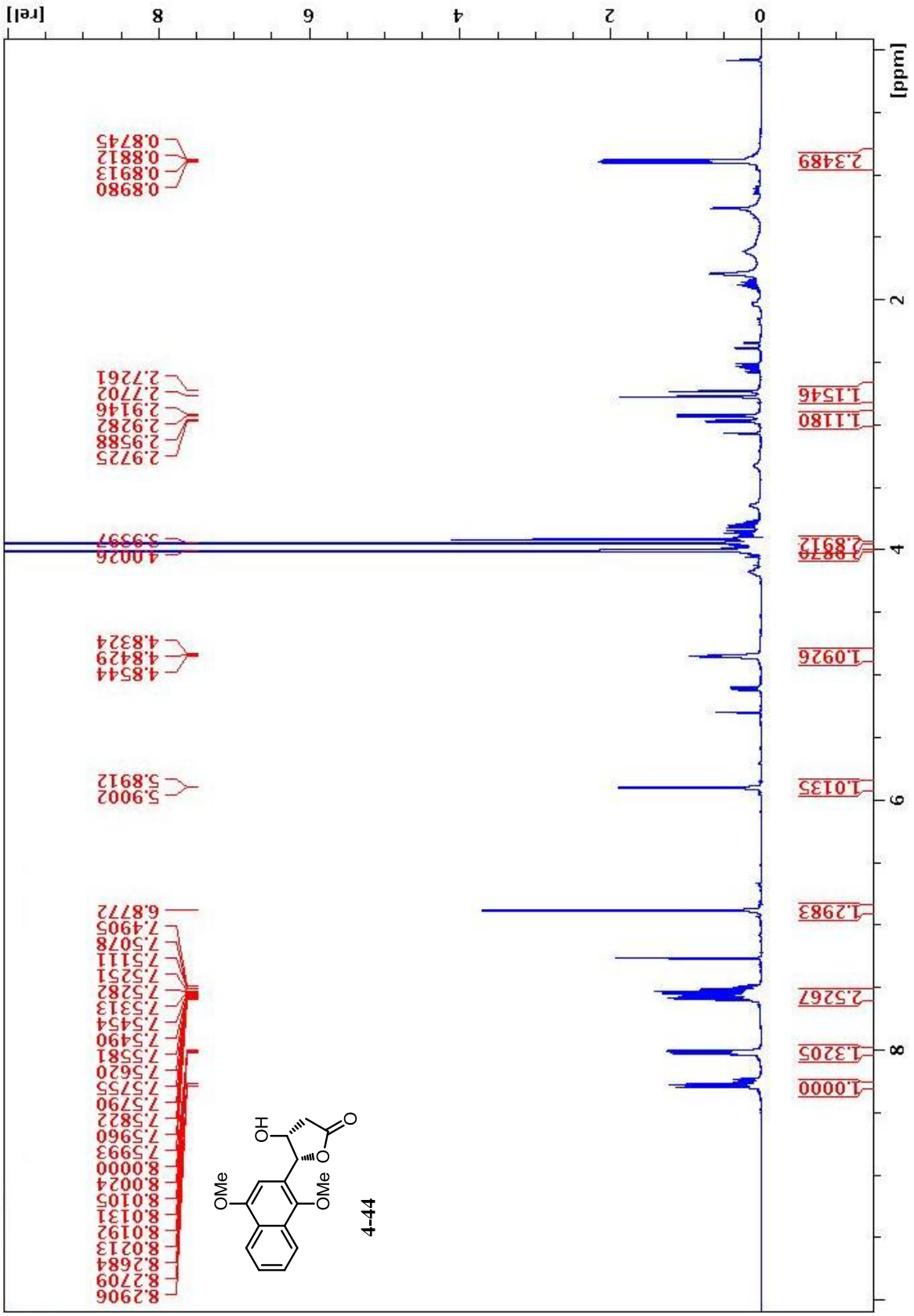
[rel]
8
6
4
2
0
[ppm]
2
4
6
8
2.3489
1.1546
1.1180
2.8912
1.0926
1.0135
1.2983
2.5267
1.3205
1.0000
0.8980
0.8913
0.8812
0.8745
2.9725
2.9588
2.9282
2.9146
2.7702
2.7261
5.9397
4.0026
4.8544
4.8429
4.8324
5.9002
5.8912
6.8772
7.4905
7.5078
7.5111
7.5251
7.5282
7.5313
7.5454
7.5490
7.5581
7.5620
7.5755
7.5790
7.5822
7.5960
7.5993
8.0000
8.0024
8.0105
8.0131
8.0192
8.0213
8.2684
8.2709
8.2906
OH
O
O
OMe
OMe
4-44

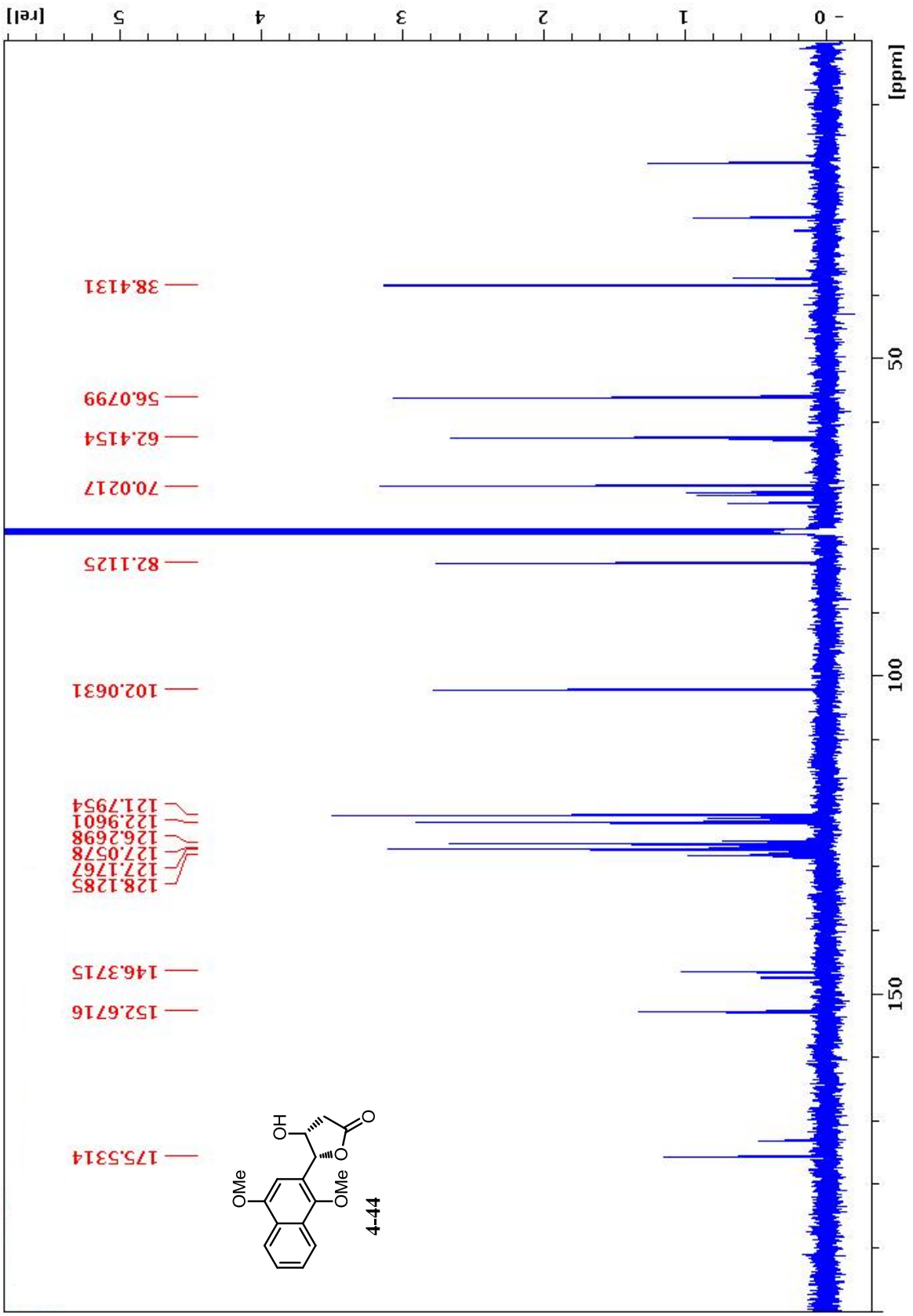
[rel]
0
1
2
3
4
5
[ppm]
50
100
150
38.4131
56.0799
62.4154
70.0217
82.1125
102.0631
121.7954
122.9601
126.2698
127.0578
127.1767
128.1285
146.3715
152.6716
175.5314
OH
O
O
OMe
OMe
4-44

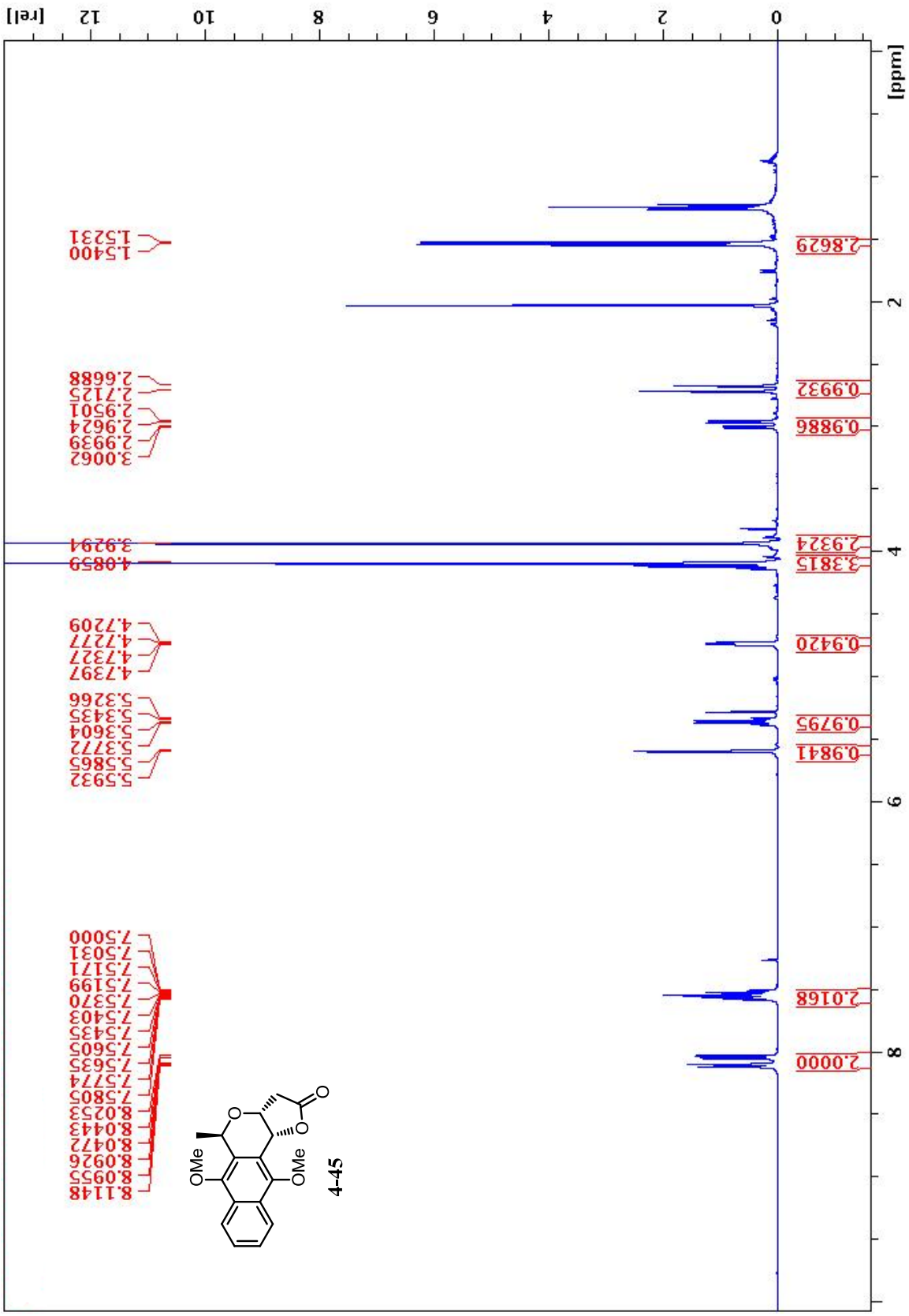
[rel]
12
10
8
6
4
2
0
[ppm]
8.1148
8.0955
8.0926
8.0472
8.0443
8.0253
7.5805
7.5774
7.5635
7.5605
7.5435
7.5403
7.5370
7.5199
7.5171
7.5031
7.5000
5.9932
5.5865
5.3772
5.3604
5.3435
5.3266
4.7397
4.7277
4.7209
4.0859
3.9291
3.0062
2.9939
2.9624
2.9501
2.7125
2.6688
1.5400
1.5231
2.0000
2.0168
0.9841
0.9795
0.9420
2.9324
3.3815
0.9886
0.9932
2.8629
OMe
OMe
4-45

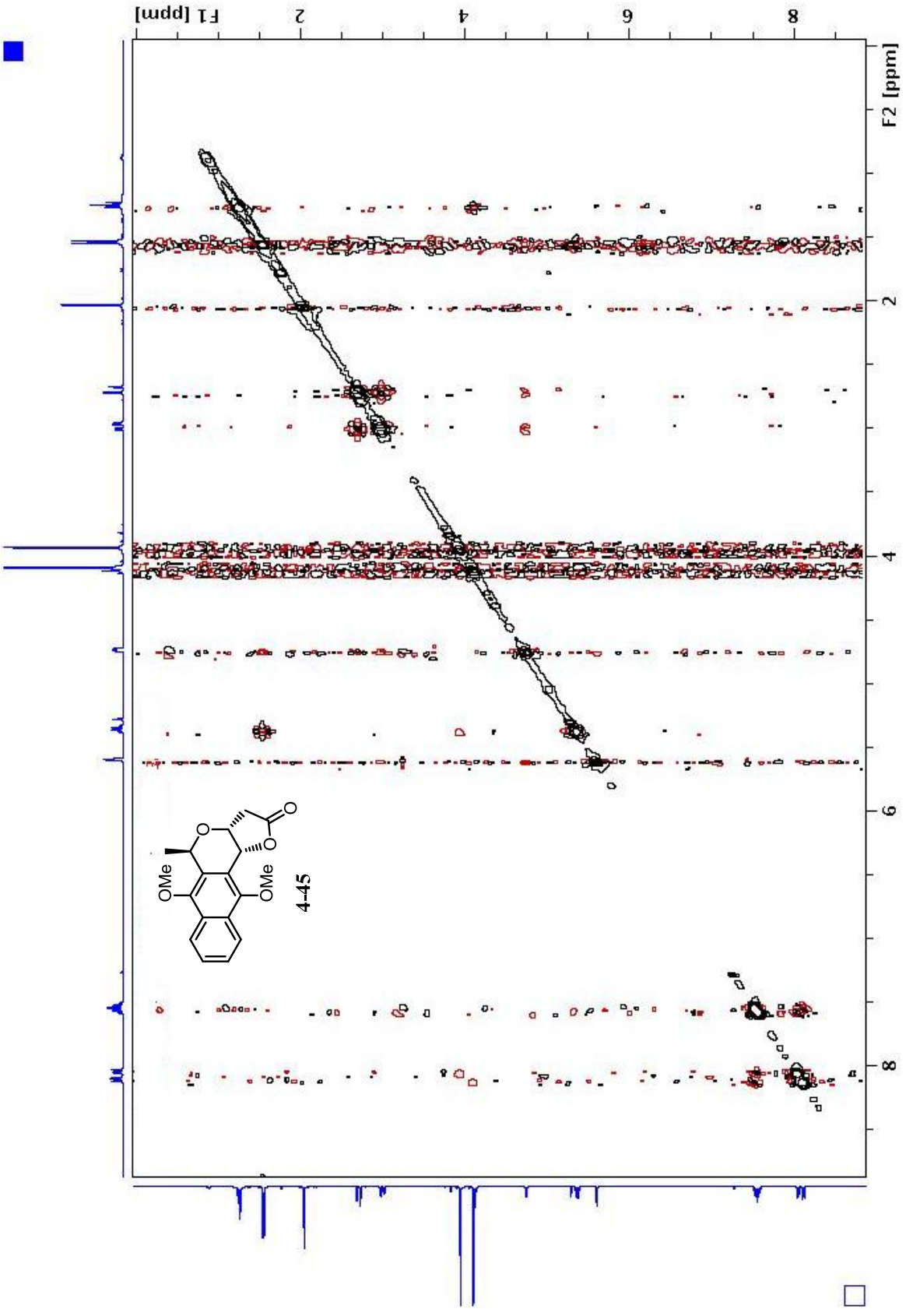
F1 [ppm]
F2 [ppm]
OMe
OMe
4-45

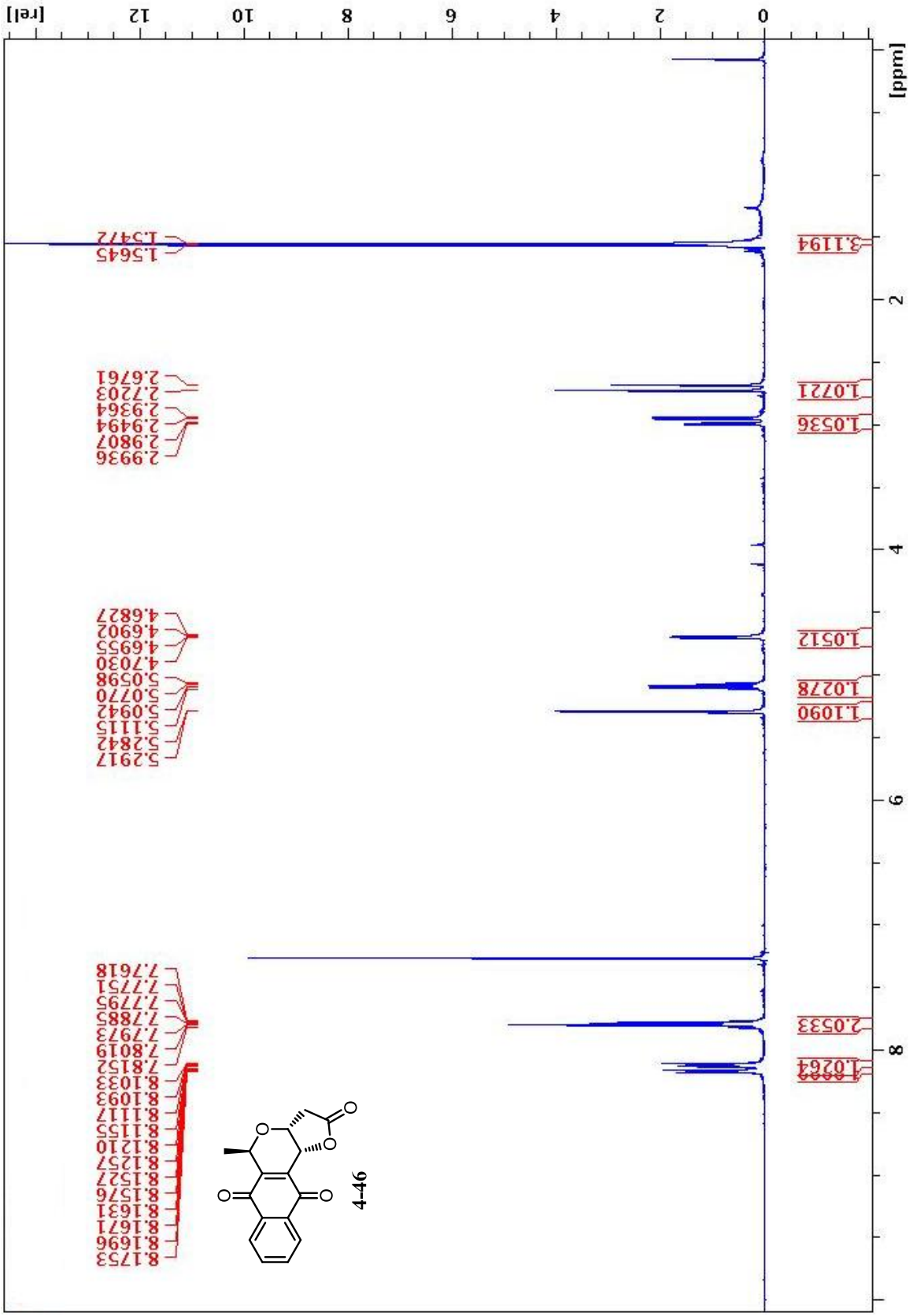
8.1753
8.1696
8.1671
8.1631
8.1576
8.1527
8.1257
8.1210
8.1155
8.1117
8.1093
8.1033
7.8152
7.8019
7.7973
7.7885
7.7795
7.7751
7.7618
5.2917
5.2842
5.1115
5.0942
5.0770
5.0598
4.7030
4.6955
4.6902
4.6827
2.9936
2.9807
2.9494
2.9364
2.7203
2.6761
1.5645
1.5472
8.0264
2.0533
1.1090
1.0278
1.0512
1.0536
1.0721
3.1194
4-46
[rel]
[ppm]

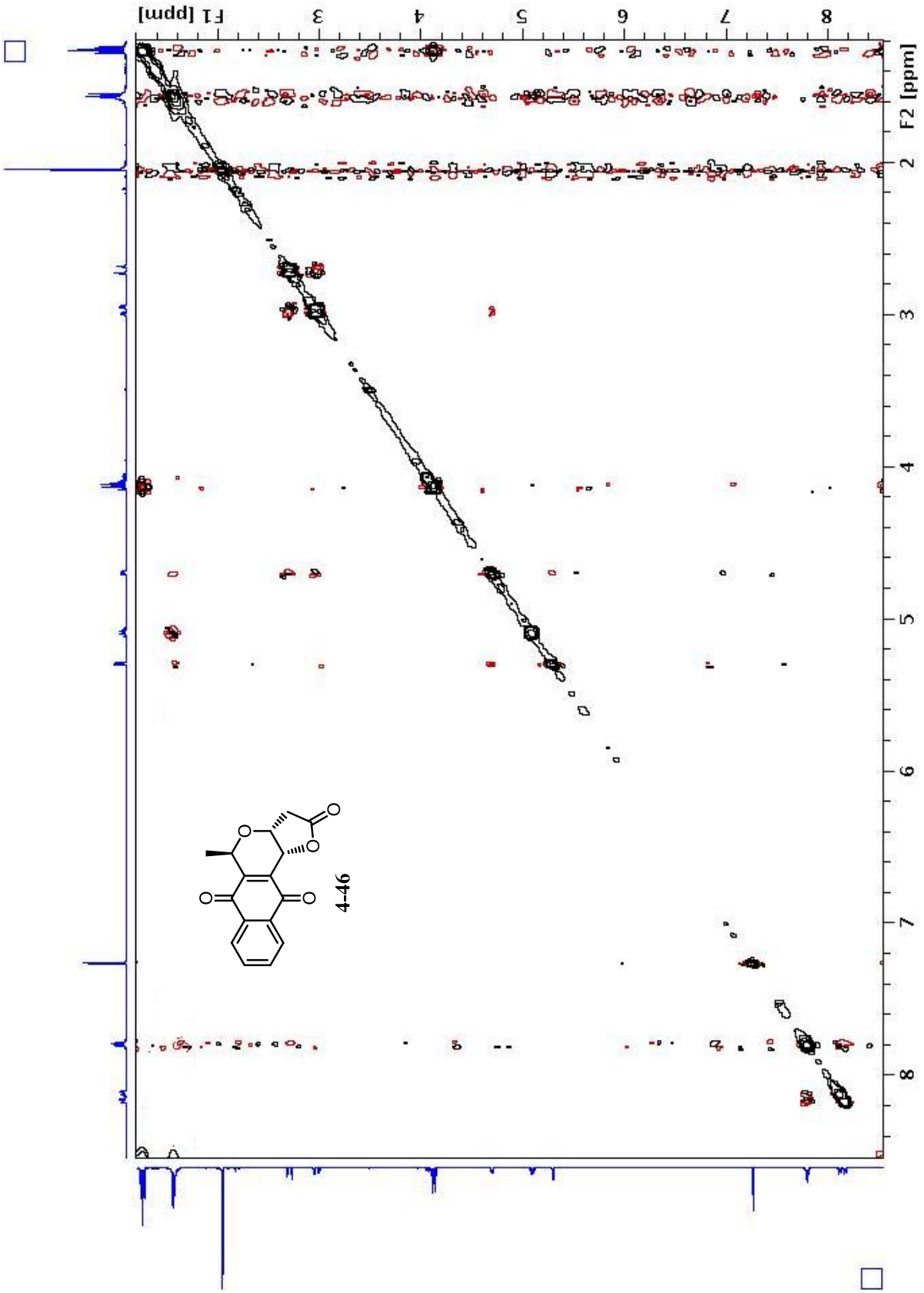
F1 [ppm]
F2 [ppm]
4-46

[rel]
4
3
2
1
0
[ppm]
50
100
150
18.6951
37.1056
68.9693
66.7749
66.6655
126.7301
126.9337
131.9296
131.9926
134.3289
134.4346
134.6030
149.6522
173.9713
182.3855
183.1780
4-46

7.6678
7.6646
7.6609
7.6479
7.6438
7.4563
7.4526
7.4460
7.4378
7.4314
7.4238
7.4200
7.4161
7.4021
7.3988
7.3877
7.3837
7.3704
7.3663
7.3621
3.5411
3.3431
2.9255
2.9112
1.8879
3.0000
O
N
OMe
Me
4-51
[rel]
15
10
5
0
[ppm]
2
4
6
8

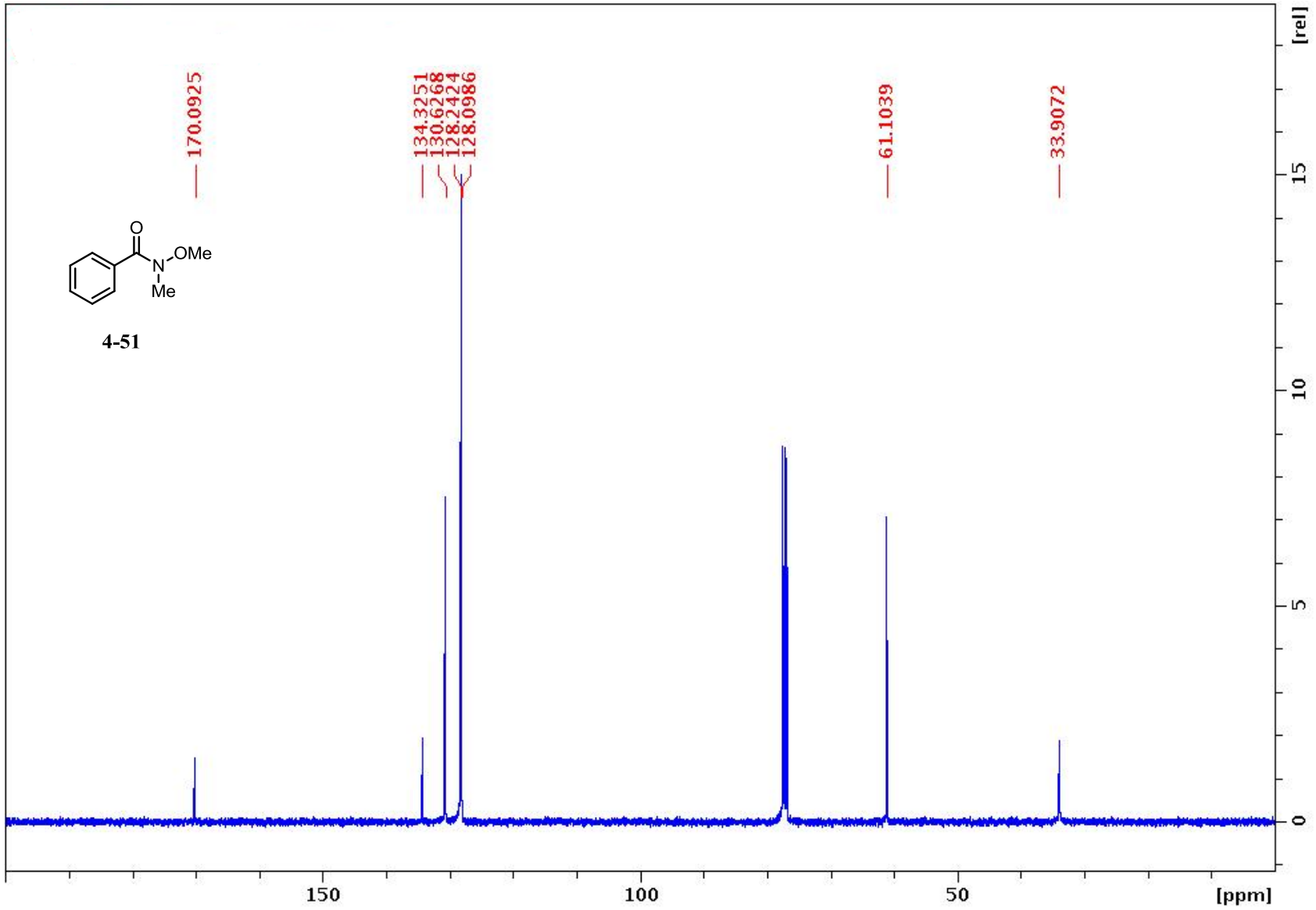
170.0925
134.3251
130.6268
128.2424
128.0986
61.1039
33.9072
O
N
OMe
Me
4-51
[rel]
15
10
5
0
150
100
50
[ppm]

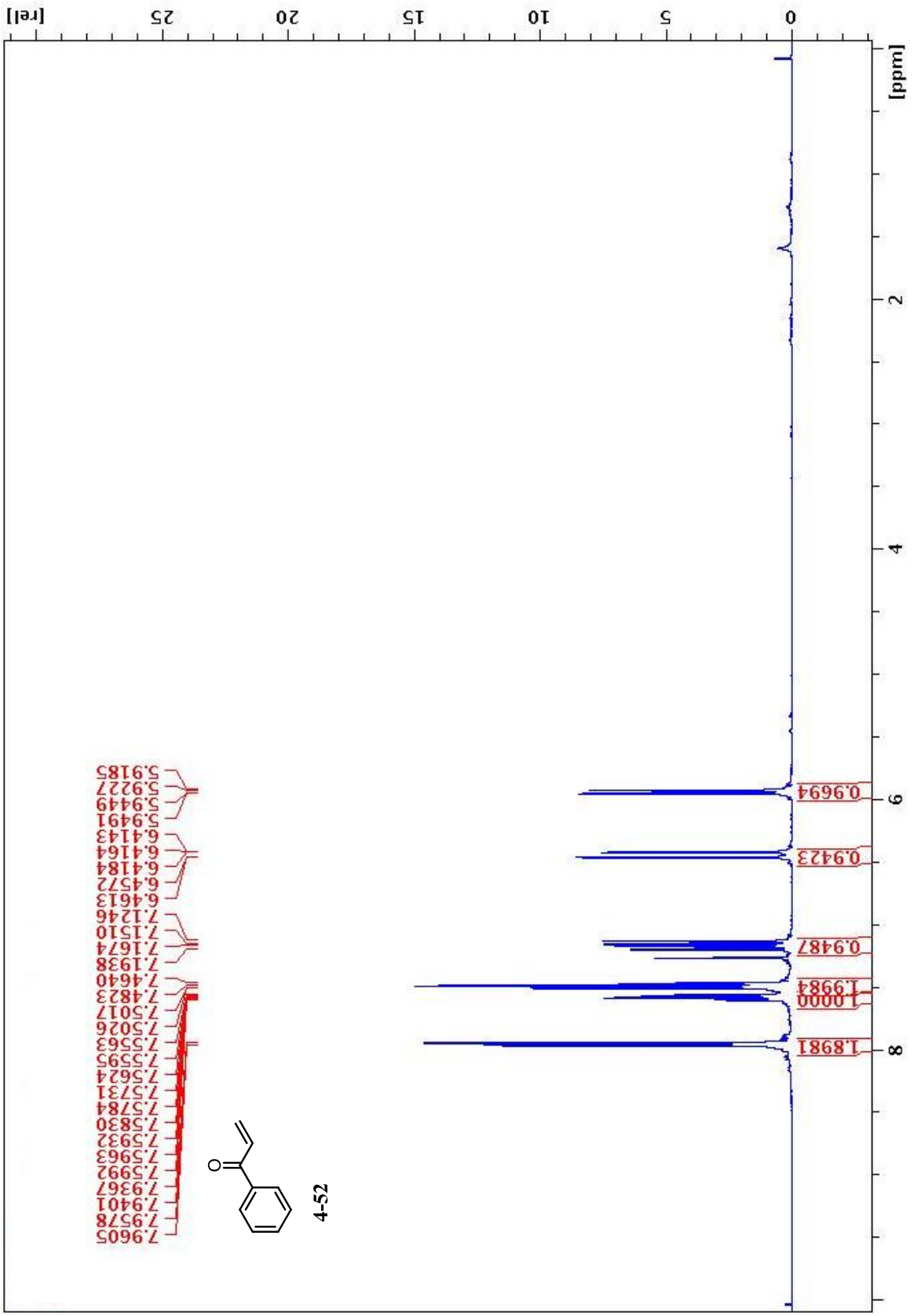
[rel]
0
5
10
15
20
25
[ppm]
2
4
6
8
0.9694
0.9423
0.9487
1.9984
1.0000
1.8981
7.9605
7.9578
7.9401
7.9367
7.5992
7.5963
7.5932
7.5830
7.5784
7.5731
7.5624
7.5595
7.5563
7.5026
7.5017
7.4823
7.4640
7.1938
7.1674
7.1510
7.1246
6.4613
6.4572
6.4184
6.4164
6.4143
5.9491
5.9449
5.9227
5.9185
4-52

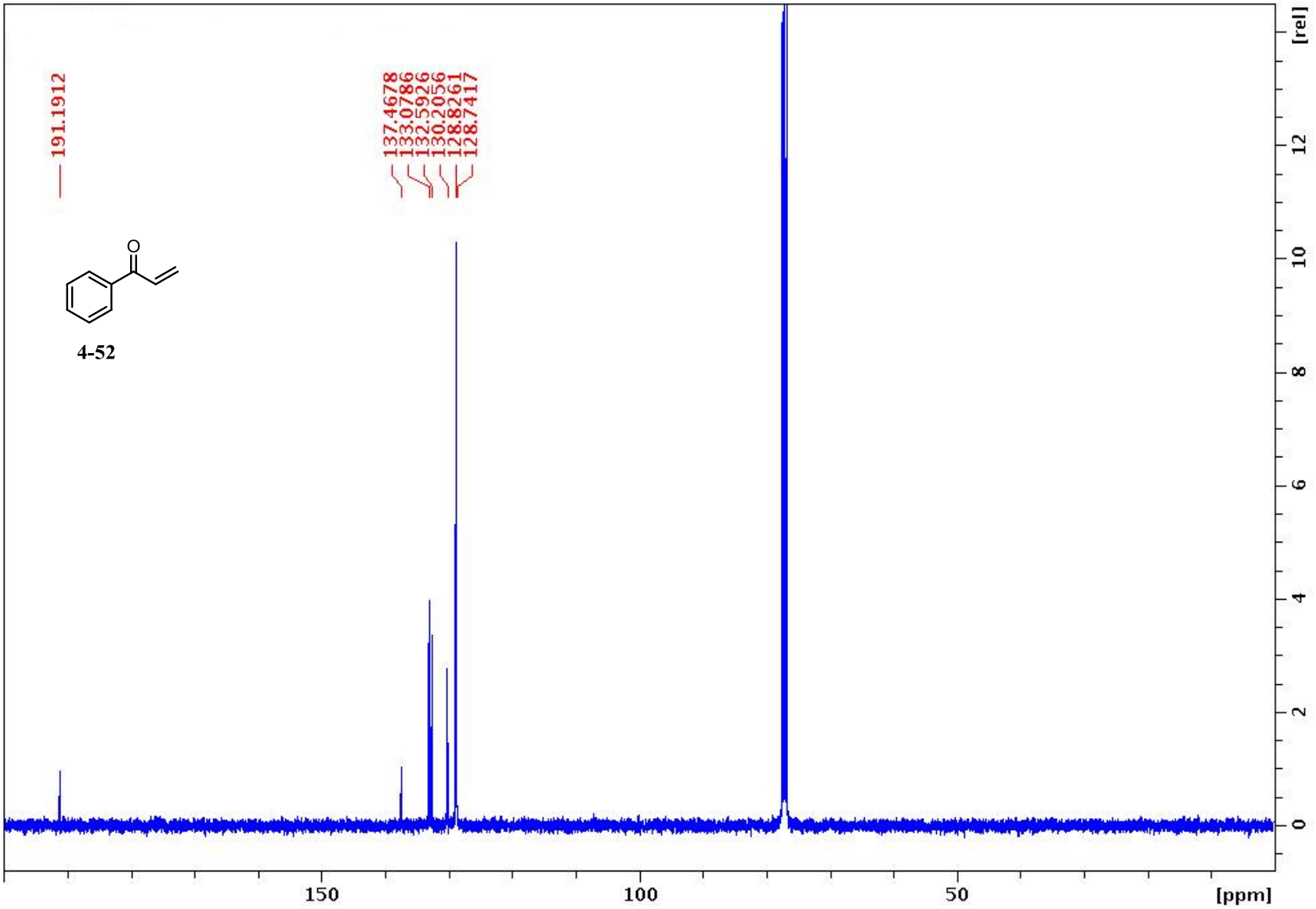
191.1912
137.4678
133.0786
132.5926
130.2056
128.8261
128.7417
4-52
150
100
50
[ppm]
[rel]

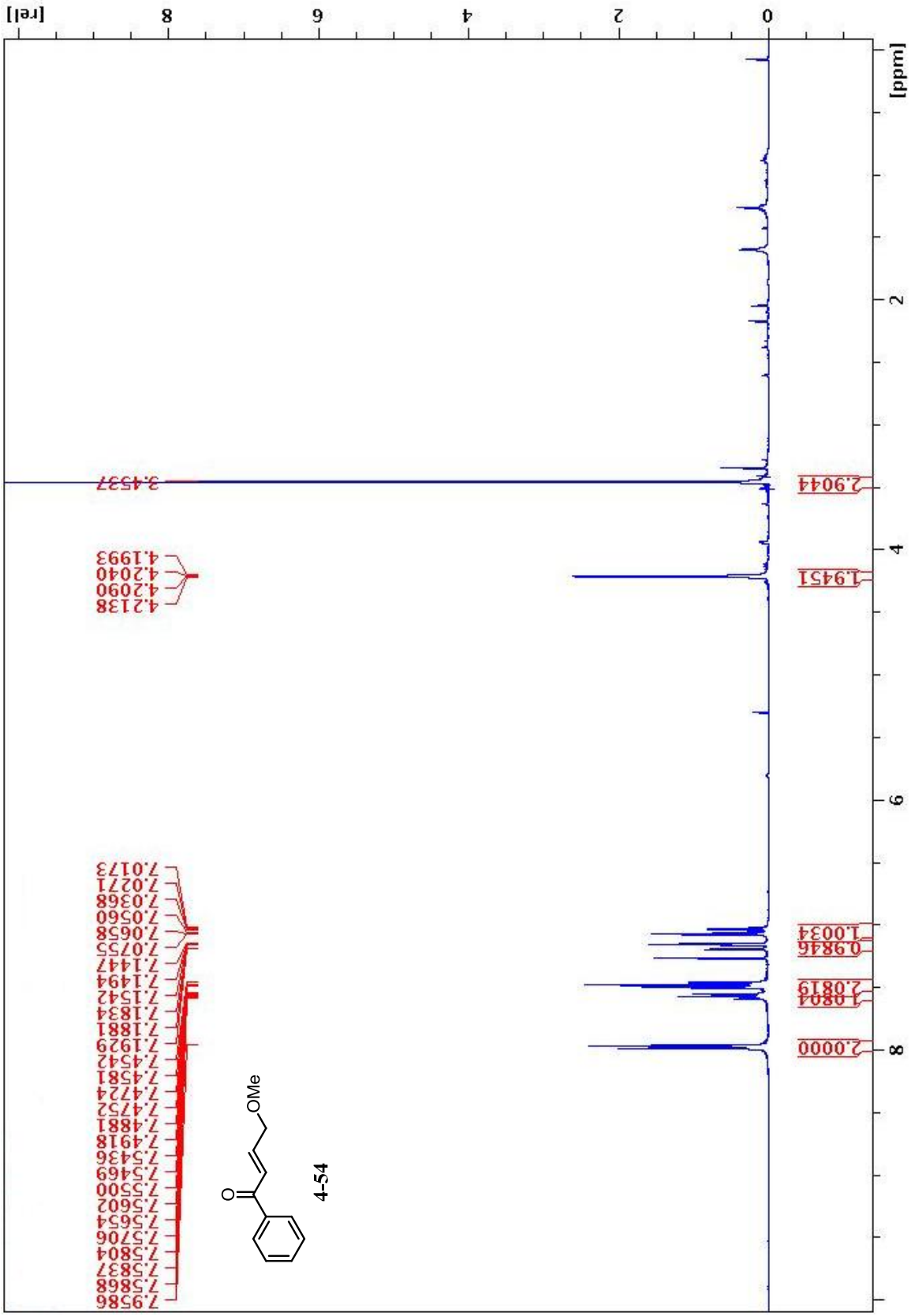
[rel]
8
6
4
2
0
[ppm]
2
4
6
8
3.4537
4.1993
4.2040
4.2090
4.2138
7.0173
7.0271
7.0368
7.0560
7.0658
7.0755
7.1447
7.1494
7.1542
7.1834
7.1881
7.1929
7.4542
7.4581
7.4724
7.4752
7.4881
7.4918
7.5436
7.5469
7.5500
7.5602
7.5654
7.5706
7.5804
7.5837
7.5868
7.9586
2.9044
1.9451
1.0034
0.9846
1.0804
2.0819
2.0000
OMe
O
4-54

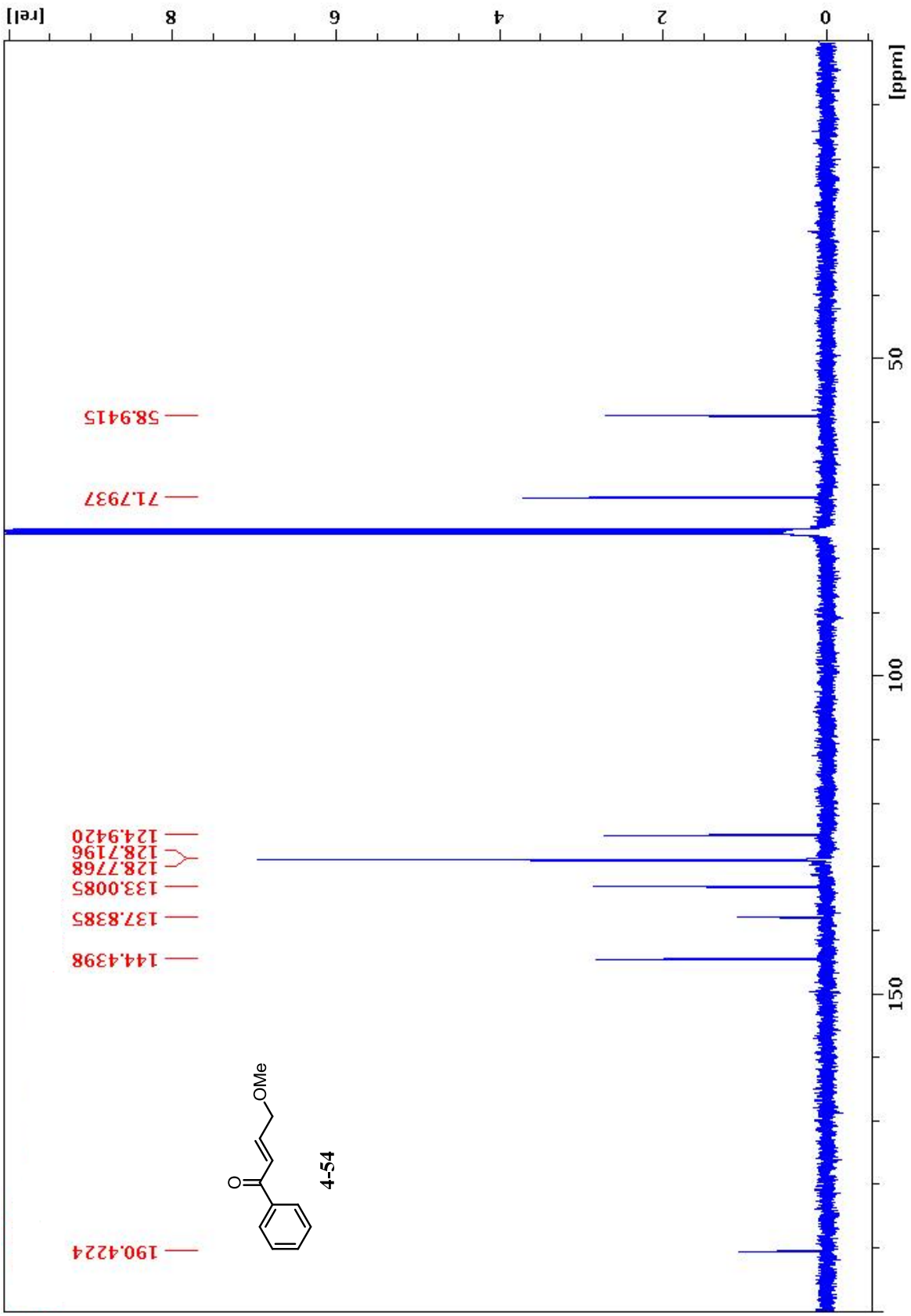
[rel]
8
6
4
2
0
[ppm]
50
100
150
190.4224
144.4398
137.8385
133.0085
128.7768
128.7196
124.9420
71.7937
58.9415
OMe
O
4-54

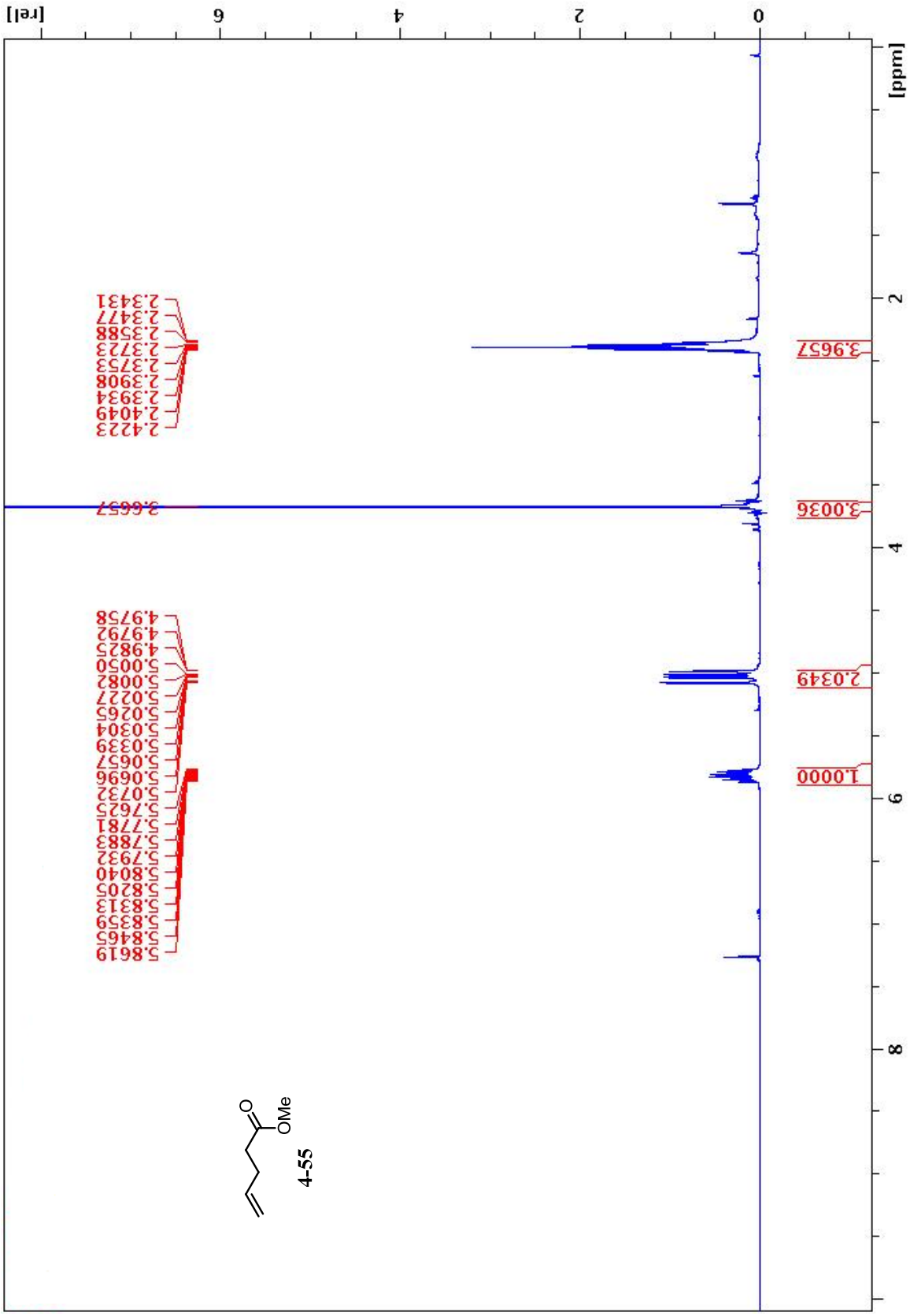
[rel]
6
4
2
0
[ppm]
2
4
6
8
3.9657
3.0036
2.0349
1.0000
2.4223
2.4049
2.3934
2.3908
2.3753
2.3723
2.3588
2.3477
2.3431
3.6657
5.8619
5.8465
5.8359
5.8313
5.8205
5.8040
5.7932
5.7883
5.7781
5.7625
5.0732
5.0696
5.0637
5.0339
5.0304
5.0265
5.0227
5.0082
5.0050
4.9825
4.9792
4.9758
OMe
O
4-55

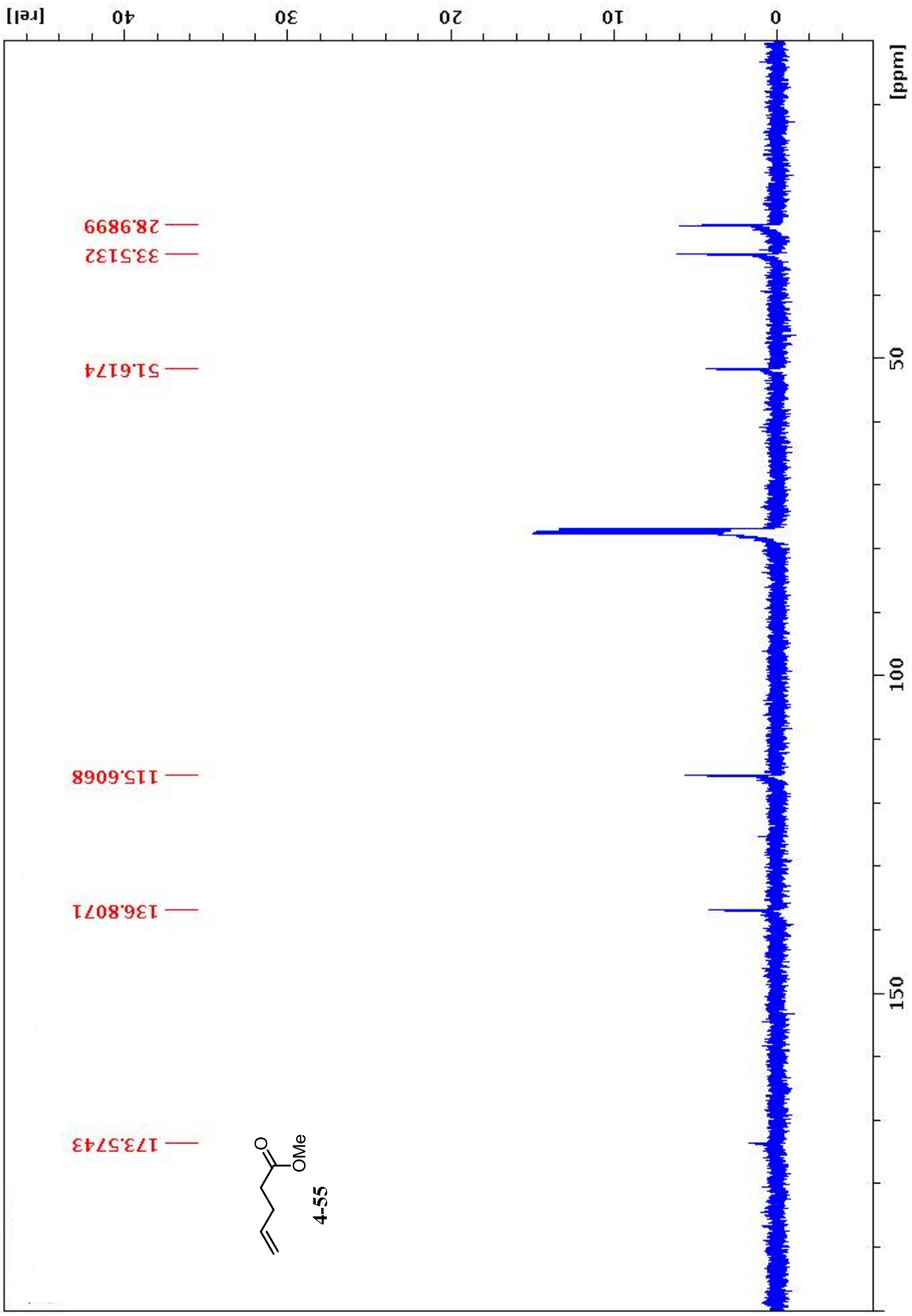
[rel]
40
30
20
10
0
[ppm]
50
100
150
28.9899
33.5132
51.6174
115.6068
136.8071
173.5743
OMe
4-55

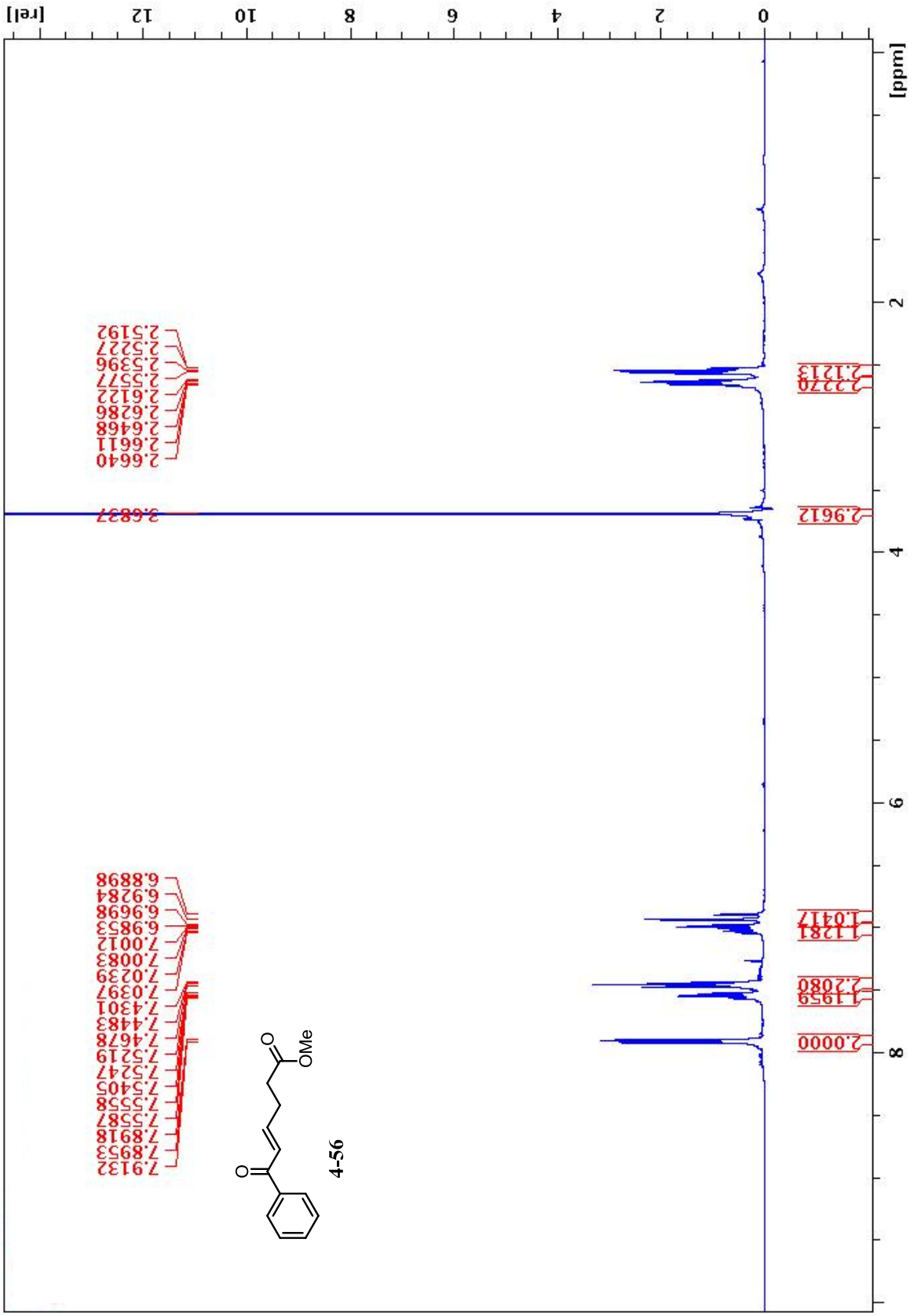
[rel]
12
10
8
6
4
2
0
[ppm]
2
4
6
8
7.9132
7.8953
7.8918
7.5587
7.5558
7.5405
7.5247
7.5219
7.4678
7.4483
7.4301
7.0397
7.0239
7.0083
7.0012
6.9853
6.9698
6.9284
6.8898
2.6640
2.6611
2.6468
2.6286
2.6122
2.5577
2.5396
2.5227
2.5192
3.6827
2.9612
2.2220
2.1213
2.0000
1.9579
2.2080
1.1281
1.0417
OMe
4-56

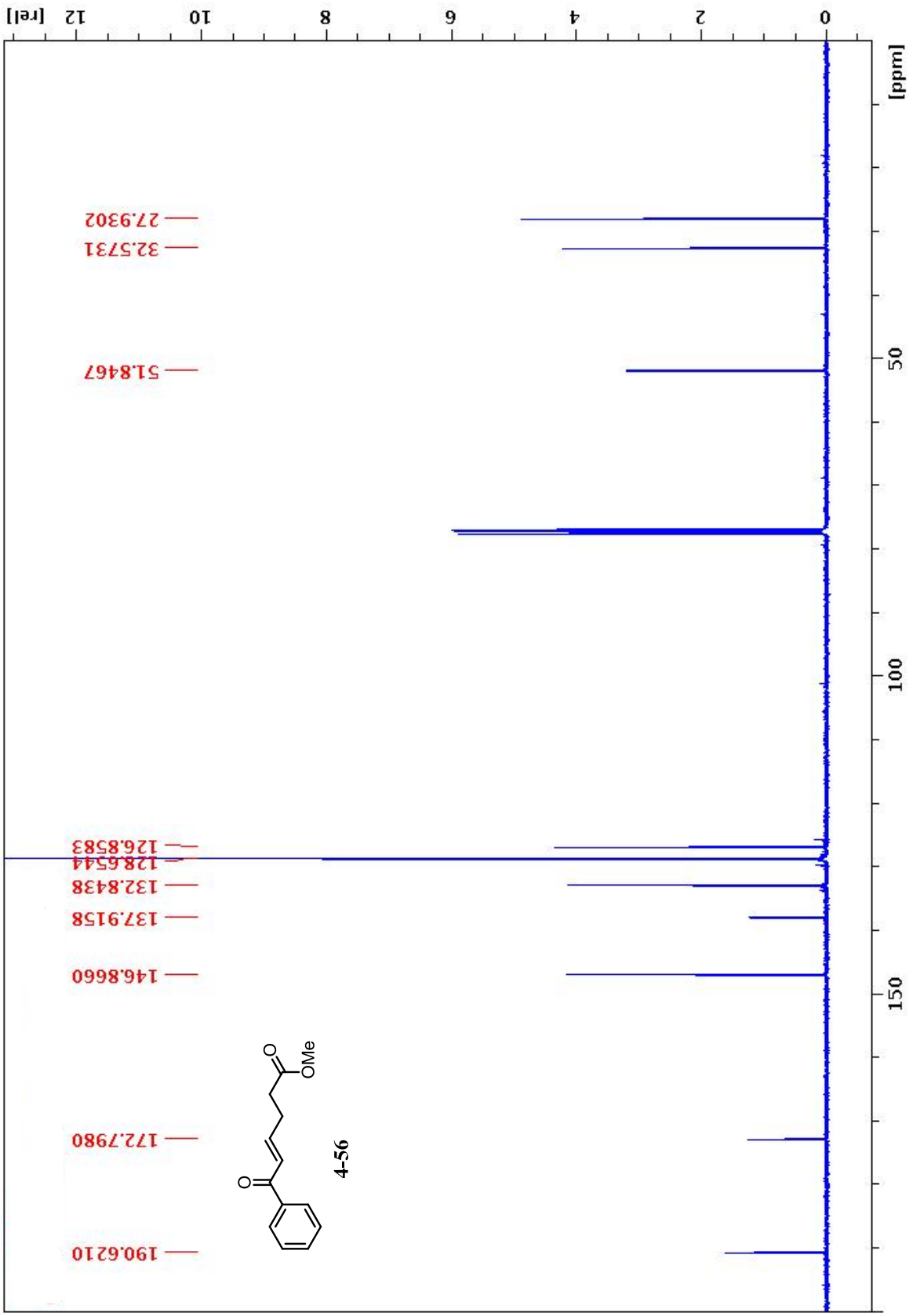
[rel]
12
10
8
6
4
2
0
[ppm]
150
100
50
27.9302
32.5731
51.8467
126.8583
128.6544
132.8438
137.9158
146.8660
172.7980
190.6210
OMe
O
O
4-56

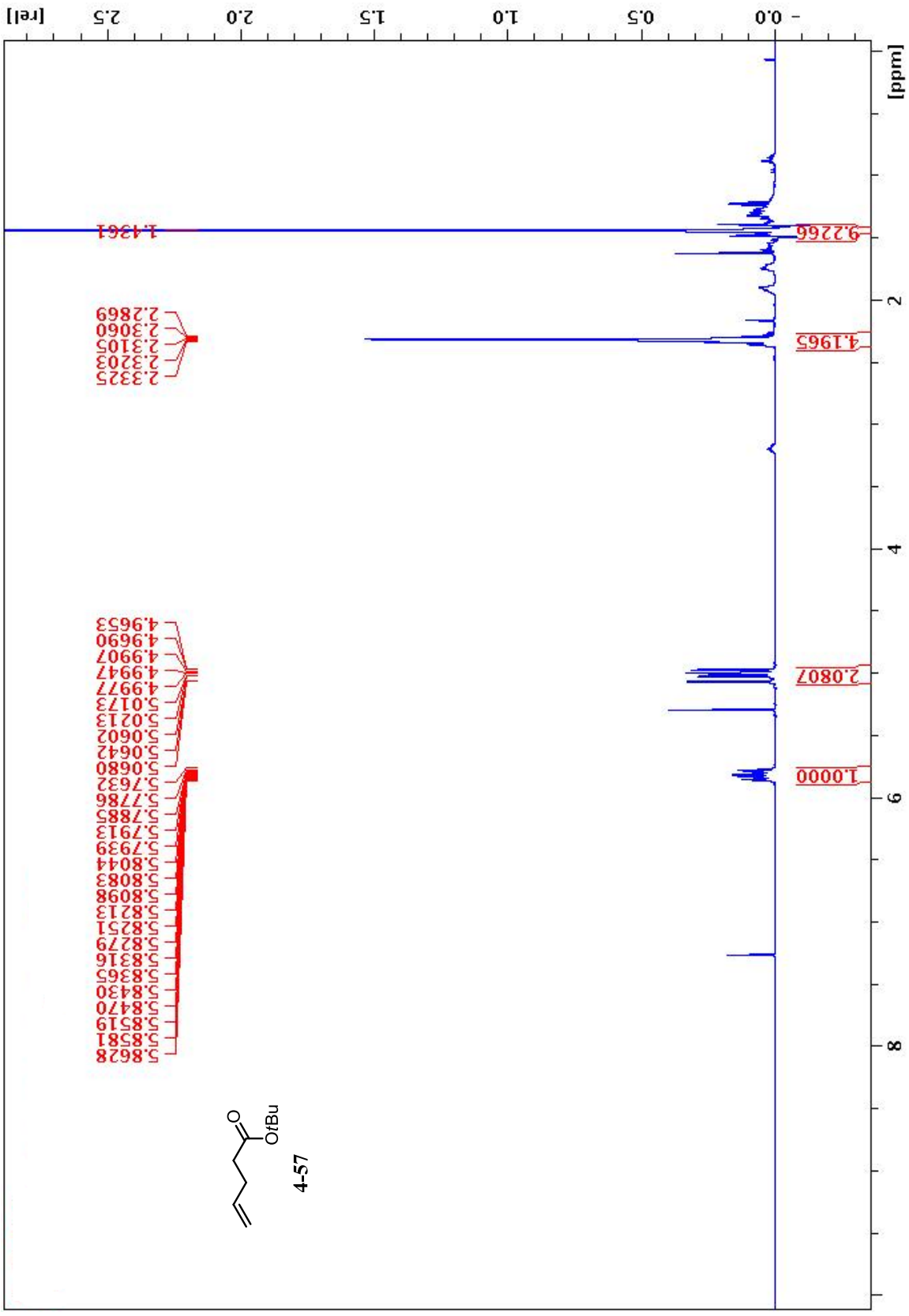
[rel]
2.5
2.0
1.5
1.0
0.5
0.0
[ppm]
2
4
6
8
1.1361
9.2266
4.1965
2.0807
1.0000
2.3325
2.3203
2.3105
2.3060
2.2869
5.8628
5.8581
5.8519
5.8470
5.8430
5.8365
5.8316
5.8279
5.8251
5.8213
5.8098
5.8083
5.8044
5.7939
5.7913
5.7885
5.7786
5.7632
5.0680
5.0642
5.0602
5.0213
5.0173
4.9977
4.9947
4.9907
4.9690
4.9653
OtBu
O
4-57

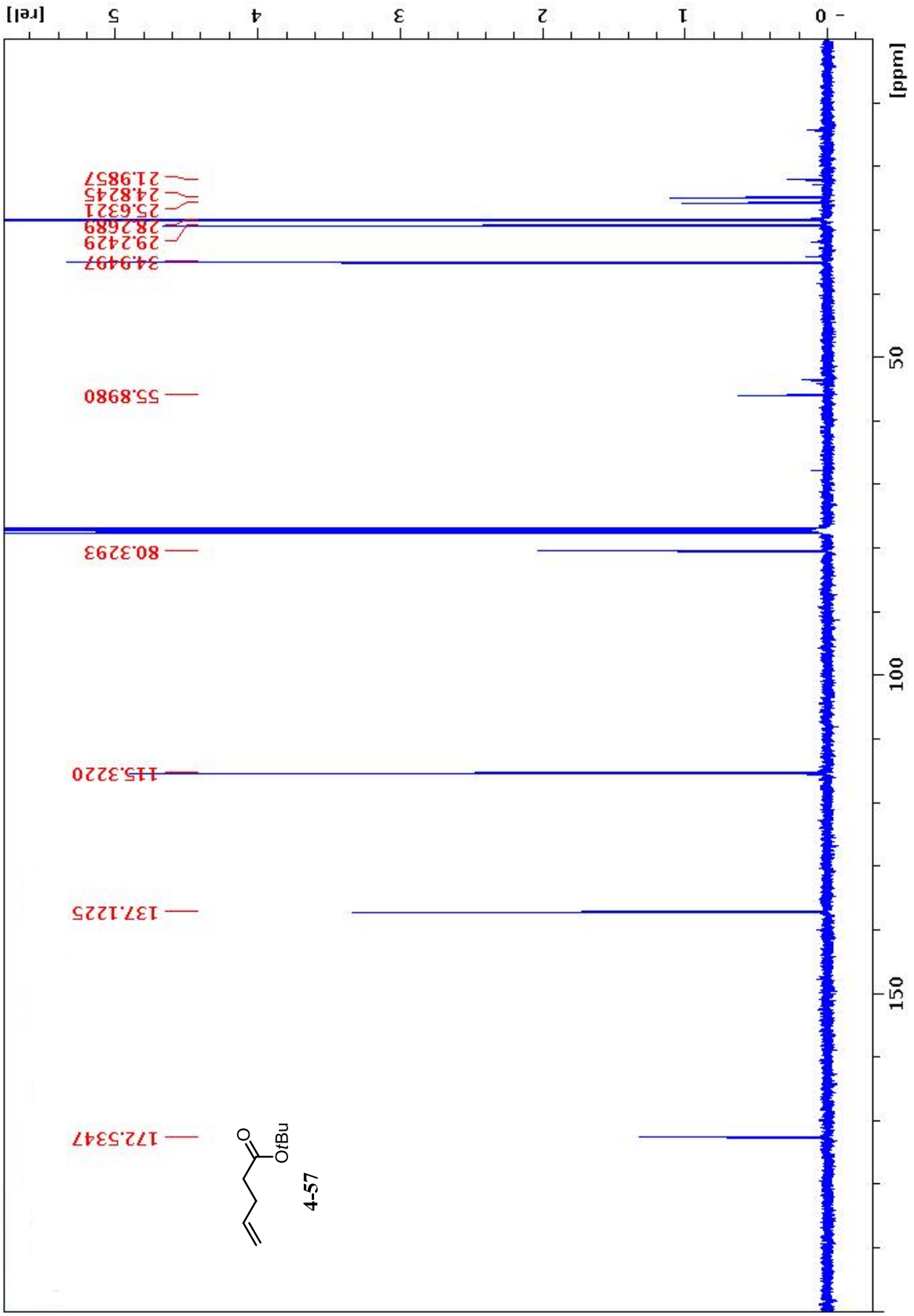
[rel]
0
1
2
3
4
5
[ppm]
50
100
150
172.5347
137.1225
115.3220
80.3293
55.8980
34.9497
29.2429
28.2689
25.6321
24.8245
21.9857
OtBu
O
4-57

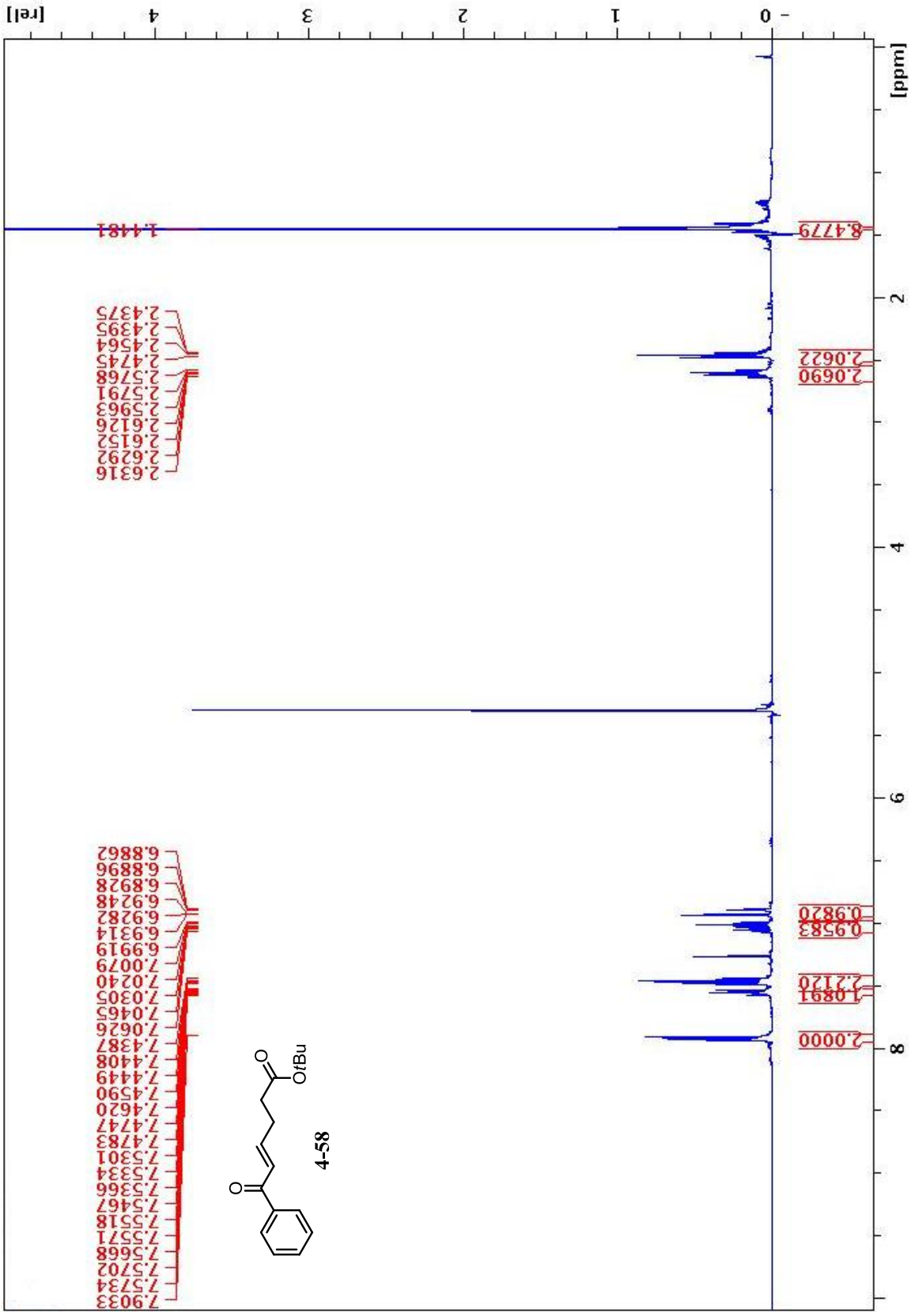
[rel]
[ppm]
OtBu
4-58

8 [rel]
6
4
2
0
[ppm]
150
100
50
190.7870
171.7719
147.4894
138.0114
132.8288
128.6924
126.7073
80.9242
53.5328
34.0248
28.2568
OtBu
O
O
4-58

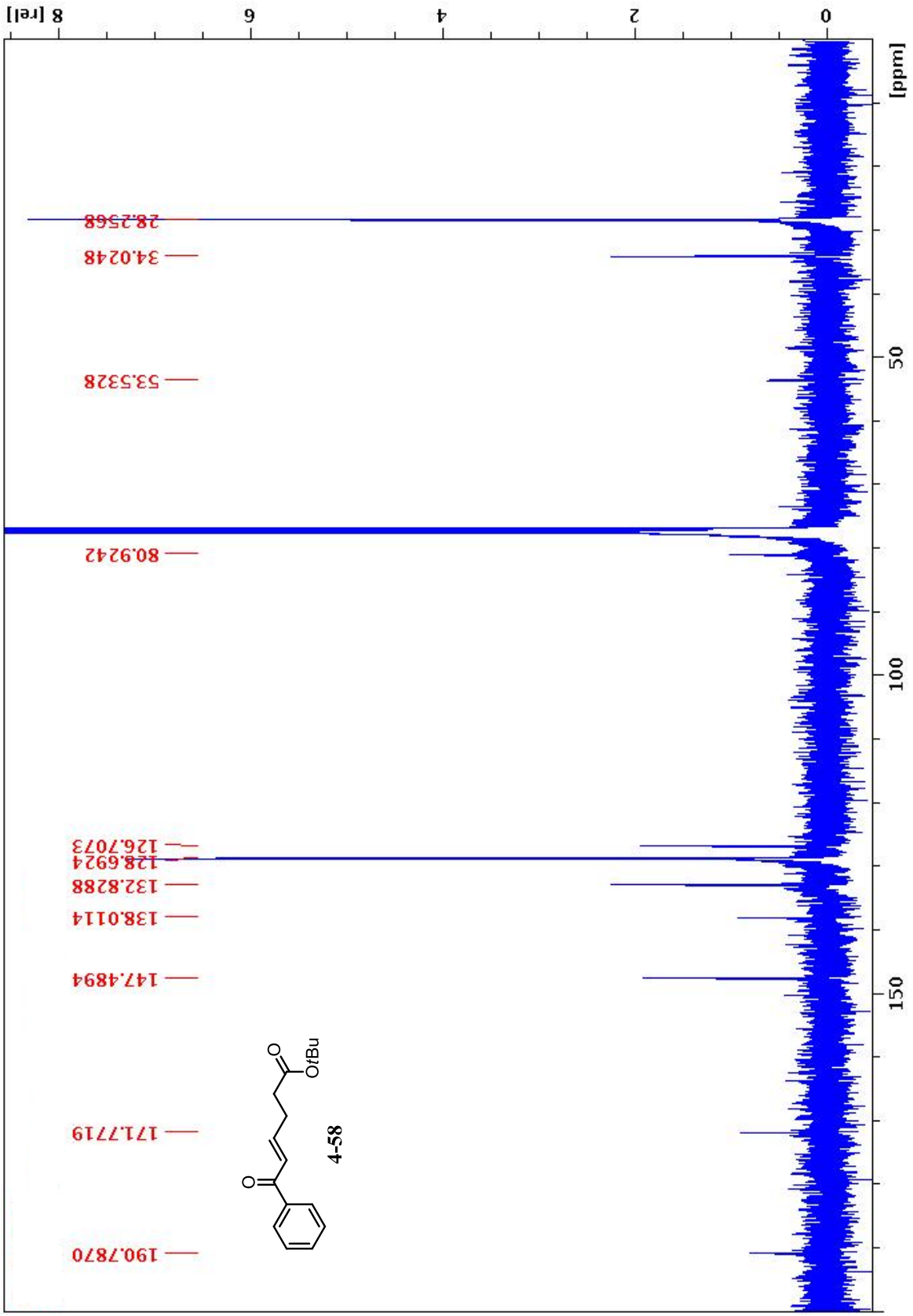
190.7870
171.7719
147.4894
138.0114
132.8288
128.6924
126.7073
80.9242
53.5328
34.0248
28.2568
OtBu
O
O
4-58
0
2
4
6
8 [rel]
150
100
50
[ppm]

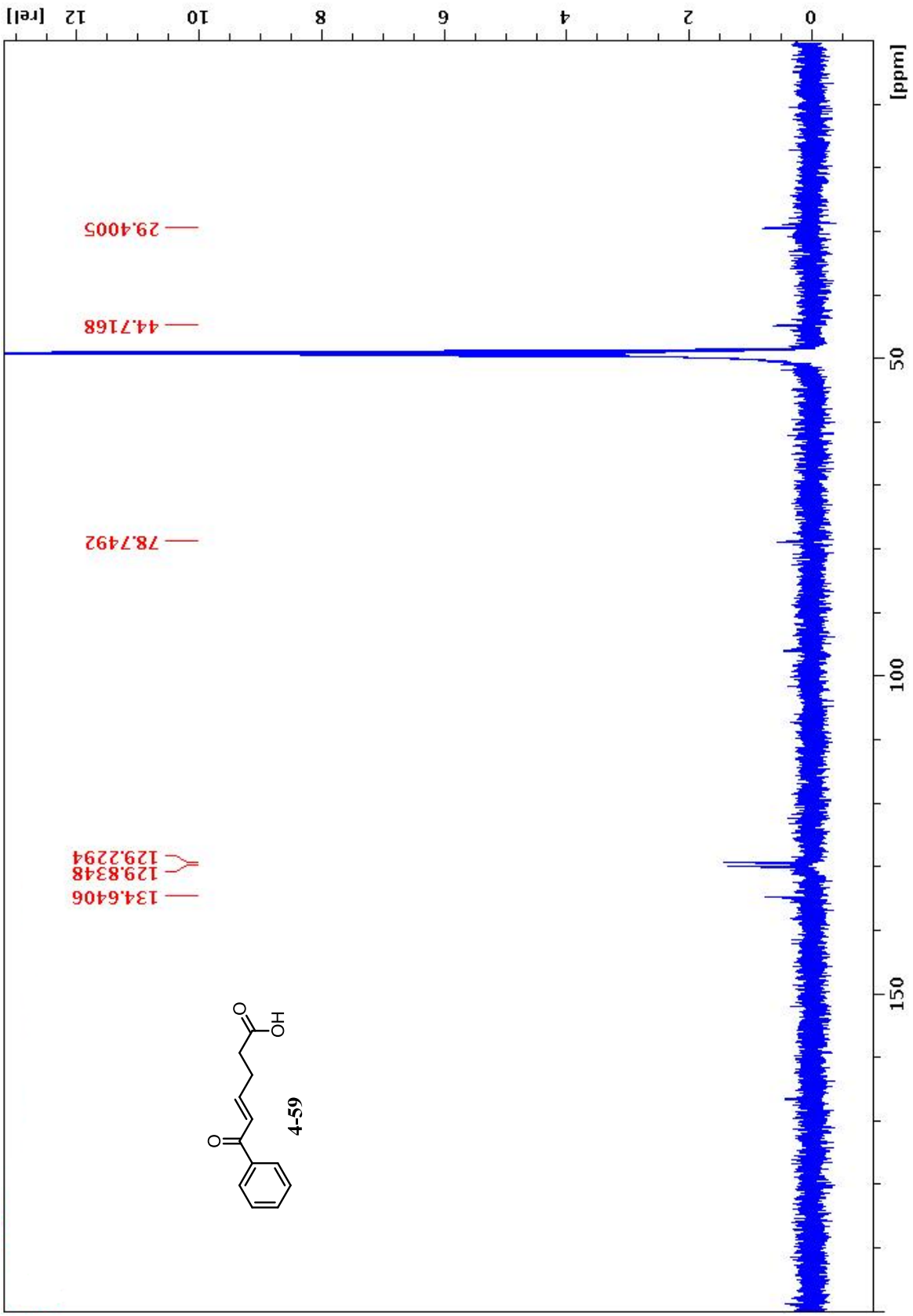
[rel]
12
10
8
6
4
2
0
[ppm]
50
100
150
29.4005
44.7168
78.7492
129.2294
129.8348
134.6406
4-59

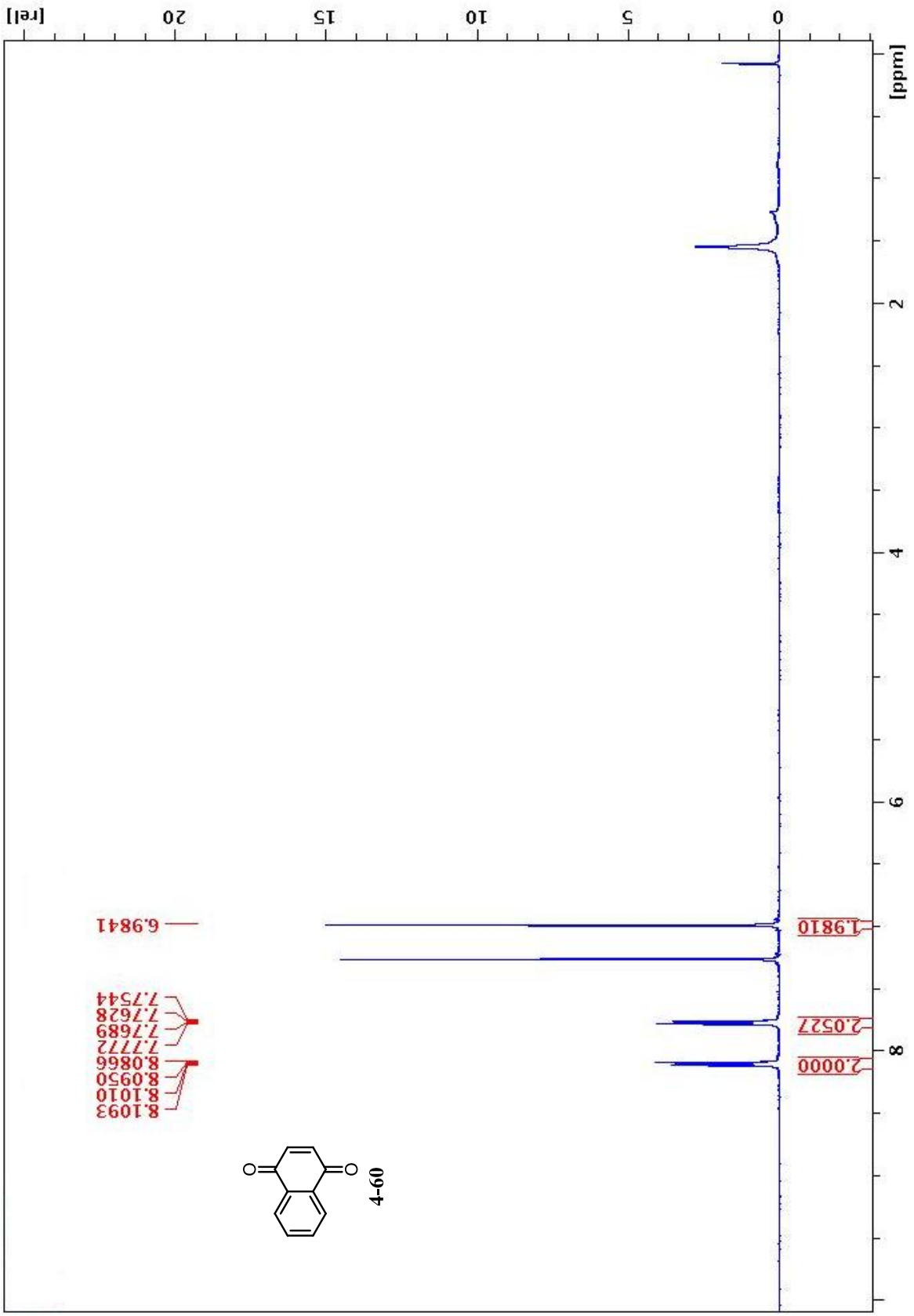
[rel]
20
15
10
5
0
[ppm]
2
4
6
8
6.9841
1.9810
2.0527
2.0000
8.1093
8.1010
8.0950
8.0866
7.7772
7.7689
7.7628
7.7544
4-60

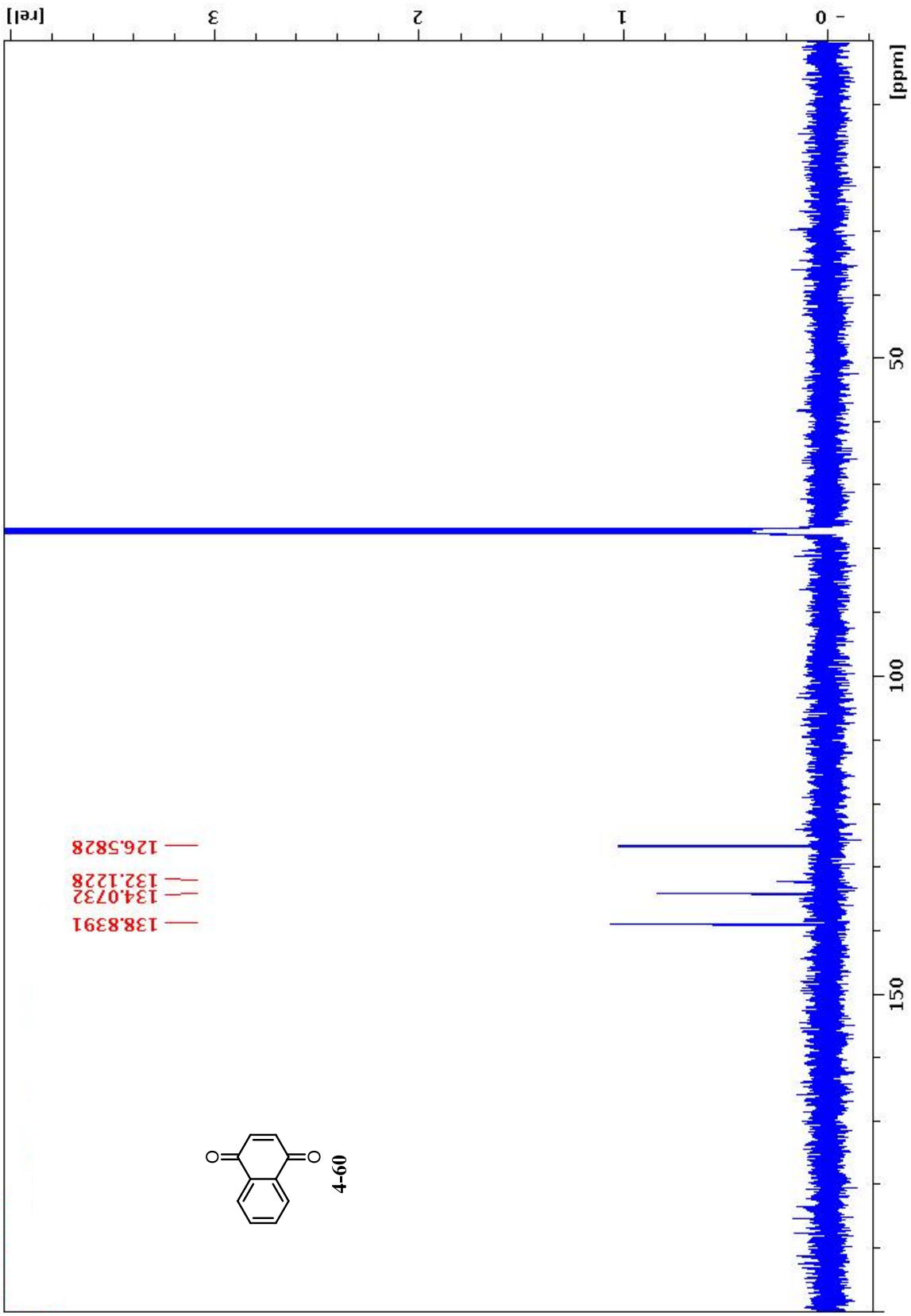
[rel]
3
2
1
0
[ppm]
50
100
150
126.5828
132.1228
134.0732
138.8391
4-60

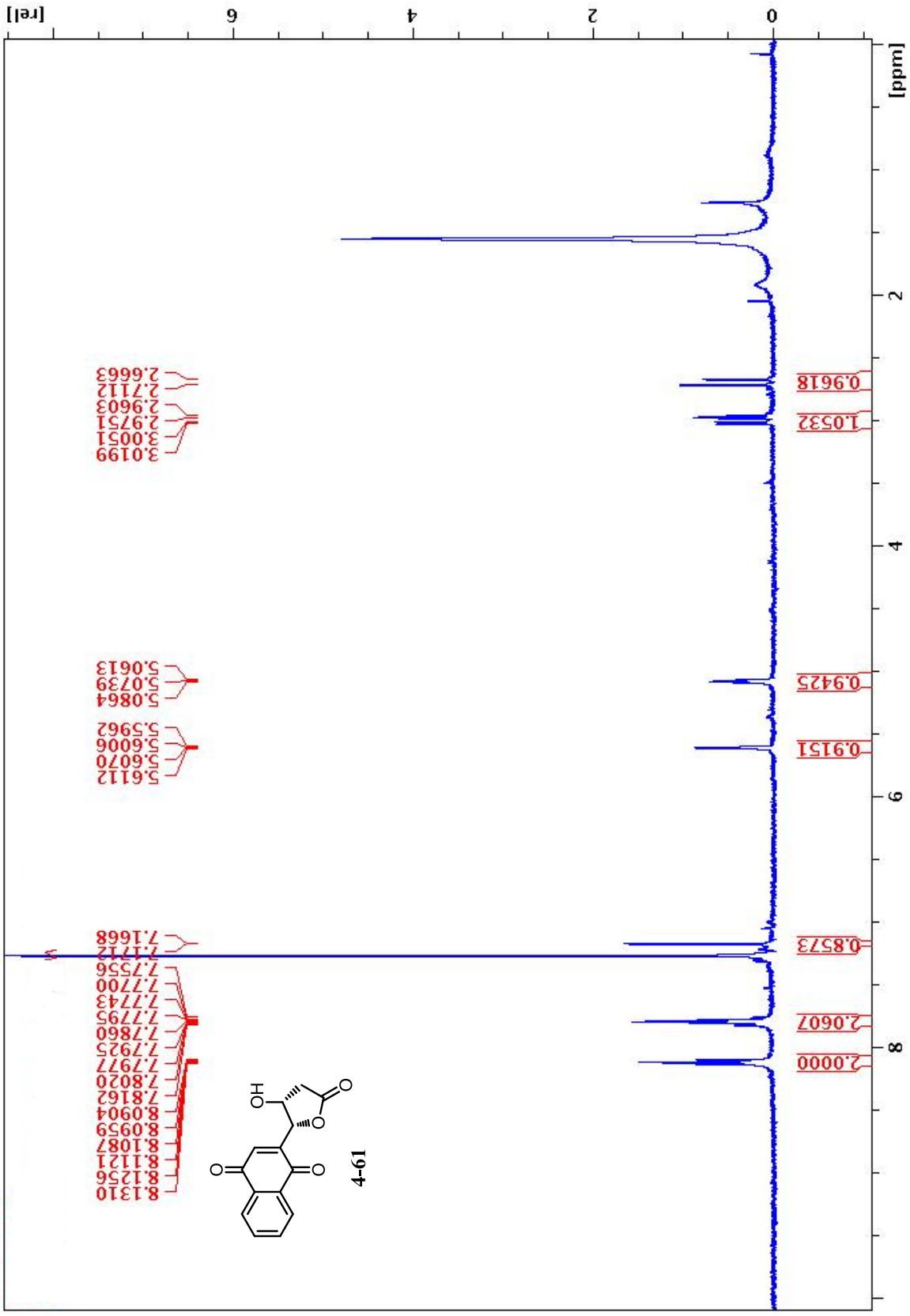
[rel]
6
4
2
0
[ppm]
2
4
6
8
8.1310
8.1256
8.1121
8.1087
8.0959
8.0904
7.8162
7.8020
7.7925
7.7860
7.7795
7.7743
7.7700
7.7556
7.1712
7.1668
5.6112
5.6070
5.6006
5.5962
5.0864
5.0739
5.0613
3.0199
3.0051
2.9751
2.9603
2.7112
2.6663
0.8573
2.0000
2.0607
0.9151
0.9425
1.0532
0.9618
OH
O
O
O
O
4-61

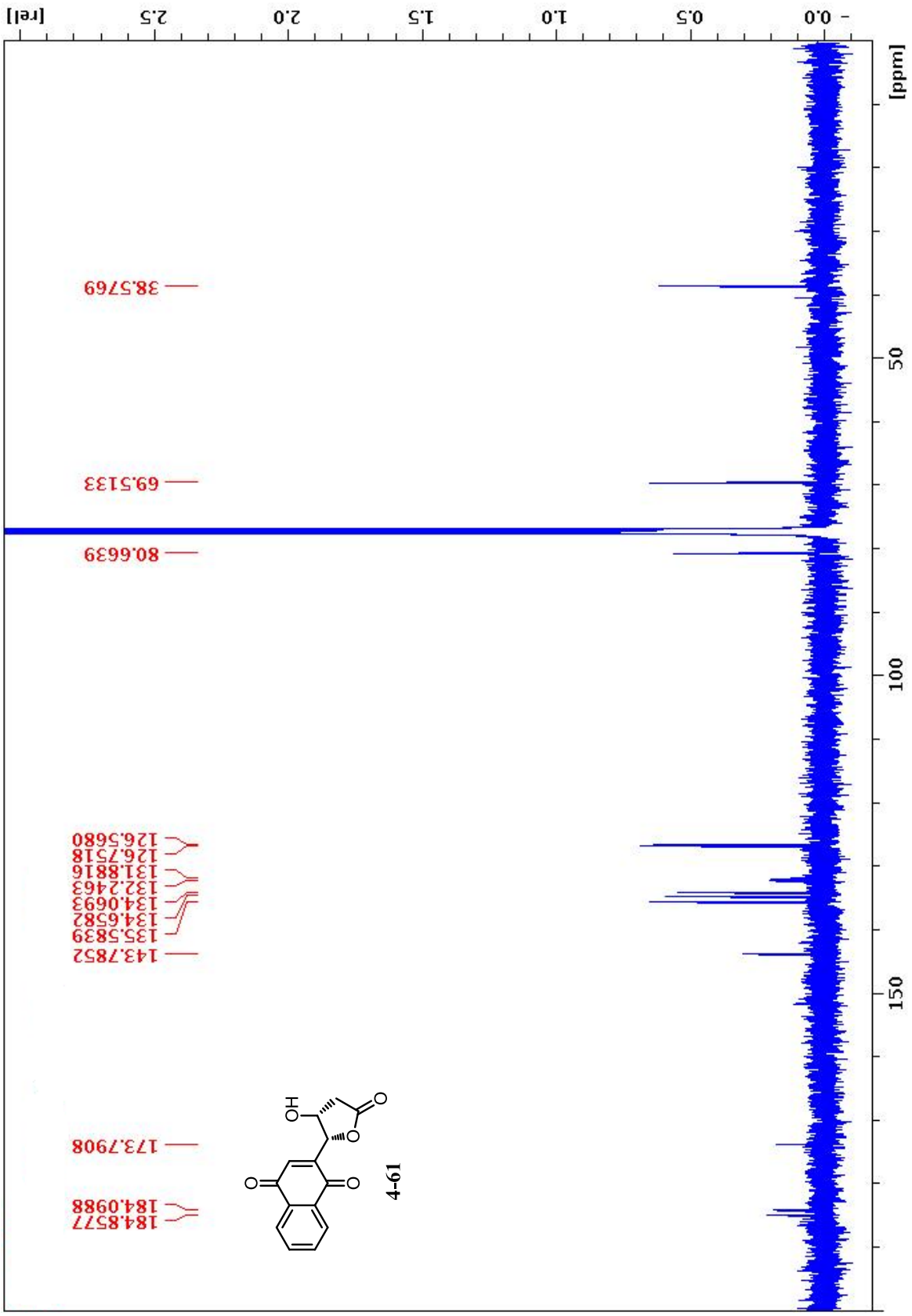
[rel]
2.5
2.0
1.5
1.0
0.5
0.0
[ppm]
50
100
150
38.5769
69.5133
80.6639
126.5680
126.7518
131.8816
132.2463
134.0693
134.6582
135.5839
143.7852
173.7908
184.0988
184.8577
4-61

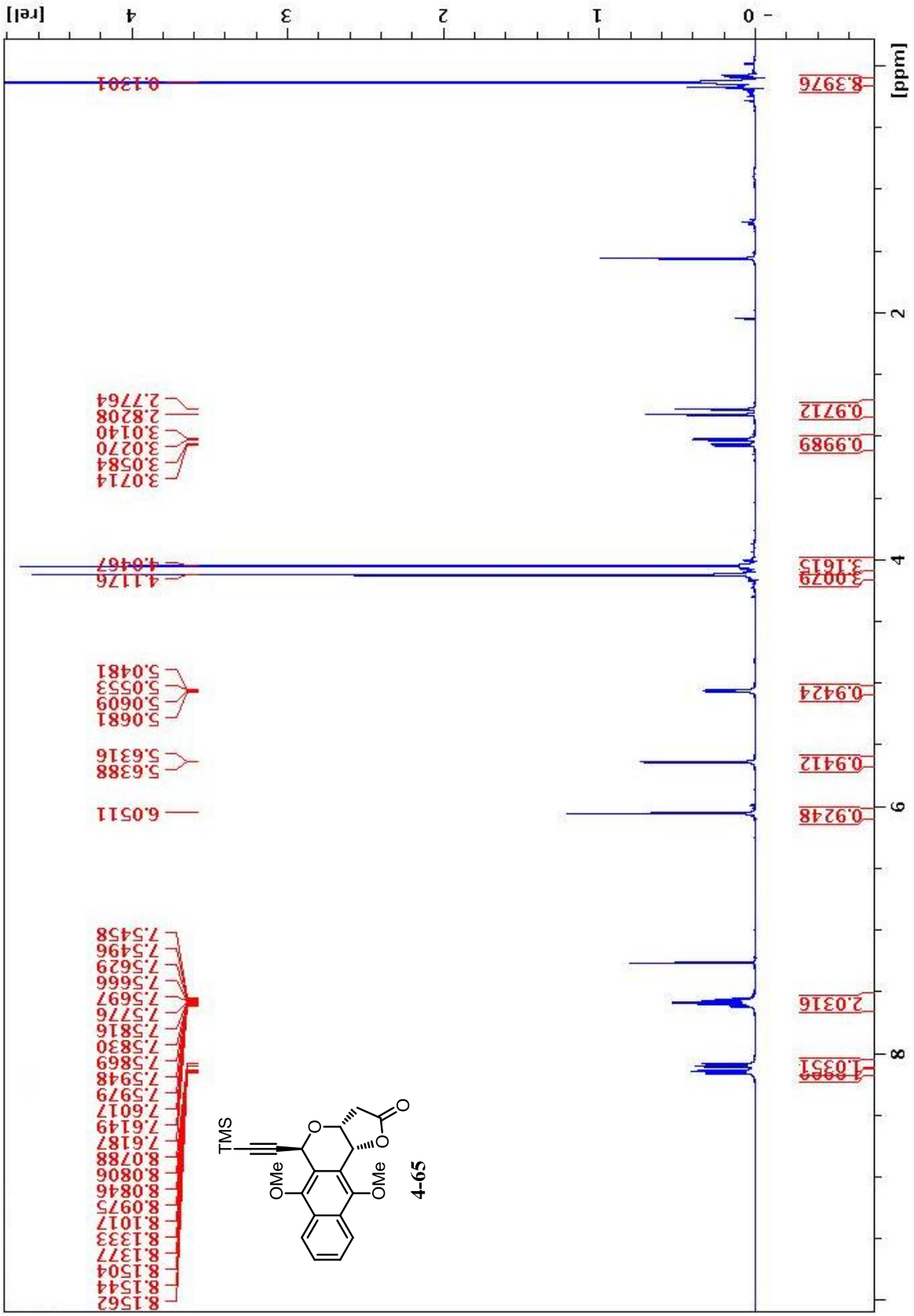
TMS
OMe
OMe
4-65

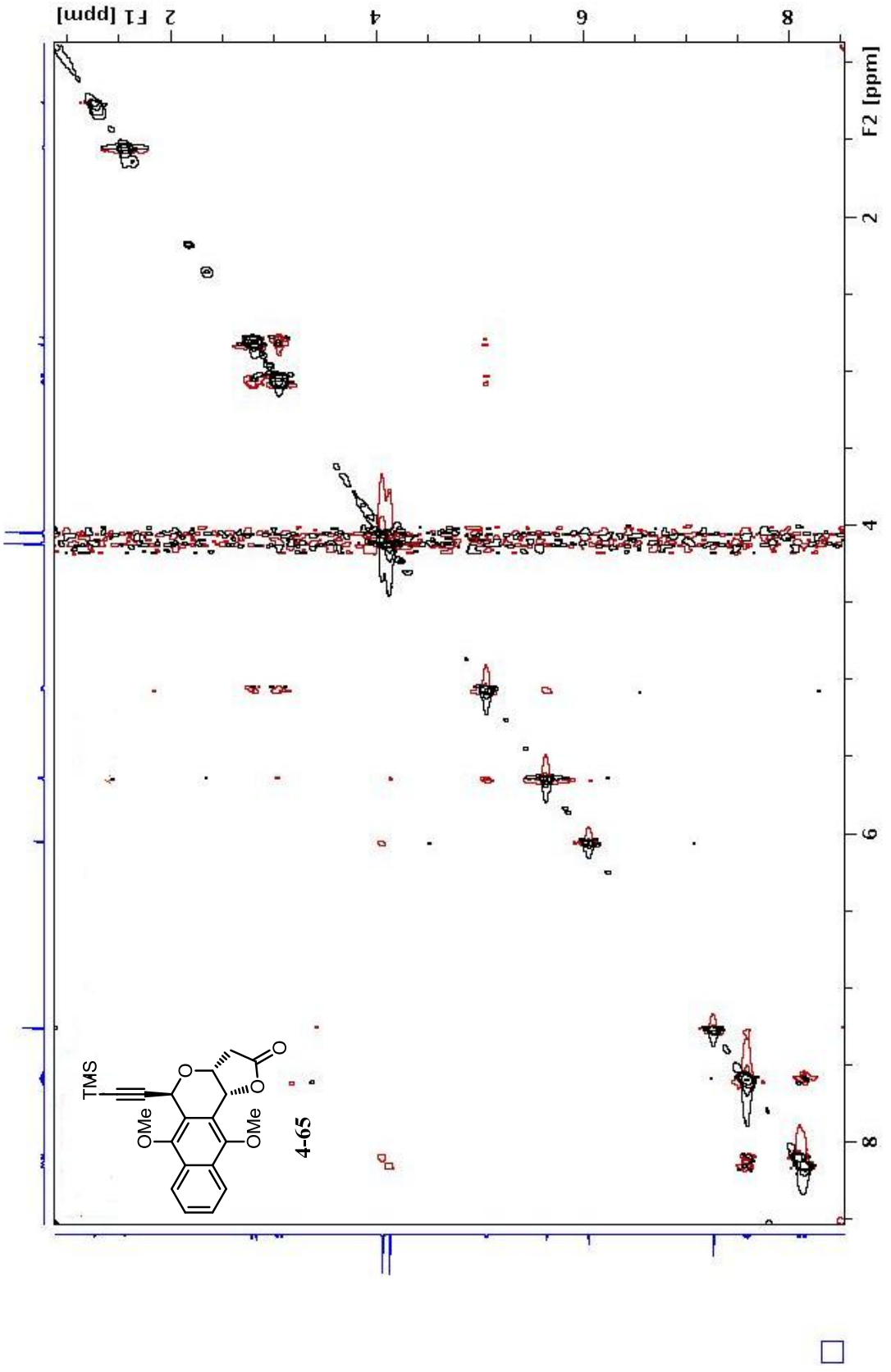
F1 [ppm]
F2 [ppm]
TMS
OMe
OMe
4-65

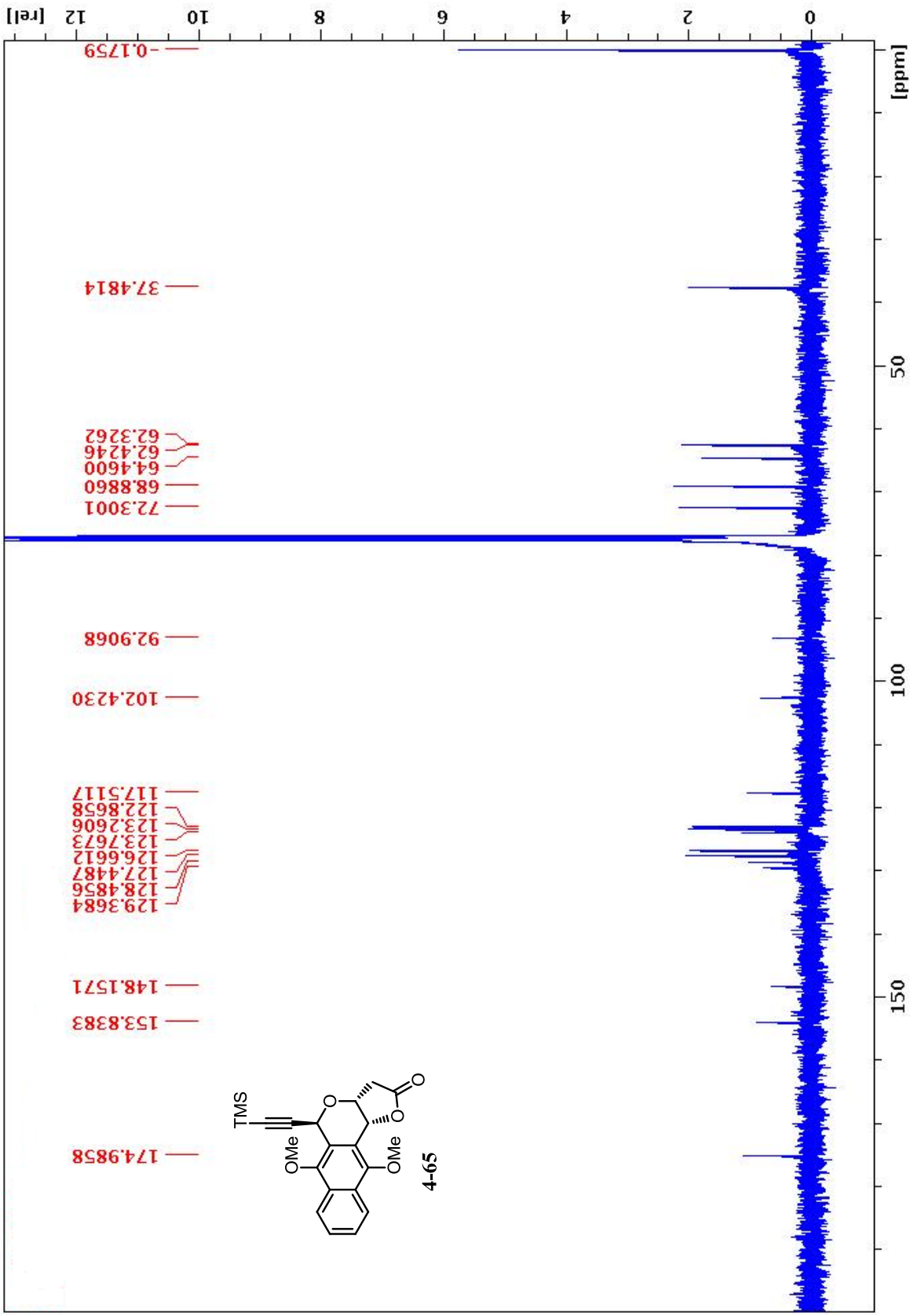
-0.1759
37.4814
62.3262
62.4246
64.4600
68.8860
72.3001
92.9068
102.4230
117.5117
122.8658
123.2606
123.7673
126.6612
127.4487
128.4856
129.3684
148.1571
153.8383
174.9858
TMS
OMe
OMe
O
O
O
4-65
[rel]
[ppm]

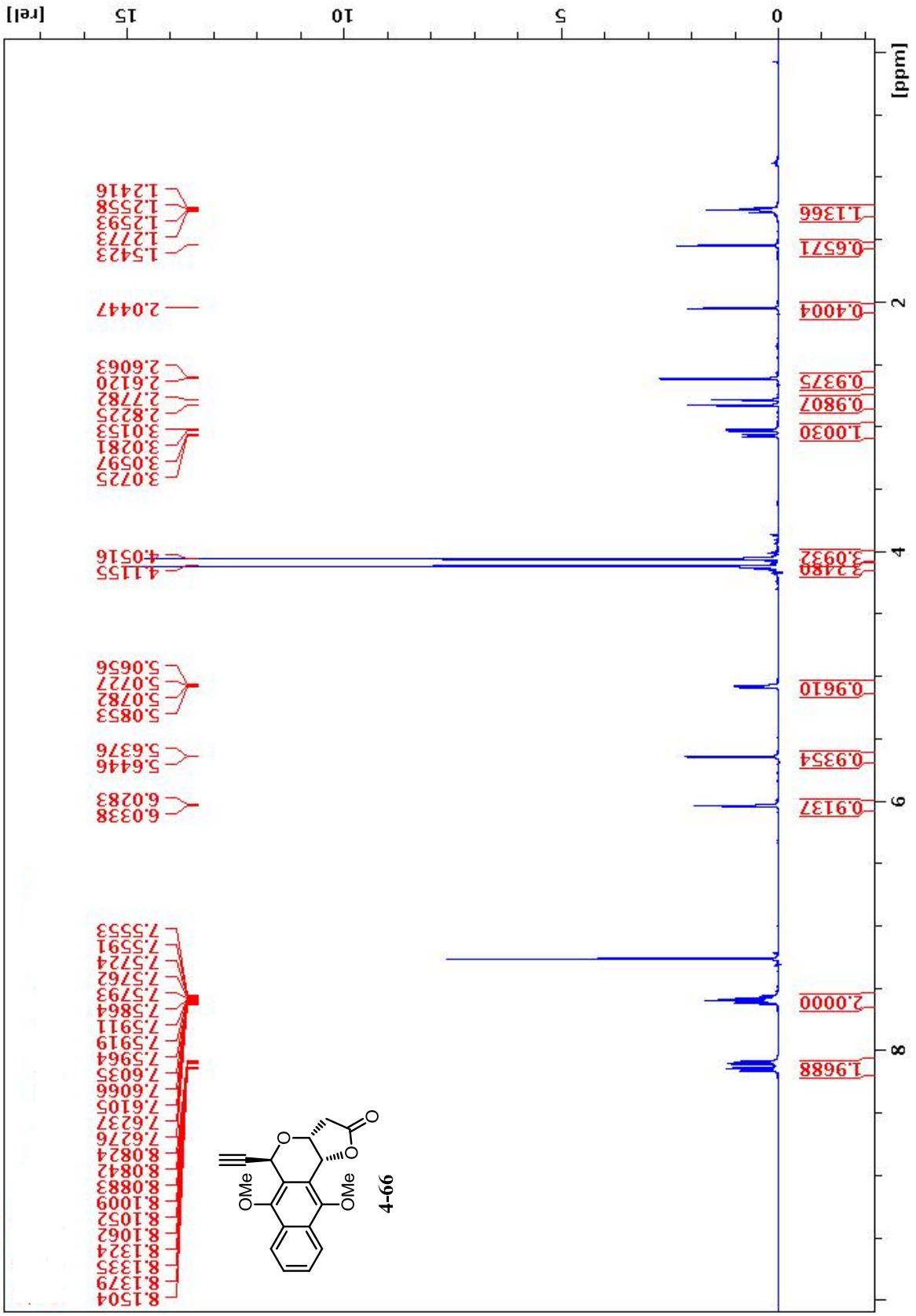
[rel]
15
10
5
0
[ppm]
2
4
6
8
1.9688
2.0000
0.9137
0.9354
0.9610
1.0030
0.9807
0.9375
0.4004
0.6571
1.1366
3.1480
3.0932
OMe
OMe
O
O
O
4-66

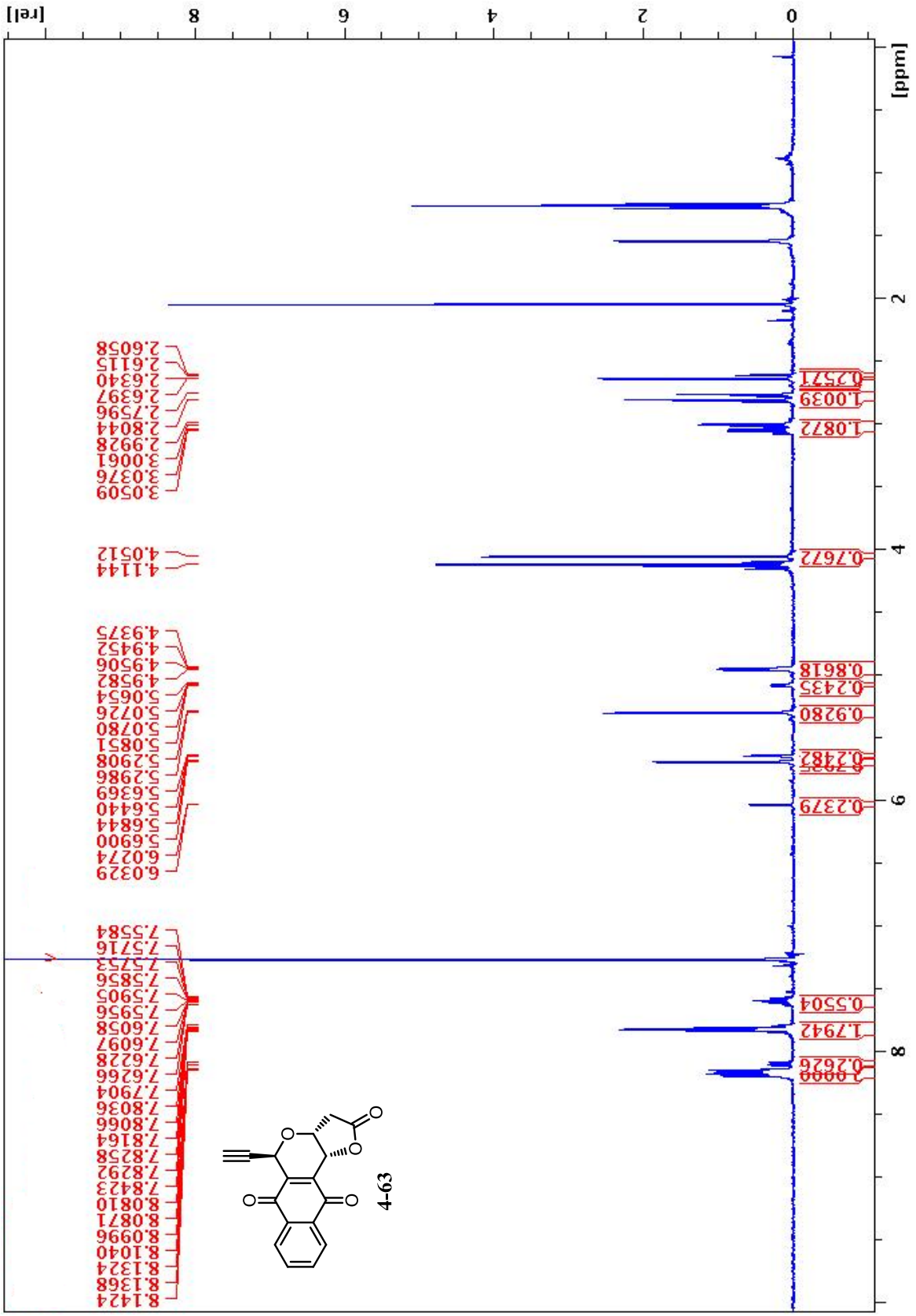
4-63

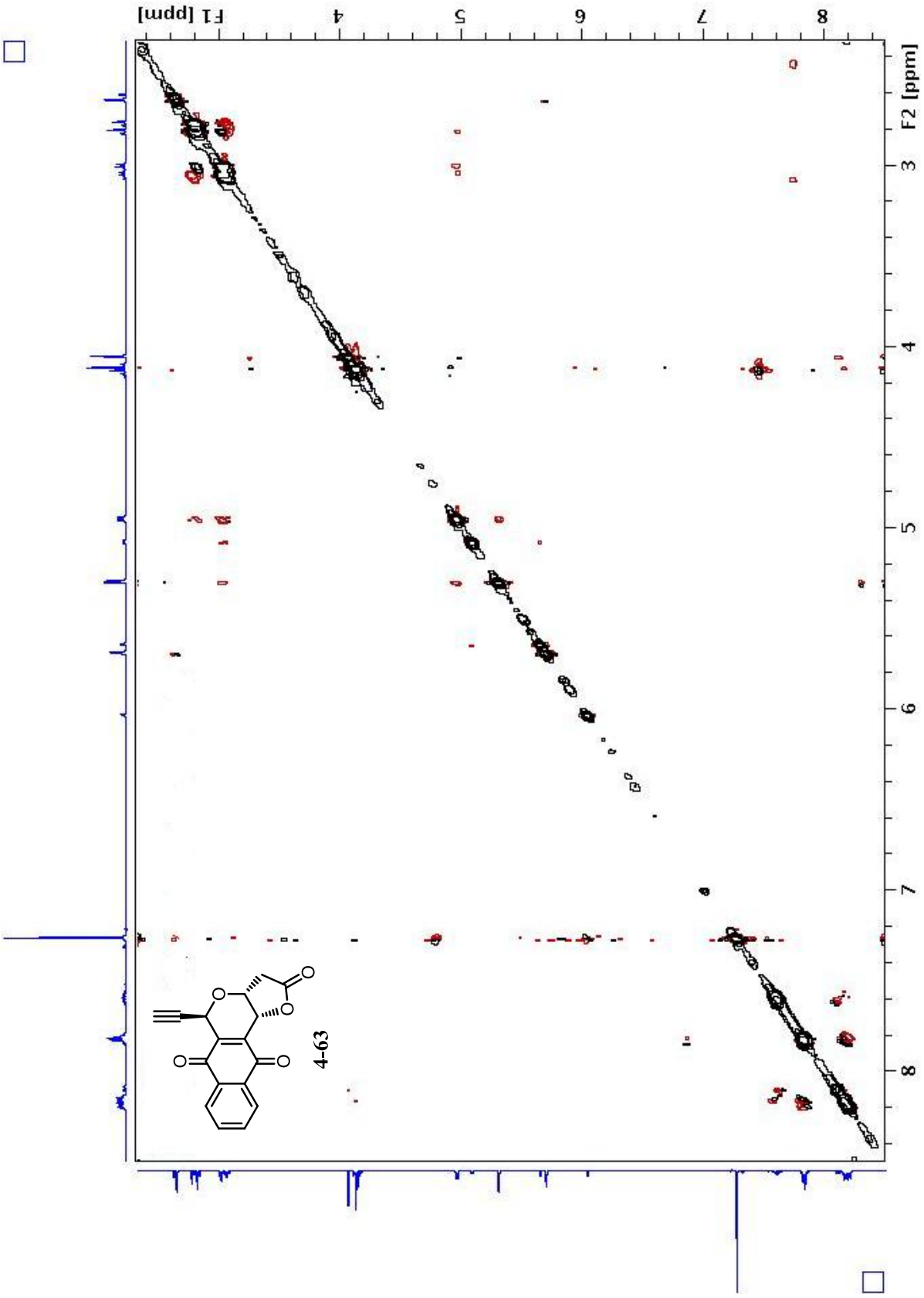
F1 [ppm]
F2 [ppm]
4-63